



**Politecnico
di Torino**

POLITECNICO DI TORINO

Master's degree in civil engineering

Master's Thesis

**Fatigue and self-healing analyses of bituminous binders modified
with a recycled plastic compound**

Supervisors:

Prof. Orazio BAGLIERI

Prof. Lucia TSANTILIS

Dott. Joseph Nicolas LA MACCHIA

Candidate:

Jakhongir DAULETIYAROV

December 2025

SUMMURY

INTRODUCTION	7
CHAPTER 1 – LITERATURE REVIEW	12
1.1 Self-Healing and Fatigue	12
1.2 Characterization of Self-Healing.....	16
1.3 Protocols for Healing Evaluation.....	19
1.4. Plastic Waste and Its Application in Asphalt Pavements	21
CHAPTER 2 – RESEARCH-BASED PROJECT.....	25
2.1 Instrumentation.....	25
2.1.1 Mixing Procedure Equipment	25
2.1.2 Rheology Test Equipment.....	27
2.2 Mixing Procedure	29
2.3 Materials	32
2.4 Sample Preparation.....	35
2.5 Methodological Approach.....	38
2.5.1 Frequency Sweep Tests.....	39
2.5.2 Linear Amplitude Sweep (LAS) Test – Fatigue Resistance	43
2.5.2 LAS-Healing (LASH) Test – Evaluation of Healing Behaviour.....	44
2.5.3 Steric Hardening Control Tests (LAS-SH).....	47
CHAPTER 3 – DATA ANALYSIS	51
3.1 Linear viscoelastic characterization.....	52
3.2 Fatigue resistance (LAS test).....	57
3.3 Self-healing (LAS-H test).....	65
3.4 LAS with Steric Hardening	75
3.5 Quantitative Evaluation of Self-Healing Behavior.....	80
3.5.1 Method 1 — Healing Assessment at a Fixed Reference Strain	83
3.5.2 Method 2 — Self-Healing Analysis Based on the AASHTO TP-101	88
CHAPTER 4 – CONCLUSION	95
BIBLIOGRAPHY	98

CONTENT OF FIGURES AND TABLES

Figure 1.1.1 - Self-healing mechanism in bituminous binders.....	12
Figure 1.1.2 - Medium severity alligator cracking.	14
Figure 1.4.1 - Plastic waste in worldwide.....	21
Figure 1.4.2 - Iterchimica Superplast Polymers.	23
Figure 2.1.1.1 - High-Shear Mixer: Operated up to 5000 RPM by Silverson model L5M-A	26
Figure 2.1.2.1 - Dynamic Shear Rheometer (DSR), Physica MCR 302, Anton Paar	27
Figure 2.1.2.2 - Measuring system. Plate- 8 mm.....	28
Figure 2.2.1 – Mixed binder with RLD-plasrtic.	31
Figure 2.2.2 - Preparation of bituminous beams.....	32
Figure 2.3.1 - A – Cutted plastic pallets; B – Plastic pallets.	34
Figure 2.4.1 - Molded bituminous binder.....	35
Table 2.1 – Tests performed on PMB with 2% of RLDP.....	49
Table 2.2 – Tests performed on PMB with 4% of RLDP.....	50
Table 3.1.1 - Master curve parameters at different reference temperatures of PMB with 2% and 4% RLDP.....	52
Figures 3.1.1 and 3.1.2 – Comparison of CA model fitting curves for PMB with 2% and 4% RLDP.	53
Figure 3.1.3 – Master curves of complex modulus ($ G $) vs. reduced frequency for Neat50/70, PMB with 2% and 4% RLDP, $T_0 = 20\text{ }^{\circ}\text{C}$	54
Figure 3.1.4 – Phase angle (δ) vs. reduced frequency comparison between Neat50/70, PMB with 2% and 4% RLDP.	55
Figure 3.1.5 – Black diagram ($ G $ vs δ) for Neat 50/70, PMB with 2% and 4% RLDP.	56
Figure 3.2.1 – LAS 15 ° stress–strain curves for Neat 50/70.	58
Figure 3.2.2 – LAS $20\text{ }^{\circ}\text{C}$ stress–strain curves for Neat 50/70.	58
Figure 3.2.3 – LAS $15\text{ }^{\circ}\text{C}$ stress–strain curves for PMB with 2 % of RLDP.....	58
Table 3.2.1 – LAS $15\text{ }^{\circ}\text{C}$ statistical analysis on consistency for PMB with 2 % of RLDP.	59
Figure 3.2.4 – LAS $20\text{ }^{\circ}\text{C}$ stress–strain curves for PMB with 2 % of RLDP.....	59
Table 3.2.2 – LAS $15\text{ }^{\circ}\text{C}$ statistical analysis on consistency for PMB with 4 % of RLDP.	60

Place Figure 3.2.5 – LAS 15 °C stress–strain curves for PMB with 4 % of RLDP..	60
Table 3.2.3 – LAS 15 °C statistical analysis on consistency for PMB with 4 % of RLDP.	61
Figure 3.2.6 – LAS 20 °C stress–strain curves for PMB with 4 % of RLDP.....	61
Table 3.2.4 – LAS 20 °C statistical analysis on consistency for PMB with 4 % of RLDP.	62
Table 3.2.5 – “Strain at maximum shear stress (γ at τ peak)”	63
Figure 3.2.7 – Comparison of LAS curves for Neat50/70, 2 %, and 4 % RLDP binders at 15 °C.	63
Figure 3.2.8 – Comparison of LAS curves for Neat50/70, 2 %, and 4 % RLDP binders at 20 °C.	64
Figure 3.3.1 – LAS-H_15 °C (2 %PMB), where Resting Time = 30min.	66
Figure 3.3.2 – LAS-H_15 °C (2 %PMB), where Resting Time = 0min.	66
Figure 3.3.3 – LAS-H_20 °C (2 %PMB), where Resting Time = 30min.	67
Figure 3.3.4 – LAS-H_20 °C (2 %PMB), where Resting Time = 0min.	67
Figure 3.3.5 – LAS-H_15 °C (4 %PMB), where Resting Time = 30min.	68
Figure 3.3.6 – LAS-H_15 °C (4 %PMB), where Resting Time = 0min.	68
Figure 3.3.7 – LAS-H_20 °C (4 %PMB), where Resting Time = 30min.	69
Figure 3.3.8 – LAS-H_20 °C (4 %PMB), where Resting Time = 0min.	69
Figure 3.3.9 – LAS-H_15 °C (2 %PMB), where Resting Time = 0min vs Resting Time = 30min.	70
Figure 3.3.10 – LAS-H_20 °C (2 %PMB), where Resting Time = 0min vs Resting Time = 30min.	71
Figure 3.3.11 – LAS-H_15 °C (4 %PMB), where Resting Time = 0min vs Resting Time = 30min.	71
Figure 3.3.12 – LAS-H_20 °C (4 %PMB), where Resting Time = 0min vs Resting Time = 30min.	72
Figure 3.3.13 – At 15 °C (2 %PMB), LASH vs LAS test results.....	72
Figure 3.3.14 – At 20 °C (2 %PMB), LASH vs LAS test results.....	73
Figure 3.3.15 – At 15 °C (4 %PMB), LASH vs LAS test results.....	74
Figure 3.3.16 – At 20 °C (4 %PMB), LASH vs LAS test results.....	74
Figure 3.4.1 – LAS-SH 2 % PMB at 15 °C	75
Figure 3.4.2 – LAS-SH 2 % PMB at 20 °C	76
Figure 3.4.3 – LAS-SH 4 % PMB at 15 °C	76

Figure 3.4.4 – LAS-SH 4 % PMB at 20 °C	77
Figure 3.4.5 – At 15 °C (2 %PMB), LAS-SH vs LAS test results.	78
Figure 3.4.6 – At 20 °C (2 %PMB), LAS-SH vs LAS test results.	78
Figure 3.4.7 – At 15 °C (4 %PMB), LAS-SH vs LAS test results.	79
Figure 3.4.8 – At 20 °C (4 %PMB), LAS-SH vs LAS test results.	79
Table 3.4.1 – Strain Values at Peak shear stress for LAS-SH Tests	80
Table 3.5.1 – Results of 2%PMB at reference γ and at peak γ	81
Table 3.5.2 – Results of 4%PMB at reference γ and at peak γ	82
Table 3.5.1.1 – Results of average values at 15°C of 2%PMB at reference γ and at peak γ	84
Figure 3.5.1.1 – At 15 °C (2 %PMB), comparison of results of all protocols used. ..	85
Table 3.5.1.2 – Results of average values at 15°C of 2%PMB at reference γ and at peak γ	85
Figure 3.5.1.2 – At 20°C (2 %PMB), comparison of results of all protocols used. ..	86
Table 3.5.1.3 – Results of average values at 15°C of 4%PMB at reference γ and at peak γ	86
Figure 3.5.1.3 – At 15°C (4%PMB), comparison of results of all protocols used. ..	87
Table 3.5.1.4– Results of average values at 20°C of 4%PMB at reference γ and at peak γ	87
Figure 3.5.1.4 – At 20°C (4%PMB), comparison of results of all protocols used. ..	88
Table 3.5.2.1– Results analysis of average values of 2%PMB, with respect to AASHTO TP 101.	90
Table 3.5.2.2– Results analysis of average values of 4%PMB, with respect to AASHTO TP 101.	91
Figure 3.5.2.1 – At 15°C (2%PMB), comparison of results of all protocols used, with respect to AASHTO TP 101.	92
Figure 3.5.2.2 – At 20°C (2%PMB), comparison of results of all protocols used, with respect to AASHTO TP 101.	92
Figure 3.5.2.3 – At 15°C (4%PMB), comparison of results of all protocols used, with respect to AASHTO TP 101.	93
Figure 3.5.2.4 – At 20°C (4%PMB), comparison of results of all protocols used, with respect to AASHTO TP 101.	93

Acknowledgment

This thesis marks the culmination of a journey that would not have been possible without the support and encouragement of many remarkable people.

I am profoundly grateful to my parents, whose unconditional love, sacrifices, and faith in me have been my greatest source of strength. Their guidance and encouragement have sustained me through every challenge, and this achievement is a reflection of their unwavering support.

To my friends, I extend heartfelt thanks for their patience, understanding, and companionship. Their encouragement and presence provided balance and joy during the demanding phases of this research, reminding me that perseverance is best carried forward with kindness and laughter.

Above all, I wish to express my deepest appreciation to my professors. Their invaluable guidance, insightful feedback, and constant encouragement shaped the direction and quality of this work. Their mentorship inspired me to pursue research with dedication and integrity.

To each person who has walked beside me on this path, I owe a debt of gratitude. This accomplishment is not mine alone, but a shared milestone made possible by your support.

Благодарность

Данная работа является итогом пути, который был бы невозможен без поддержки и участия многих замечательных людей.

Прежде всего я выражаю глубочайшую признательность своим родителям. Их безусловная любовь, жертвы и вера в меня стали моим главным источником силы. Их руководство и поддержка помогли мне преодолевать все трудности, и этот результат — отражение их неизменной заботы.

Моим друзьям я искренне благодарен за терпение, понимание и дружеское участие. Их поддержка и присутствие дарили мне радость и равновесие в самые напряжённые периоды исследования, напоминая, что настойчивость легче сохранять, когда рядом есть доброта и смех.

Особую благодарность я хочу выразить своим профессорам. Их бесценные советы, внимательные замечания и постоянное поощрение определили направление и качество данной работы. Их наставничество вдохновило меня заниматься научными исследованиями с преданностью и честностью.

Каждому, кто сопровождал меня на этом пути, я обязан благодарностью. Это достижение — не только моё, но и общий результат, ставший возможным благодаря вашей поддержке.

ABSTRACT

In recent years, the asphalt industry has focused on improving pavement performance and durability while adopting more sustainable construction practices. Recycled plastic materials have become increasingly relevant for achieving these goals, as they can enhance material properties and reduce environmental impact. However, the direct use of recycled plastics in binder modification—especially those originally designed for hybrid or dry modification methods—is still not widely explored. This thesis investigates the fatigue and self-healing behaviour of bituminous binders modified with Recycled Low-Density Plastic (RLDP). Two modified binders containing 2% and 4% RLDP by total binder mass were tested, along with a neat 50/70 penetration grade binder used as a reference. The Dynamic Shear Rheometer (DSR) was employed to evaluate fatigue and healing performance through Frequency Sweep (FS), Linear Amplitude Sweep (LAS), and LAS-Healing (LASH) tests. The results showed that RLDP addition increased binder stiffness and elasticity while maintaining thermorheological consistency. The 4% RLDP binder demonstrated better resistance to fatigue damage, whereas the 2% RLDP binder showed higher self-healing efficiency, recovering more stiffness after rest periods due to greater molecular mobility.

Overall, the study confirms that recycled plastic modification, especially at moderate dosages, can enhance both fatigue resistance and self-healing capacity of bituminous binders, offering a practical and sustainable alternative to traditional polymer modification in pavement engineering.

INTRODUCTION

The increasing pressure on road networks, combined with the demand for sustainable infrastructure, has directed significant research efforts toward improving the performance and durability of asphalt pavements. Flexible pavements, which are the most widely used pavement type, consist of several layers where the surface and binder courses are composed of asphalt mixtures. These mixtures must simultaneously fulfill functional requirements, such as smoothness, skid resistance, and comfort, and structural requirements, such as the ability to distribute traffic loads to the subgrade while resisting mechanical and environmental distress.

Despite advances in pavement engineering, flexible pavements remain vulnerable to several deterioration mechanisms. Permanent deformation (rutting), thermal cracking, and particularly fatigue cracking is the most common. Among these, fatigue cracking is considered one of the primary factors that determine the service life of asphalt pavements. It originates from the initiation and propagation of microcracks under repeated load cycles, leading to stiffness reduction, structural weakening, and eventual failure.

Within the asphalt mixture, the bituminous binder is the most sensitive component to mechanical fatigue and environmental variations. Continuous loading causes micro-damage in the binder, which can develop into interconnected cracks in the pavement surface. However, bitumen exhibits a unique property: the ability to partially recover mechanical properties such as stiffness and strength during periods of rest. This phenomenon, known as self-healing, has been recognized as a fundamental mechanism in extending the fatigue life of pavements.

The self-healing process occurs when, after partial damage, the bitumen molecules undergo flow, diffusion, and re-adhesion across microcrack interfaces, leading to a recovery of mechanical integrity. Although this recovery is rarely complete, it is sufficient to delay further damage and extend pavement service life. The study of this property is therefore essential not only from a structural perspective but also in terms of economic and environmental sustainability, as it can reduce maintenance frequency and material consumption.

Over the last two decades, various methodologies have been developed to evaluate the self-healing potential of bituminous binders. Laboratory testing has largely relied on the Dynamic Shear Rheometer (DSR), which allows for controlled application of oscillatory shear to characterize binder response under linear and nonlinear viscoelastic conditions.

Furthermore, the incorporation of the Time–Temperature Superposition Principle (TTSP) allows researchers to account for the influence of temperature, one of the most critical factors in binder performance and healing potential. More recently, emphasis has been placed on the role of nonlinear viscoelastic behaviour, recognizing that high deformation levels can induce integrity losses that are not solely attributable to fatigue damage.

In parallel with the development of self-healing evaluation methods, the use of plastics in asphalt technology has emerged as a promising strategy to enhance pavement performance while addressing global sustainability challenges. Plastics can be incorporated into pavements through two main routes: the wet process, where plastic materials are blended directly into the hot bituminous binder, and the dry process, where plastic particles are added into the aggregate mix before binder incorporation.

In this thesis, the wet modification method is adopted for the preparation of Recycled Low-Density Plastic (RLDP)-modified binders. This process allows the plastic to be melted and uniformly dispersed within the bitumen using a high-shear mixer operating up to 5000 rpm, ensuring complete homogenization and stable polymer–bitumen interaction. The wet method was chosen because it enables precise control of mixing temperature, shear rate, and dispersion, producing consistent and reproducible laboratory samples suitable for advanced rheological characterization.

In both laboratory and field studies, the incorporation of plastic within the binder phase has been shown to enhance elastic recovery, rutting resistance, and temperature stability, thereby extending pavement service life and reducing maintenance frequency. Depending on their origin and properties, plastics used for binder modification can be broadly classified into:

- *Virgin polymers*, such as styrene–butadiene–styrene (SBS), ethylene–vinyl–acetate (EVA), and polyethylene (PE), which are conventionally employed to improve elasticity, stiffness, and fatigue resistance; and
- *Recycled plastics*, including low-density polyethylene (LDPE), high-density polyethylene (HDPE), polypropylene (PP), and polyethylene terephthalate (PET), which offer similar benefits while contributing to waste reduction and environmental sustainability [14,15,21,22].

Among these materials, Recycled Low-Density Plastic (RLDP) has demonstrated particular promise due to its low melting point, high ductility, and good compatibility with bituminous binders. When blended through the wet process, RLDP improves binder stiffness, deformation resistance, and may enhance fatigue and healing behaviour by reinforcing the bitumen matrix and improving molecular mobility across damaged zones.

The integration of recycled plastics in bitumen therefore represents a dual advantage: it enhances the mechanical and durability performance of asphalt pavements while reducing the environmental burden associated with plastic waste disposal. As such, it aligns with the broader principles of green infrastructure, circular economy, and sustainable pavement engineering, contributing simultaneously to technical innovation and environmental conservation [21,22].

While many studies have been conducted on neat and SBS-modified binders, there is still limited knowledge regarding the comparative healing behaviour of binders modified with alternative additives such as recycled plastics. Moreover, the influence of additive dosage on self-healing efficiency remains insufficiently quantified. Understanding how different modification strategies affect both fatigue resistance and healing potential is crucial for developing binders that can deliver improved long-term performance under realistic traffic and environmental conditions.

The present thesis aims to contribute to the understanding of fatigue performance and self-healing behaviour in bituminous binders through a comparative rheological investigation of both newly prepared and pre-characterized materials. The study focuses on assessing the influence of Recycled Low-Density Plastic (RLDP) as a

sustainable additive, examining its effect on the viscoelastic and fatigue-healing response of the binder.

To ensure a comprehensive evaluation, the research includes experimental testing of RLDP-modified binders prepared in the laboratory, combined with a comparative analysis against reference materials obtained from previous research activities. The binders considered in this work are as follows:

- Neat binder (50/70 penetration grade): serves as the reference material, representing the unmodified baseline for mechanical and rheological comparison.
- RLDP-modified binder (2% additive content): prepared and tested within this thesis using the wet process to investigate the effect of a lower recycled plastic concentration on viscoelastic and healing performance.
- RLDP-modified binder (4% additive content): similarly prepared and tested to evaluate the influence of a higher RLDP concentration and to identify potential thresholds for optimal self-healing and fatigue resistance.

In this framework, the mixing and rheological characterization of the RLDP-modified binders constitute the experimental core of the present research. The neat data, obtained from prior experimental campaigns, are used as reference datasets for comparative analysis.

This approach enables a systematic evaluation of performance trends across different binder types and modification levels, providing insight into the role of recycled plastic content on the mechanical integrity and healing potential of bituminous materials. Furthermore, it establishes a methodological continuity with previous studies while introducing an original contribution through the preparation, testing, and analysis of 2% and 4% RLDP binders.

The experimental program consists of:

- Linear viscoelastic characterization through frequency sweep tests, with master curves constructed using the CA model with time-temperature superposition principle;

- Fatigue resistance assessment using the LAS protocol (Linear Amplitude Sweep);
- Healing potential analysis using the LASH protocol (LAS-based Healing), complemented with steric hardening tests to exclude structural stiffening effects.

The outcomes of this research are expected to provide new insights into how plastic and RLDP modifications influence the healing ability of binders in comparison with conventional bitumen. By linking experimental results with analytical modelling, the study seeks to clarify whether these modifications can contribute to extended fatigue life, reduced maintenance needs, and more sustainable pavement solutions.

In particular, the use of Recycled Low-Density Plastic (RLDP) represents a dual benefit: it enhances the mechanical and healing properties of asphalt binders while simultaneously addressing the environmental challenge of plastic waste management. Thus, this research not only explores technical performance but also contributes to circular economy practices by promoting the reuse of waste plastics in road construction. In a broader context, the study aligns with global sustainability goals, aiming to develop binders that combine enhanced structural performance with reduced environmental impact and longer service lives.

CHAPTER 1 – LITERATURE REVIEW

1.1 Self-Healing and Fatigue

One of the most distinctive features of asphalt materials, compared to other construction materials such as concrete or steel, is their inherent ability to self-heal. Self-healing can be defined as the natural capacity of a bituminous binder to recover part of its mechanical properties after being subjected to micro-damage, provided that sufficient rest time is given [1,2]. Unlike external repair strategies, self-healing occurs spontaneously, driven by the material's viscoelastic and adhesive characteristics.

The mechanisms governing healing have been the subject of significant research. While the process is not yet fully understood at the molecular scale, several studies agree that it can be explained through a multi-stage mechanism: (i) the flow of binder into the crack zone, (ii) the adhesion between opposing crack surfaces, and (iii) molecular diffusion across the crack interface, which gradually restores structural continuity [2,3,11]. Qiu [3] highlighted the importance of these mechanisms in the development of a fundamental understanding of healing, while Bhasin et al. [11] proposed frameworks to quantify the extent of recovery based on measurable material properties.

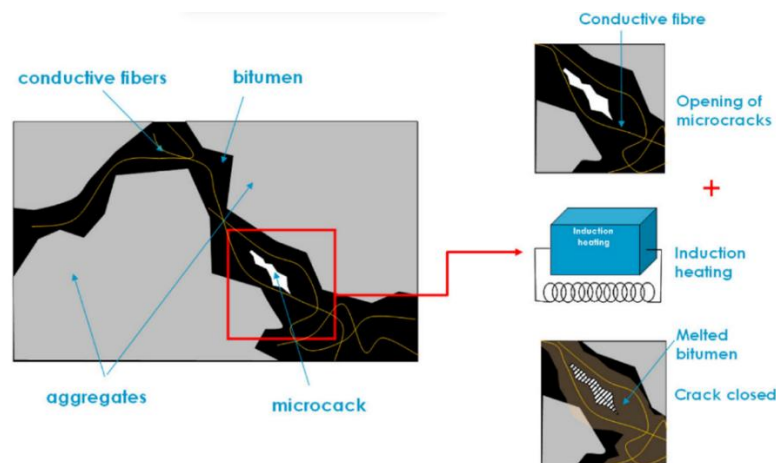


Figure 1.1.1 - Self-healing mechanism in bituminous binders

* Figure 1. Adapted from "Concept of self-healing in asphalt using encapsulated rejuvenators" in *Synthesis and Characterization of Alginate-Based Capsules Containing Waste Cooking Oil for Asphalt Self-Healing*

Although complete recovery of the original mechanical state is rarely possible, even partial healing has significant engineering value. Research has consistently shown that the ability of binders and mixtures to heal micro-damage extends pavement life, reduces the rate of crack propagation, and delays costly maintenance interventions [7,13].

In flexible pavements, fatigue cracking is one of the most critical modes of distress, often determining the end of service life. Fatigue is induced by the repeated application of traffic loads, which cause the accumulation of damage even when stress levels remain below the binder's ultimate strength [4,5,9]. The process begins with the nucleation of micro-cracks, typically at the bottom of the asphalt layers where tensile stresses are concentrated. These cracks propagate with successive loading cycles, eventually forming interconnected networks recognized as *alligator cracking* (Fig. 2) [6].

The significance of fatigue in pavement deterioration has been widely reported in the literature. Di Benedetto et al. [5] described fatigue as a progressive process in which the material gradually loses its load-bearing capacity. Collop and Cebon [9], through theoretical modelling, demonstrated how repeated load applications—even below conventional failure thresholds—could lead to long-term crack growth. To address this, Carpenter and Shen [6] introduced the concept of a fatigue endurance limit, a threshold strain level below which micro-damage does not accumulate. However, in practice, traffic loads, temperature fluctuations, and aging often push pavements beyond this limit, making fatigue cracking inevitable without mechanisms such as healing.

Self-healing plays a crucial role in mitigating fatigue. When traffic is discontinuous—as in periods of low traffic volume or at night—micro-cracks may partially close and the binder may regain part of its structural capacity (Fig. 1). Laboratory studies confirm that introducing rest periods in fatigue loading significantly extends binder and mixture life [7,8]. Liu et al. [8] demonstrated that both temperature and rest time are critical factors in determining healing efficiency, highlighting that binders recover more effectively at intermediate service temperatures and under longer rest durations.



Figure 1.1.2 - Medium severity alligator cracking.

The interaction between fatigue and self-healing is highly dependent on both external conditions and intrinsic binder properties. Externally, temperature, loading frequency, and rest periods are decisive [7,8]. For instance, higher service temperatures enhance molecular mobility, thereby accelerating healing, whereas colder temperatures restrict binder flow and reduce recovery potential. Similarly, longer rest periods between load cycles allow for greater healing, while continuous heavy traffic limits the opportunity for recovery.

Intrinsic material properties are equally important. Binder composition, polarity, and modification strongly influence its ability to resist fatigue and recover from damage [2,10]. Mazzoni [10] highlighted the interplay between fatigue, self-healing, and *thixotropy* in bituminous mastics, stressing that structural changes in the binder during rest can be mistakenly interpreted as healing if not properly distinguished. This underlines the importance of accurate experimental methodologies to isolate true healing effects.

Over the past decades, various modification strategies have been employed to improve both fatigue resistance and healing potential. Polymers, such as SBS (styrene-butadiene-styrene), are known to enhance elasticity and crack-bridging capacity, thereby improving durability and healing efficiency [14,15]. More recently, attention has shifted towards the use of recycled plastics as modifiers, motivated not only by performance enhancement but also by sustainability considerations. Giustozzi and colleagues [21,22] demonstrated that incorporating recycled plastics into binders can

improve mechanical properties while simultaneously reducing environmental impacts by valorizing waste streams.

In the broader context of bituminous binder modification, numerous studies have explored the mechanical enhancement and self-healing potential introduced by polymeric and plastic-based additives [1,14,15,21,22]. Conventional polymer modifiers such as styrene–butadiene–styrene (SBS) have long been employed to improve elasticity, fatigue resistance, and temperature susceptibility. More recently, increasing attention has been directed toward the utilization of recycled plastic wastes as alternative modifiers, providing both mechanical improvement and environmental benefit.

Building on these developments, the present research compares several binder systems characterized by different modification approaches and additive concentrations. The analysis includes both previously investigated reference materials and newly prepared RLDP-modified binders, allowing a direct evaluation of the effects of recycled plastic addition on fatigue resistance and healing behaviour. The binder systems considered are the following:

- Neat 50/70 penetration grade binder: representing the unmodified reference binder, commonly used as a control material in rheological investigations.
- RLDP-modified binder (2% additive by total mass): newly prepared within this study to investigate the influence of a low recycled plastic concentration on viscoelastic and self-healing characteristics.
- RLDP-modified binder (4% additive by total mass): also prepared in this research, representing a higher dosage intended to examine concentration-dependent changes in stiffness, fatigue response, and recovery efficiency.

The datasets corresponding to the Neat 50/70 binder were made available from the experimental work of MSc student N. Fatlavi, carried out during a previous research phase. These results serve as benchmark references for comparative evaluation. The current thesis extends that work by focusing on the preparation, rheological testing, and performance analysis of the 2% and 4% RLDP-modified binders, enabling a

critical comparison between conventional, commercial, and recycled-plastic modification strategies.

Through this approach, the study not only verifies the consistency of recycled plastic performance against established polymer systems but also identifies potential advantages and limitations associated with increasing RLDP content. This comparative framework strengthens the scientific basis for employing recycled low-density plastics as sustainable modifiers in asphalt technology, bridging the gap between traditional polymer modification and circular-material innovation in bituminous binder engineering.

This comparison is motivated by the dual objective of performance improvement and sustainability. On the one hand, it seeks to clarify how polymeric and plastic additives influence the fundamental mechanisms of fatigue and healing at the binder scale. On the other, it addresses the growing demand for environmentally responsible materials in road construction. By combining rheological testing, fatigue protocols, and healing assessment, the study aims to provide new insights into how neat, plastic-modified, and RLDP-modified binders perform under cyclic loading and rest, and how they contribute to the overall durability of asphalt pavements [1,2,21,22].

1.2 Characterization of Self-Healing

While the concept of self-healing in asphalt binders is well recognized, its quantification and characterization remain complex. The main difficulty arises because several time-dependent phenomena, such as *thixotropy* and steric *hardening*, may produce apparent increases in stiffness or modulus during rest, which can be mistakenly interpreted as healing [10,19]. Mazzoni [10] highlighted that bituminous mastics show significant structural rebuilding during rest, while Santagata et al. [19] demonstrated that steric hardening alone can account for a substantial portion of the recovery observed in conventional tests. This makes it crucial to distinguish between true healing, which involves micro-crack closure and molecular diffusion, and pseudo-healing, which is only reversible stiffening unrelated to damage recovery. For this reason, researchers have developed specialized testing protocols and

analytical frameworks to accurately capture the genuine contribution of healing [1,16].

Self-healing in binders is generally considered a multi-step process. First, binder flow allows the damaged material to refill micro-cracks. Second, adhesion re-establishes contact between opposing crack surfaces. Finally, molecular diffusion occurs across the interface, restoring structural continuity [2,3,11]. Each step is strongly influenced by the material's viscoelastic balance and its chemical composition.

Indicators used to characterize healing include:

- Stiffness recovery (through dynamic shear rheometry),
- Reduction in crack growth rate (observed under repeated loading),
- Extension of fatigue life when rest periods are introduced into cyclic loading [7,8,11].

Qiu [3] emphasized the importance of time and temperature in enabling molecular diffusion, while Liu et al. [8] identified optimal healing temperatures and rest durations at which recovery efficiency is maximized. These findings highlight the necessity of tailoring test conditions to simulate realistic service environments.

Binder type and modification strongly affect healing capacity. Neat binders such as 50/70 penetration grade show a natural but limited ability to heal [12]. Polymer modification, especially using SBS, has been shown to improve healing due to enhanced elasticity and better crack-bridging behaviour [14,15]. Tabakovic and Schlangen [13] further confirmed that engineered self-healing systems, including encapsulated rejuvenators, can extend binder performance by repeatedly restoring mechanical integrity.

More recently, research has explored the use of recycled plastics as modifiers, not only for their mechanical benefits but also for their environmental contribution. Giustozzi and Nizamuddin [21] [22] reported that road-grade recycled plastics can enhance both stiffness and fatigue resistance while aligning with circular economy goals. These findings support the hypothesis that recycled low-density plastic (RLDP)

could positively influence the healing capacity of binders by increasing molecular mobility and improving viscoelastic behaviour.

Given the complexity of isolating healing effects, international efforts have been made to standardize testing procedures. The *RILEM TC 278-CHA committee* [16] has proposed methodological frameworks to evaluate binder self-healing, stressing the need to control for steric hardening and nonlinear effects. Baglieri et al. [24] also highlighted how *nonlinearity* and *thixotropy* affect LAS-based healing evaluations, underlining the need for careful interpretation of test results. Ultimately, accurate characterization requires combining laboratory experiments with analytical models to ensure that healing is not overestimated and to provide results that can be translated into pavement design.

In this thesis, the characterization of self-healing behaviour is conducted through the analysis of three binder systems: neat 50/70, and RLDP-modified binders with 2 %, and 4 % of total binder mass. Among these, the 2 % and 4 % RLDP binders were prepared and experimentally analysed within this research, while the neat 50/70 binder were provided from previous Master's-level work and used as reference datasets for comparison. The experimental design explicitly considers steric hardening effects through the implementation of LAS-SH control protocols, ensuring that the observed recovery in mechanical properties is attributed to genuine self-healing phenomena rather than structural stiffening.

By integrating advanced rheological testing—Frequency Sweep (FS), Linear Amplitude Sweep (LAS), and LAS-based Healing (LASH)—with analytical modelling approaches, this thesis provides a reliable quantification of the healing capacity of RLDP-modified binders, distinguishing true molecular recovery from other time-dependent effects. This methodological rigor is necessary to answer the central research question: Can recycled plastics not only reinforce asphalt binders but also enhance their natural self-healing ability? The outcome of this characterization will serve as the foundation for comparing binder systems in terms of both durability and sustainability [1,2,16,21,22].

1.3 Protocols for Healing Evaluation

Despite decades of research, one of the most significant challenges in the study of asphalt binders remains the quantification of self-healing. Unlike properties such as viscosity or stiffness, healing does not have a direct measurable parameter. Instead, it manifests indirectly through recovery of modulus, delay in crack propagation, or extension of fatigue life [1,2]. As a result, different researchers have relied on diverse test protocols, each capturing a specific aspect of the healing process.

A further complication arises from the fact that healing often overlaps with other time-dependent processes such as *thixotropy* and *steric hardening* [10,19]. If these are not properly controlled, results may overestimate the actual healing contribution. Thus, modern approaches focus on test designs that allow clear separation between reversible structural stiffening and true damage recovery [16,24].

Early studies evaluated healing by comparing fatigue tests with and without rest periods, observing the relative increase in fatigue life [7,9]. While useful, such approaches lacked precision and often failed to isolate steric hardening. Recent developments have introduced more sophisticated methods using Dynamic Shear Rheometer (DSR) protocols, which allow precise control of strain, stress, and temperature.

Key protocols include:

1. Time Sweep (TS):
 - Involves applying cyclic loading at constant strain or stress for a defined period, followed by a rest interval, and then reloading.
 - Healing efficiency is calculated by comparing the recovery in modulus or phase angle after rest [25].
 - Limitations: TS tests are time-consuming and may still include steric hardening effects if not corrected.
2. Linear Amplitude Sweep (LAS):
 - Standardized in AASHTO TP101-14 [18] and AASHTO T391-20 [23], LAS applies strain-controlled cyclic loading with gradually increasing amplitude until failure.

- Healing is not directly assessed, but LAS provides baseline fatigue performance necessary for comparison with healing-modified protocols.
3. LAS with Healing (LASH):
- A modification of LAS where rest periods are introduced at predetermined damage levels (e.g., 25%, 50%, or 75% of fatigue life).
 - Recovery is quantified by comparing post-rest fatigue response with the expected response without rest [18].
 - Liu et al. [8] demonstrated how healing efficiency depends strongly on rest duration and temperature, confirming the sensitivity of this protocol to realistic service conditions.
4. LAS with Steric Hardening Control (LAS-SH):
- Proposed to explicitly account for stiffening not caused by healing. A “control” LAS test with rest but without prior damage is performed, isolating steric hardening contributions [19,24].
 - Subtracting steric hardening from total recovery yields the true healing component.

The need for standardized healing protocols has been highlighted by international efforts such as the *RILEM TC 278-CHA committee* [16]. Their work emphasizes that reliable healing evaluation requires:

- Integration of fatigue and healing protocols within a unified framework,
- Explicit consideration of *steric hardening* and *thixotropy*,
- Testing conditions representative of field environments (temperature, load frequency, rest periods).

This thesis adopts a *multi-protocol strategy* to evaluate the healing potential of neat, and RLDP-modified binders. The approach integrates:

- Frequency Sweep (FS): to establish master curves and viscoelastic behaviour [17],
- LAS and LASH: to measure fatigue life and healing efficiency under controlled loading [18,23],

- LAS-SH: to isolate steric hardening and ensure healing is not overestimated [19],

By applying this comprehensive methodology, the thesis aims to deliver a rigorous and unbiased assessment of healing capacity. The comparison across neat, and RLDP-modified binders will clarify whether waste-derived additives can improve not only binder stiffness and fatigue life, but also the fundamental self-healing mechanisms that govern long-term pavement durability [1,2,21,22].

1.4. Plastic Waste and Its Application in Asphalt Pavements

The rapid urbanization and industrial expansion of recent decades have led to an exponential increase in global plastic production. According to Giustozzi and Nizamuddin (2022) [21], more than 400 million tonnes of plastic are produced annually worldwide, with a significant portion classified as non-recyclable or difficult-to-process waste. Traditional disposal practices, such as landfilling and incineration, have proven inadequate and environmentally harmful, leading to severe pollution of soils, waterways, and marine ecosystems. Consequently, finding sustainable and large-scale reuse pathways for waste plastics has become an urgent global priority.



Figure 1.4.1 - Plastic waste in worldwide.

In this context, pavement engineering presents a promising opportunity to repurpose plastic waste in a circular and sustainable manner. Asphalt pavements, which already

consume millions of tonnes of materials annually, provide an ideal platform for large-scale waste reutilization. By integrating waste plastics into asphalt, it is possible to not only enhance pavement durability but also reduce the environmental footprint of road construction, aligning with the United Nations' Sustainable Development Goals (SDGs) — particularly those targeting responsible consumption, innovation, and climate action.

The use of plastic waste in asphalt materials contributes to sustainability in multiple ways:

- 1) Waste reduction: diverts significant volumes of non-recyclable plastics from landfills and the environment.
- 2) Material efficiency: decreases the reliance on virgin bitumen and synthetic polymers, reducing fossil fuel demand.
- 3) Extended pavement life: leads to fewer maintenance cycles, lowering overall CO₂ emissions from reconstruction.
- 4) Circular economy integration: transforms waste materials into valuable infrastructure resources.

From a materials-engineering perspective, plastic additives offer thermoplastic and viscoelastic properties that can improve stiffness, rutting resistance, and fatigue performance of bituminous mixtures when properly blended [21,22]. Depending on the blending technique, these materials can act as reinforcing polymers or as fillers improving the microstructure of the binder matrix.

Two primary incorporation techniques exist: the dry process and the wet process.

In the dry process, plastic particles are mixed with hot aggregates before binder addition. The plastic partially melts, coating aggregate surfaces and improving cohesion. This process is simple and cost-effective, making it popular in developing countries.

In the wet process, the plastic is melted and blended directly into the binder using high-shear mixing at elevated temperatures. This method achieves better dispersion

and stronger interaction between the bitumen and polymer phases, but it requires stricter temperature control and specialized equipment.

Recent research [22] highlights that road-grade recycled plastics — such as polyethylene (PE), polypropylene (PP), and polyethylene terephthalate (PET) — can significantly enhance binder rheology when used appropriately. Among these, Recycled Low-Density Polyethylene (RLDP) has proven particularly suitable due to its relatively low melting temperature, high ductility, and chemical compatibility with bitumen. Optimal dosages typically range between 2% and 4%, where mechanical improvements are achieved without excessive increases in viscosity, ensuring good workability during mixing and compaction.

Despite the potential benefits, several challenges remain: the heterogeneity of waste plastics, variation in melting behaviour, and uncertainty regarding long-term ageing and recyclability of modified asphalt. Giustozzi et al. (2022) [22] emphasize that not all plastics are suitable for direct binder modification and that specific formulations initially designed for the dry method may behave differently when used in the wet process.



Figure 1.4.2 - Iterchimica Superplast Polymers.

In this study, the SUPERPLAST ECO additive — a patented polymeric compound by Iterchimica S.p.A. — was selected to evaluate this hypothesis. Although originally designed for dry modification, it was experimentally tested using the wet blending method to explore its potential when directly incorporated into the bituminous binder. This approach represents an innovative application, combining sustainability

objectives with advanced rheological characterization. The goal is to determine whether recycled plastic additives, when blended at the molecular level, can effectively contribute to fatigue resistance and self-healing properties, thereby extending pavement lifespan.

Overall, the integration of recycled plastics into asphalt pavements demonstrates how waste valorization and sustainable engineering can work hand in hand. This approach not only mitigates one of the most pressing environmental issues of our time — plastic waste accumulation — but also contributes to resource-efficient, low-carbon, and long-lasting pavement solutions. Such advancements mark a significant step toward the development of green infrastructure systems that support circular economy principles and the long-term sustainability of the road construction industry [21,22].

CHAPTER 2 – RESEARCH-BASED PROJECT

2.1 Instrumentation

The experimental activities conducted in this study required a combination of *mixing* and *rheological testing instruments*. The instrumentation was selected to ensure high precision, repeatability, and compliance with relevant European and AASHTO standards.

The laboratory workflow was divided into two primary stages:

1. *Preparation of modified binders*, where a *high-shear mixer* and related devices were used to achieve a homogeneous dispersion of plastic and RLDP (Recycled Low-Density Plastic) additives within the bitumen.
2. *Rheological testing*, where a *Dynamic Shear Rheometer (DSR)* was employed to evaluate the linear and nonlinear viscoelastic characteristics of the binders through Frequency Sweep (FS), Linear Amplitude Sweep (LAS), LAS with Healing (LASH), and LAS with Steric Hardening Control (LAS-SH) protocols.

The use of precise and calibrated instrumentation was crucial to ensure that the rheological results could be meaningfully correlated with the physical modification processes.

2.1.1 Mixing Procedure Equipment

The first stage of the research involved the preparation of modified binders incorporating plastic and RLDP additives. The aim was to obtain a stable and uniform dispersion of these materials in the neat 50/70 base binder, ensuring reproducible rheological behaviour in subsequent testing.

High-Shear Mixer

A high-shear mixer (Silverson model L5M-A) capable of rotational speeds up to 5000 rpm was used to promote efficient blending between the bituminous matrix and the polymeric modifiers. The device is equipped with a digital heating system, allowing simultaneous control of temperature and shear rate during the mixing process. The

high shearing action breaks down polymer agglomerates and ensures a fine distribution of plastic particles throughout the binder, preventing phase separation and guaranteeing the homogeneity of the final product [21,22].



Figure 2.1.1.1 - High-Shear Mixer: Operated up to 5000 RPM by Silverson model L5M-A

Convection Oven

A convection oven was employed to preheat both the neat binder and additive materials prior to mixing. The oven was maintained at a constant temperature of 185 ± 2 °C, in accordance with EN 12594, to ensure proper fluidity of the binder and prevent premature thermal degradation. Pre-conditioning of materials at a stable temperature also improves mixing consistency and repeatability between samples [23].

Precision Balance

All materials were weighed using a precision analytical balance with a sensitivity of ± 0.01 g. This level of accuracy was essential for maintaining the required additive proportions (2% and 4% by total mass of binder) and ensuring consistency between different mix formulations [23].

Temperature Monitoring Devices

Continuous temperature control was maintained throughout the mixing process using thermocouples and infrared sensors, allowing real-time tracking of the binder temperature. This monitoring ensured that the mixing temperature remained stable,

preventing overheating or localized polymer degradation that could compromise binder properties [23].

Silicone Moulds and Storage Containers

After mixing, the binders were poured into silicone moulds and left to cool under controlled laboratory conditions. Once solidified, the specimens were stored in airtight aluminum containers to minimize oxidation and aging prior to rheological testing. These storage procedures ensured consistent binder conditions across all tests and prevented the formation of surface skins or volatiles that might alter the material's rheological response.

2.1.2 Rheology Test Equipment

Dynamic Shear Rheometer (DSR)

The Dynamic Shear Rheometer (DSR) represents the principal instrument used in this research for evaluating the rheological, viscoelastic, and fatigue–healing behaviour of the tested bituminous binders. This equipment allows the application of a sinusoidal shear load under controlled stress or strain, while precisely maintaining the sample temperature. The DSR provides quantitative measurements of the complex shear modulus ($|G^*|$) and phase angle (δ), two fundamental parameters that describe the ability of the binder to resist deformation and recover its original structure. These parameters define the binder's viscoelastic nature, allowing the distinction between the elastic (recoverable) and viscous (irreversible) components of its mechanical response [17,18,26].



Figure 2.1.2.1 - Dynamic Shear Rheometer (DSR), Physica MCR 302, Anton Paar

The DSR used in this study is a controlled-strain rheometer equipped with parallel-plate geometry, typically 8 mm and 25 mm in diameter, selected according to the binder stiffness and testing temperature. The gap between the plates was adjusted within the range of 1.0 to 2.0 mm, ensuring a uniform stress distribution across the specimen.



Figure 2.1.2.2 - Measuring system. Plate- 8 mm.

To maintain accurate temperature control, the DSR includes a Peltier temperature-regulated chamber capable of operating between -10°C and 100°C . This precision allows simulation of both field-representative low-temperature conditions and high-temperature service behaviour. The binder sample is preheated, poured between the plates, and trimmed to the proper geometry before testing. The upper plate oscillates sinusoidally, imposing a shear strain (γ) or stress (τ), while the rheometer measures the corresponding response.

The instrument calibration was carried out before each testing session following the manufacturer's recommendations and the guidelines of AASHTO T315 [17]. The calibration includes torque and normal force checks, plate alignment, and verification of the phase angle accuracy using standard silicone oil samples.

To ensure measurement precision, all tests were performed using freshly prepared binder samples, conditioned for 15–30 minutes at testing temperature before initiation. The applied strain amplitudes were kept below the LVE limit (previously determined through amplitude sweeps) to avoid premature structural damage during FS tests.

Torque limits, temperature stability, and strain control were continuously monitored by the rheometer's feedback system. The DSR's sensitivity allowed the detection of subtle variations in modulus and phase angle, crucial for identifying transitions between elastic, viscoelastic, and viscous domains. Each test was repeated at least three times per binder type to verify reproducibility. Data were post-processed using the instrument's proprietary software and exported for further analysis and modelling in Excel.

The Dynamic Shear Rheometer served as the central analytical instrument linking the microstructural effects of binder modification with macroscopic rheological response. Through the systematic use of FS, LAS, LASH, and LAS-SH protocols, the DSR enabled a comprehensive understanding of:

- The temperature–frequency dependence of binder stiffness;
- The transition between linear and nonlinear viscoelastic regimes;
- The fatigue–healing balance influenced by plastic and RLDP modifiers.

This multi-layered rheological characterization allowed the identification of performance improvements due to recycled additives and provided the quantitative basis for comparing neat, plastic-modified, and RLDP-modified binders under controlled laboratory conditions [21–26].

2.2 Mixing Procedure

The preparation of the RLDP-modified binders was carried out following a controlled wet-mixing protocol, specifically designed to ensure uniform dispersion of the plastic additive within the bituminous matrix while preserving the thermal stability of both components. The entire procedure was conducted in a temperature-controlled environment to minimize the risk of overheating, oxidation, or premature degradation of the polymeric phase.

Pre-Heating of the Binder

Prior to mixing, the neat 50/70 penetration-grade binder was pre-heated in a convection oven at 185 ± 2 °C for approximately 1.5 hours to ensure complete fluidity

and eliminate any residual moisture. After this initial conditioning, approximately 551 g for 2% and 521 g for 4% of the binder was transferred into a metallic container, which was subsequently placed back into the oven and maintained at the same temperature for an additional 30 minutes. This step allowed for uniform temperature distribution throughout the binder volume, ensuring stable viscosity and facilitating proper incorporation of the RLDP additive during mixing.

Weighing and Conditioning of Additives

The Recycled Low-Density Plastic (RLDP) additive, supplied in granular form as SUPERPLAST ECO (Iterchimica S.p.A.), was weighed using a high-precision analytical balance with an accuracy of ± 0.01 g. The amount of additive was calculated according to the target modification level 2 % or 4 % of the total binder mass. For the 2 % formulation, approximately 11.0 g of RLDP was used, while 20.88 g was used for the 4 % formulation.

To improve handling and reduce electrostatic adhesion between pellets, the RLDP granules were gently pre-heated to approximately 40 °C prior to mixing. This pre-conditioning step ensured smoother feeding into the molten binder and prevented the formation of clusters that could hinder homogeneity during the blending phase.

High-Shear Mixing

The actual blending process was conducted using a Silverson L5M-A high-shear mixer, pre-heated for about five minutes to stabilize the working chamber temperature. The metallic container with the molten binder was placed into the mixer assembly, and the temperature was maintained between 170 °C and 180 °C throughout the entire operation.

Mixing was performed at a constant rotational speed of 5000 revolutions per minute (RPM) for a total duration of 25 minutes. The RLDP pellets were introduced gradually during the first 10 minutes of mixing to ensure their progressive melting and uniform dispersion within the bitumen matrix, avoiding the formation of unmelted agglomerates or local over-shearing. During the process, the temperature was monitored every 3 minutes using a thermocouple probe to ensure consistency within

the target range; adjustments were made when necessary, by reducing or increasing the heating intensity.

The high-shear mixing process promotes mechanical dispersion and partial dissolution of the plastic particles within the binder, resulting in a stable and homogeneous blend. This is a critical step for the wet modification method, as uniformity of the polymer distribution directly influences the resulting binder's rheological and self-healing performance.

Post-Mixing Handling and Homogeneity Verification

Immediately after completion of the mixing stage, the hot binder was manually stirred with a pre-heated stainless-steel spatula to visually assess its homogeneity and to break any residual air bubbles or superficial films formed during agitation. The resulting mixture was observed to exhibit a smooth, viscous consistency, indicating satisfactory polymer dispersion. Subsequently, the binder was allowed to rest for approximately five minutes before casting, allowing entrapped air to escape naturally.



Figure 2.2.1 – Mixed binder with RLD-plastic.

Casting and Conditioning of Specimens

Following the mixing phase, the binders were cast into silicone moulds of rectangular geometry (approximately $80 \times 20 \times 5$ mm). These dimensions were selected to

facilitate consistent specimen preparation for subsequent rheological testing. The moulds were left to cool under ambient laboratory conditions until the surface layer began to solidify, after which they were transferred into a refrigeration chamber maintained at 5 ± 1 °C for a minimum of two hours. This controlled cooling phase ensured gradual solidification of the binder and minimized the presence of thermal stresses or internal voids.



Figure 2.2.2 - Preparation of bituminous beams.

After solidification, the specimens were carefully demoulded and stored in sealed aluminium containers to prevent oxidation and contamination prior to rheological testing. All samples were labelled with their respective compositions and stored in a dark, temperature-stable environment until the initiation of the experimental campaign.

2.3 Materials

Bituminous Binders

This research investigates three different bituminous binders, representing a progressive range of modification strategies—from conventional polymer modification to innovative sustainable solutions using recycled plastics. Each binder was characterized in terms of its viscoelastic and fatigue–healing behaviour. One of the binders (Neat 50/70) were adopted from the experimental work of MSc student N. Fatlavi, while two binders (RLDP 2% and RLDP 4%) were prepared and tested within this thesis using the same experimental framework to ensure methodological consistency.

1. Neat 50/70 Penetration Grade Binder

The 50/70 penetration-grade binder was selected as the reference material due to its extensive use in European road construction and its well-documented rheological properties [12, 23]. This binder serves as the baseline for assessing how polymer and recycled-plastic modification affect viscoelastic and self-healing performance.

The corresponding dataset was obtained from the previous Master's research by N. Fatlavi, ensuring continuity with prior investigations.

2. RLDP-Modified Binder (2 % Recycled Low-Density Plastic)

The 2 % RLDP-modified binder was prepared and tested within this thesis, representing the lower concentration of recycled plastic modification. It was produced by incorporating approximately 11.0 g of SUPERPLAST ECO into 551 g of 50/70 binder using the wet blending method. This dosage was selected to determine the minimum RLDP concentration capable of improving viscoelastic and healing properties without adversely affecting binder workability.

3. RLDP-Modified Binder (4 % Recycled Low-Density Plastic)

The 4 % RLDP-modified binder was also prepared and investigated within this thesis, following the same wet mixing procedure used for the 2 % formulation. Here, 20.88 g of SUPERPLAST ECO was blended with 522 g of 50/70 binder under controlled temperature and shear conditions. This higher concentration was selected to evaluate the effects of increased RLDP dosage on stiffness, fatigue resistance, and self-healing capacity, and to identify the potential threshold at which excessive hardening could reduce the material's ductility or healing ability. Both binders (2 % and 4 %) underwent identical pre-heating, blending, and cooling protocols to ensure homogeneity and repeatability.

Plastic Additive: SUPERPLAST ECO

The SUPERPLAST ECO additive used in this research is a patented polymeric compound developed by Iterchimica S.p.A. (Italy) to enable the valorisation of non-recyclable plastics within road construction materials [21, 22]. The additive consists of techno-selected recycled plastics engineered to enhance bitumen stiffness,

deformation resistance, and fatigue performance, while promoting circular-economy principles.

Although SUPERPLAST ECO is primarily designed for use in the *dry modification* process—where plastic is blended with aggregates before binder addition — this study explores its experimental application in the *wet modification* process. The objective is to assess its compatibility and performance when directly incorporated into the bituminous binder phase.



Figure 2.3.1 - A – Cutted plastic pallets; B – Plastic pallets.

According to the manufacturer's technical data sheet, the main physical characteristics are:

- Form: Granular, light grey;
- Density: 0.40–0.60 g/cm³;
- Softening point: 160–180 °C;
- Recommended dosage: 4–10 % by binder mass (depending on the desired mechanical properties).

In this study, dosages of 2 %, and 4 % were selected to examine the influence of increasing RLDP content on binder rheology and fatigue–healing behaviour. These concentrations were based on previous findings indicating that moderate plastic

dosages can improve performance while preserving workability and viscosity within acceptable limits [21, 22].

2.4 Sample Preparation

The preparation of binder specimens for rheological testing was carried out in accordance with the procedures outlined in EN 12594:2014 (Bitumen and bituminous binders – Preparation of test samples) and EN 14023:2010 (Polymer-modified bituminous binders – Specifications), with methodological adaptations derived from De Leonardis (2022) to accommodate the specific characteristics of the recycled plastic-modified binders investigated in this study. All operations were performed under controlled laboratory conditions to ensure consistency, accuracy, and reproducibility of results.

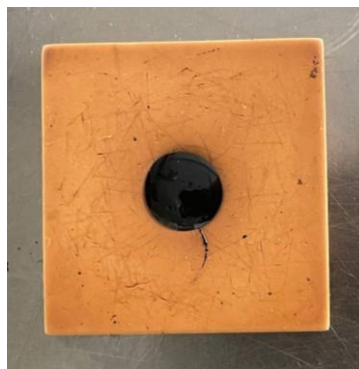


Figure 2.4.1 - Molded bituminous binder.

For each test performed with the Dynamic Shear Rheometer (DSR), approximately 0.230–0.250 g of binder material was required per specimen. After mixing and conditioning, the binders—neat, and RLDP-modified (2 %, and 4 %)—were first cast into rectangular strips using silicone moulds (approximately $80 \times 20 \times 5$ mm). Once solidified, these strips were manually cut into smaller fragments suitable for mounting onto the DSR testing plates. Each fragment was subsequently placed into circular silicone moulds having a diameter corresponding to that of the 8 mm parallel plates used in the rheometer. This step ensured consistent geometry and full compatibility between the specimen and the DSR testing configuration. The use of silicone moulds prevented adhesion during demoulding and maintained specimen integrity, thus

avoiding any distortion or air inclusion that might affect subsequent mechanical response measurements.

Proper thermal conditioning of binder specimens prior to rheological testing is essential to achieve adequate fluidity, facilitate mounting between the DSR plates, and ensure reproducibility across all binder types.

The pre-heating temperature and duration were tailored according to the material composition to reflect their distinct thermal sensitivities:

- Neat 50/70 binder: pre-heated at 130 °C for 5 minutes to reach the desired viscosity without promoting oxidation.
- RLDP-modified binders (2 %, and 4 %): pre-heated at a slightly higher temperature of 150 °C for 10 minutes, ensuring sufficient softening to allow proper placement and adhesion during the DSR setup phase.

Following the heating step, all samples were subjected to a two-stage cooling process:

- Ambient cooling at laboratory temperature for approximately 5 minutes to prevent thermal shock, and
- Refrigeration at 5 ± 1 °C for another 5 minutes to achieve a stable and uniform temperature throughout the sample before mechanical testing.

This dual-stage cooling regime was adopted to minimize the risk of uneven hardening or temperature gradients within the binder, both of which could influence rheological response during the initial loading cycles.

The rheological testing was conducted using a Dynamic Shear Rheometer (DSR) equipped with 8 mm parallel plates and an integrated Peltier environmental chamber for precise temperature control. To ensure optimal adhesion and minimize slippage during testing, the lower plate of the DSR was pre-heated to an appropriate adhesion temperature as 45 °C.

A pre-conditioned binder fragment was then carefully positioned on the centre of the lower plate using a pre-heated spatula. The upper plate was lowered slowly until a 2.1 mm gap was achieved, allowing the binder to spread uniformly across the testing area. Excess binder extruded from the edges was trimmed off immediately using the same pre-heated spatula to ensure a smooth and symmetrical specimen profile. Once the trimming was completed, the gap was further adjusted to 2.0 mm, corresponding to the final test geometry specified in EN 14770 (Bitumen and bituminous binders – Determination of complex shear modulus and phase angle using a dynamic shear rheometer).

The environmental chamber was then closed to maintain a stable test temperature, minimizing the influence of external air currents or humidity variations during thermal equilibration. The sample was left to equilibrate for several minutes until a uniform thermal condition across the specimen was reached.

The adopted procedure was designed to ensure maximum repeatability, minimal oxidation, and uniform geometry among all tested specimens.

In particular:

- Adhesion and Slippage Prevention:

The pre-heating of DSR plates promotes proper wetting of the binder surface, guaranteeing full contact between the binder and metal plates, thereby preventing sample slippage during oscillatory shear testing.

- Controlled Geometry and Thickness:

By adjusting the specimen thickness to precisely 2.0 mm, consistent stress distribution across all specimens was achieved, ensuring comparability of rheological parameters such as complex modulus (G^*) and phase angle (δ).

- Reduced Thermal Aging:

Short pre-heating times, combined with rapid stabilization at low temperature prior to testing, minimized oxidative aging and hardening of the binder—factors known to artificially increase stiffness and reduce the apparent healing potential.

This methodology, adapted from De Leonardis (2022) and refined to suit RLDP-modified binders, provided reliable sample integrity and repeatable conditions for both linear viscoelastic (LVE) and nonlinear fatigue–healing evaluations.

As a result, the prepared specimens were considered fully representative of the binder systems investigated and suitable for subsequent frequency sweep, LAS, and LASH testing procedures.

2.5 Methodological Approach

The methodological approach adopted in this thesis is designed to provide a comprehensive evaluation of fatigue and self-healing behaviour in bituminous binders, combining experimental protocols with analytical modelling. The procedure follows recent advances in binder characterization and aligns with international standards (EN, ASTM, AASHTO) and recommendations from RILEM TC CHA [16, 17, 18].

The methodology aims to:

1. Quantify the linear viscoelastic behaviour of neat, and RLDP-modified binders (2 %, and 4 %).
2. Characterize fatigue resistance under repeated loading conditions using the LAS test protocol [18, 25].
3. Evaluate healing efficiency by incorporating rest phases, distinguishing true recovery from steric hardening effects [16, 19, 24].
4. Compare the influence of binder modification (neat vs. RLDP 2 %, and 4 %) in terms of mechanical performance, durability, and sustainability [1, 21, 22].

This integrated approach ensures a complete understanding of the rheological, fatigue, and self-healing response of binders. By combining standardized testing procedures with advanced damage modelling, the methodology provides a reliable foundation for assessing how recycled low-density plastic modification affects the mechanical integrity and healing potential of bituminous binders.

2.5.1 Frequency Sweep Tests

The frequency-sweep (FS) test represents the cornerstone of the rheological characterization of bituminous binders, providing the parameters required to describe their linear-viscoelastic (LVE) behaviour. Within the framework of this study, FS testing was employed to quantify the complex shear modulus (G^*) and phase angle (δ) across a wide range of frequencies and temperatures, thereby defining the materials' stiffness and viscoelastic balance. The method conforms to the guidelines established by EN 14770, AASHTO T 315-12 [17], and the procedures adopted by De Leonardis (2022), with specific adjustments introduced to account for the modified rheological nature of RLDP-containing binders.

The FS test was selected as the principal tool for investigating the time- and temperature-dependent response of bituminous binders in the small-strain domain, where the material behaves linearly and the relationship between stress and strain remains proportional. By applying sinusoidal shear deformations of constant amplitude over a range of frequencies, it is possible to determine both the elastic (storage) component G' and the viscous (loss) component G'' of the complex modulus, expressed as:

$$G^* = \sqrt{(G')^2 + (G'')^2}$$

The phase angle (δ) quantifies the lag between stress and strain, indicating the material's relative viscous or elastic character. At higher temperatures or lower loading frequencies, viscous effects dominate (large δ), while at lower temperatures or higher frequencies, the material exhibits elastic-solid behaviour (small δ). These relationships are essential for interpreting the binder's ability to resist deformation under traffic loading and for predicting its fatigue and self-healing tendencies [2, 4, 16].

All rheological measurements were performed using a Dynamic Shear Rheometer (DSR) equipped with 8 mm parallel plates and an integrated Peltier environmental control chamber, allowing temperature regulation within ± 0.1 °C. The sample thickness was maintained at 2.0 mm, following the standard geometry used for intermediate-temperature characterization of binders [17].

A small strain amplitude of 0.1 % was selected to ensure that all tests were conducted within the linear-viscoelastic range, as previously verified through strain-sweep (amplitude-sweep) pre-tests. This condition guarantees that the measured responses reflect intrinsic material properties, unaffected by non-linear damage or structural rearrangements [5, 10, 20].

Temperature equilibration time was fixed at 10 minutes before each frequency step to guarantee uniform thermal distribution across the specimen.

The instrument's torque calibration and compliance corrections were verified before each testing session in accordance with the manufacturer's procedures.

Test Procedure

Each binder (Neat 50/70, RLDP 2 %, and 4 %) was tested over a temperature range from 4 °C to 34 °C, in increments of 6 °C, varying the angular frequency between 1 rad/s and 100 rad/s and the strain between 1% and 0.01% recording 19 points at each temperature. At every combination of temperature and frequency, the DSR recorded the complex modulus (G^*) and the phase angle (δ).

To ensure data reliability:

- Each measurement was repeated at least twice, and the average value was used for analysis.
- Deviations between repeated runs were kept below 5 % for both G^* and δ , in line with AASHTO T 315 precision limits.
- The binder surface was trimmed and cleaned after each test to avoid contamination or residue build-up between runs.

Master Curve Construction

The experimental results were processed to construct master curves of G^* versus reduced frequency using the time-temperature superposition principle (TTSP). The reference temperature (T_0) was set at 25 °C, as commonly adopted in previous

studies [1, 2, 3, 16]. The shift factors a_t were determined through the Williams–Landel–Ferry (WLF) model:

$$\log a_T = -\frac{C_1(T - T_0)}{C_2 + (T - T_0)}$$

where C_1 and C_2 are empirical constants dependent on the binder's molecular structure. The resulting master curves provided a continuous representation of the binder stiffness over a wide frequency domain equivalent to $10^{-4} - 10^4$ Hz, thus simulating traffic loading from slow-moving heavy vehicles to high-speed traffic conditions [7, 25].

The experimental data from the frequency-sweep tests were processed to construct master curves of the complex shear modulus (G^*) as a function of reduced frequency, representing the viscoelastic response of the binders over a wide range of loading conditions. To achieve this, the Christensen–Anderson (CA) model was adopted, which provides a physically based formulation for describing the linear viscoelastic (LVE) behaviour of bituminous binders [2, 5, 9, 25].

The CA model expresses the dependency of the complex modulus on frequency through the following relationship:

$$G^*(w) = G_g \left[1 + \left(\frac{w_0}{w} \right)^{\frac{\log 2}{R}} \right]^{-\frac{R}{\log 2}}$$

where:

- G_g is the glassy modulus, representing the upper asymptotic modulus at very high frequencies (elastic solid behaviour),
- w_c is the crossover frequency at which $|G^*|$ reaches half of its maximum value, corresponding to the onset of the transition between elastic and viscous behaviour,
- w is the angular frequency (rad/s).
- R describes the slope of the transition region between glassy and viscous states.

This model provides a continuous and smooth representation of the complex modulus over the full frequency domain, allowing extrapolation beyond the measured range.

It captures both the low-frequency viscous plateau and the high-frequency elastic limit, which are critical for characterizing the full relaxation spectrum of modified binders [5, 9].

The master curves were constructed by applying the time–temperature superposition principle (TTSP), using 20 °C as the reference temperature (T_0). Data at other temperatures were shifted horizontally along the frequency axis to form a continuous curve. The shift factors (a_t) were determined through curve fitting within the CA model framework, ensuring thermo-rheological consistency for both neat and modified binders.

The resulting master curves provided a detailed visualization of the temperature- and frequency-dependent stiffness behaviour of the binders, covering an equivalent frequency domain from 10^{-4} to 10^4 Hz. This range effectively simulates the deformation response of pavements under diverse traffic conditions—from slow heavy loads to rapid vehicle motion.

One of the objectives of the Frequency Sweep (FS) analysis was to determine the equirigidity temperature, i.e., the temperature at which the binder attains a specified level of stiffness, expressed by the complex shear modulus ($|G^*|$). In this study, two reference stiffness values—5 MPa and 35 MPa—were adopted, corresponding respectively to the softening and transition zones of binder behaviour under service conditions. The equirigidity temperatures were identified by interpolating the master curve of $|G^*|$ versus temperature obtained from the Christensen–Anderson (CA) model for each binder system (neat, and RLDP 2 %, 4 %).

This parameter provides a direct indication of the temperature sensitivity and performance grade of the binder:

- A lower temperature at 5 MPa reflects better flexibility and low-temperature crack resistance,
- Whereas a higher temperature at 35 MPa indicates improved stiffness and rutting resistance at high service temperatures.

The CA model thus enabled the quantification of differences in modulus evolution and temperature susceptibility between the five binders investigated (Neat 50/70, and RLDP at 2 %, and 4 %), providing a reliable foundation for the subsequent fatigue (LAS) and healing (LASH) analyses.

2.5.2 Linear Amplitude Sweep (LAS) Test – Fatigue Resistance

The Linear Amplitude Sweep (LAS) test was performed to evaluate the fatigue resistance of bituminous binders under cyclic loading, following the standardized procedure described in AASHTO TP 101 [18] and the experimental framework presented by De Leonardis (2022). This method enables the determination of the material's fatigue life (N_f) and the strain level at maximum shear stress, providing key input parameters for subsequent healing assessments (LASH tests).

The primary goal of the LAS test is to quantify the fatigue resistance of bituminous binders when subjected to repeated oscillatory shear deformation at increasing strain levels. It evaluates how quickly the material loses stiffness due to micro-damage accumulation and identifies the strain threshold that initiates structural failure.

A further key objective is to determine the strain amplitude corresponding to the maximum shear stress (γ_{\max}). This value represents the critical deformation level at which the binder transitions from a predominantly viscoelastic to a damage-dominated behaviour.

In this study, γ_{\max} derived from the LAS test was subsequently used as the reference strain input for the LAS-Healing (LASH) protocol, ensuring that the healing evaluation was performed under realistic and comparable stress conditions [16, 18, 19]. This dual purpose makes the LAS test fundamental both for fatigue characterization and for setting up healing experiments, providing a consistent methodological link between the two investigations [2, 5, 25].

All LAS tests were conducted using the Anton Paar MCR 301 DSR with 8 mm parallel plates and an environmental Peltier system ensuring temperature stability (± 0.1 °C). Samples were prepared according to the procedure outlined in Section 3.3,

maintaining a 2.0 mm gap and ensuring uniform adhesion between the binder and plates.

The test temperature was set at 15°C and 20°C, representative of intermediate pavement service conditions. Each sample was equilibrated for 10 minutes before testing to achieve uniform temperature distribution.

The LAS protocol consists of two sequential phases:

Phase 1 – Linear Viscoelastic Calibration

A 0.1 % strain amplitude oscillation at 10 rad/s was applied to define the undamaged reference modulus (G_0^*). This phase ensures that the material response is linear.

Phase 2 – Amplitude Sweep (Fatigue Loading)

In this phase, the strain amplitude was linearly increased from 0.1 % to 30 % over 3600 loading cycles at a frequency of 10 Hz.

The DSR continuously recorded the evolution of complex modulus (G^*), phase angle (δ), and shear stress as functions of time. The maximum shear stress point—corresponding to the transition from the stable to the damage regime—was automatically identified by the instrument software. This γ_{\max} value was later employed in the LAS-Healing tests, ensuring consistency between fatigue and healing evaluation procedures.

Each LAS test was repeated at least twice for every binder type, with results averaged to minimize variability. Deviations in G^* and δ between repetitions remained within ± 5 %, in line with AASHTO TP 101 precision limits. Instrument calibration was checked daily using the neat 50/70 binder, and the DSR plates were cleaned and reconditioned after every test to prevent residue accumulation or slippage.

2.5.2 LAS-Healing (LASH) Test – Evaluation of Healing Behaviour

The LAS-Healing (LASH) test represents the extension of the Linear Amplitude Sweep (LAS) procedure and was conducted to evaluate the self-healing capacity of bituminous binders after controlled damage. The methodology follows the principles

introduced by AASHTO TP 101 [18] and further developed by Santagata et al. (2013) and Baglieri et al. (2024) within the RILEM TC CHA framework [16, 19, 24, 25]. This approach allows the quantification of the binder's ability to recover stiffness after rest periods, separating true molecular healing effects from structural stiffening, known as steric hardening.

The LASH protocol was applied to the same five binders tested in the LAS phase: Neat 50/70, and RLDP-modified binders at 2 %, and 4 % additive content. Among these, the 2 % and 4 % RLDP binders were prepared and experimentally analysed within this thesis, while the remaining binders were used as reference datasets obtained from prior Master's research.

The main objective of the LASH test is to evaluate the intrinsic healing potential of binders following fatigue damage induced under controlled conditions. Unlike the LAS test, which focuses solely on fatigue resistance, the LASH protocol introduces rest periods between two loading stages to monitor the material's recovery in stiffness and phase response. The strain amplitude corresponding to the maximum shear stress (γ_{\max}), previously identified in the LAS test (Section 3.4.2), was adopted as the damage-inducing strain level for each binder. By using this critical value, the test ensures that the material is damaged to a comparable extent before the healing phase begins, providing a consistent basis for evaluating and comparing the healing efficiency (H) among binders [16, 18, 19].

All tests were performed using the same Anton Paar MCR 301 DSR with 8 mm parallel plates and a 2.0 mm gap, under strict temperature control (± 0.1 °C). Each binder specimen was conditioned at 15°C and 20°C, ensuring identical thermal conditions as in the LAS tests. The test consisted of three sequential phases, adapted from De Leonardis (2022) and recent RILEM CHA guidelines.

Phase 1 – Initial Loading (Damage Stage)

The binder was subjected to oscillatory shear at a constant strain amplitude equal to γ_{\max} (as obtained from LAS), with a frequency of 10 Hz. This phase continued until a predetermined level of damage was reached, typically defined by a 30 % reduction

in the initial complex modulus (G_0^*). This ensured comparable damage across all binders, allowing uniform conditions for subsequent healing analysis.

Phase 2 – Rest Period (Healing Stage)

After the first loading stage, the specimen was left undisturbed for 30 minutes at the same temperatures (15°C and 20°C). No external deformation was applied during this period, allowing the material to undergo molecular diffusion, flow, and reconnection at the micro-crack interfaces. This process is considered representative of field rest conditions, such as traffic interruptions or nighttime cooling cycles, during which self-healing can occur [2, 5, 16]. The temperature and plate positions were kept constant to prevent artefacts caused by thermal expansion or relaxation.

Phase 3 – Reloading (Post-Healing Stage)

After the rest period, the same oscillatory loading as in Phase 1 was reapplied under identical strain and frequency conditions. The recovered modulus and phase angle were recorded to quantify the degree of healing achieved by each binder.

In addition to the standard LAS-Healing protocol with a 30-minute rest period, a series of control tests without any rest interval was also performed, following the comparative approach proposed by De Leonardis (2022). In these tests, the two loading phases were executed consecutively under identical strain and frequency conditions, omitting the rest stage entirely. This configuration allowed direct evaluation of the effect of rest duration on the mechanical recovery of the binder. By comparing the results from the non-resting tests and those with a 30-minute rest, it was possible to distinguish the portion of modulus recovery attributable to true self-healing phenomena—such as molecular flow and crack closure—from that resulting from viscoelastic relaxation or reversible structural rearrangement. This comparison provided an essential reference for quantifying the net healing contribution, especially for RLDP-modified binders, where the interplay between polymer mobility and relaxation kinetics is particularly significant.

2.5.3 Steric Hardening Control Tests (LAS-SH)

The phenomenon of steric hardening (also referred to as physical or structural hardening) represents the time-dependent increase in stiffness of bituminous binders when kept at rest under constant temperature, in the absence of external loading. This effect arises from molecular reorientation, crystallization of waxes, and structural rearrangement within the colloidal bitumen system, rather than from true healing of fatigue-induced damage. To accurately quantify the self-healing capacity of binders in the LASH tests, it was therefore essential to conduct dedicated control tests to isolate and correct for the contribution of steric hardening [16, 19, 24].

The objective of the steric hardening control tests was to determine the extent to which binder stiffness naturally increases during rest periods, independent of prior mechanical loading. By quantifying this intrinsic stiffening, it becomes possible to differentiate between actual self-healing (due to crack closure and molecular diffusion) and physico-chemical recovery that occurs in undamaged samples. This distinction ensures that the healing efficiency (H) calculated from the LASH procedure truly represents damage recovery, not simple structural aging or reorganization [19, 24, 25].

The test design was adapted from Santagata et al. (2013) and De Leonardis (2022), following the same temperature and timing conditions as those used in the LASH experiments to allow direct comparison. The steric hardening control tests were performed on fresh, undamaged binder specimens, using the same Dynamic Shear Rheometer (DSR) setup adopted for LAS and LASH testing. Each binder type—Neat 50/70, and RLDP-modified (2 %, and 4 %)—was subjected to an identical thermal and temporal protocol to ensure consistency.

The procedure comprised the following steps:

- Initial Reference Measurement:

A small oscillatory strain of 0.1 % at 10 rad/s was then applied to measure the initial complex shear modulus (G_o^*), ensuring that the sample response remained within the linear viscoelastic range.

- Rest Period (No Loading):

The specimen was maintained at 15°C and 20°C for a 30-minute rest period, matching the duration and thermal conditions of the LASH test.

During this time, no mechanical loading or strain was applied; the sample remained between the plates with a constant gap of 2.0 mm, preventing moisture loss or oxidation.

- Post-Rest Measurement:

At the end of the rest phase, the same oscillatory shear (0.1 % strain, 10 rad/s) was reapplied to measure the new modulus, $G^*(\text{rest})$. The increase in modulus during the rest period reflects the steric or physical hardening that occurs naturally in the binder structure.

The tables below summarize the experimental program carried out in this research, including the types of tests performed, testing temperatures, rest periods, and the number of repetitions for each binder. The “Important values and feedbacks” column provides information on the convergence of the individual trials. Due to occasional measurement inconsistencies or machine-related errors, not all trials exhibited satisfactory convergence. To ensure the reliability of the results, statistical analyses—outlined in Chapter 3—were applied to identify and select only the consistent and representative trials for further evaluation and comparison.

For the LAS-H (Linear Amplitude Sweep-based Healing) tests, two trials were considered for each temperature and rest time, as all repetitions demonstrated satisfactory convergence. The tables therefore indicate which specific trials were deemed valid and included in the subsequent comparative analyses.

Material	Test	Temperature	Important values and feedbacks	Times to rest	Repetitions
Neat bindet 50/70 + 2% of RLDP by total mass of binder	Frequency Sweep Test (FS)	4-6-10-16-22-28-34 °C	-	-	trial 1
					trial 2
					trial 3
	Linear Amplitude Sweep Test (LAS) Resistance to fatigue	T=15°C	not converged	-	trial 1
			not converged		trial 2
			not converged		trial 3
			not converged		trial 4
			not converged		trial 5
			converged		trial 6
			not converged		trial 7
			converged		trial 8
			converged		trial 9
		T=20°C	not converged	-	trial 1
			not converged		trial 2
			not converged		trial 3
			converged		trial 4
			converged		trial 5
			converged		trial 6
	Linear Amplitude Sweep with Steric Hardening Test (LAS-SH)	T=15°C	not converged	30 min.	trial 1
			not converged		trial 2
			converged		trial 3
			converged		trial 4
		T=20°C	not converged	30 min.	trial 1
			converged		trial 2
			not converged		trial 3
			not converged		trial 4
			converged		trial 5
			converged		trial 6
	Linear Amplitude Sweep based Healing (LASH)	T=15°C	not converged	30 min.	trial 1
			not converged		trial 2
			converged		trial 3
			converged		trial 4
			converged		trial 5
			converged		trial 6
			converged	0 min.	trial 1
			converged		trial 2
		T=20°C	not converged	30 min.	trial 3
			not converged		trial 1
			not converged		trial 2
			converged		trial 3
			not converged		trial 4
			converged		trial 5
			not converged	0 min.	trial 1
			not converged		trial 2
			not converged		trial 3
			converged		trial 4
			converged		trial 5

Table 2.1 – Tests performed on PMB with 2% of RLDP.

Material	Test	Temperature	Important values and feedbacks	Times to rest	Repetitions
Neat bindet 50/70 + 4% of RLDP by total mass of binder	Frequency Sweep Test (FS)	4-6-10-16-22-28-34 °C	-	-	trial 1
					trial 2
					trial 3
	Linear Amplitude Sweep Test (LAS) Resistance to fatigue	T=15°C	converged	-	trial 1
			not converged		trial 2
			not converged		trial 3
			not converged		trial 4
			not converged		trial 5
			not converged		trial 6
			converged		trial 7
		T=20°C	converged	-	trial 1
			converged		trial 2
	Linear Amplitude Sweep with Steric Hardening Test (LAS-SH)	T=15°C	converged	30 min.	trial 1
			not converged		trial 2
			not converged		trial 3
			not converged		trial 4
			converged		trial 5
			converged		trial 6
		T=20°C	converged	30 min.	trial 1
			not converged		trial 2
			not converged		trial 3
			converged		trial 4
			not converged		trial 5
			converged		trial 6
	Linear Amplitude Sweep based Healing (LASH)	T=15°C	converged	30 min.	trial 1
			converged		trial 2
			converged		trial 3
			converged		trial 4
			converged	0 min.	trial 1
			converged		trial 2
			converged		trial 3
		T=20°C	not converged	30 min.	trial 1
			not converged		trial 2
			converged		trial 3
			converged		Trial 4
			converged	0 min.	trial 1
			converged		trial 2
			converged		trial 3

Table 2.2 – Tests performed on PMB with 4% of RLDP.

CHAPTER 3 – DATA ANALYSIS

This chapter presents the processing, analysis, and interpretation of the experimental data obtained from the rheological characterization of the two investigated binders: the RLDP-modified binders containing 2 %, and 4 % recycled low-density plastic, with respect to known results of the reference Neat 50/70. The aim is to integrate the results from the different testing protocols into a coherent framework describing the viscoelastic, fatigue, and healing behaviour of the materials.

In the first part, the results of the Frequency Sweep (FS) tests are processed and analysed to characterise the linear-viscoelastic (LVE) response of the binders. The data are shifted according to the time–temperature superposition principle, and the experimental curves are fitted using the Christensen–Anderson (CA) model to obtain the master curves of complex modulus and phase angle. From these curves, the fundamental viscoelastic parameters—such as stiffness, temperature susceptibility, and equirigidity temperatures (5 MPa and 35 MPa)—are determined, providing a reference basis for subsequent analyses.

The second part of the chapter focuses on the Linear Amplitude Sweep (LAS) tests, which enable evaluation of fatigue resistance. The LAS data are interpreted through the new model as comparing the results of LAS, LAS-H, and LAS-ST tests to identify the strain at maximum shear stress (γ_{\max}) and to quantify the relationship between applied strain and fatigue life. These parameters also serve as input for the following LAS-Healing (LASH) tests.

The next section presents the results of the LASH tests, aimed at assessing the self-healing capacity of the binders through controlled rest periods of 30 minutes, together with comparative tests conducted without rest time, in order to distinguish true healing from instantaneous viscoelastic recovery. The influence of steric hardening is evaluated separately through dedicated control tests, allowing correction of the measured recovery values and determination of the net healing efficiency.

Finally, the chapter introduces the integrated data analysis, combining the outcomes of FS, LAS, and LASH tests within the quantitative modelling framework. The discussion includes the construction of master curves, the computation of healing indices, and the investigation of non-linear effects on material integrity loss. Through this comprehensive approach, the chapter aims to establish clear correlations between binder composition, plastic modification level, and mechanical performance, providing insight into the rheological and self-healing mechanisms governing RLDP-modified bituminous binders.

3.1 Linear viscoelastic characterization

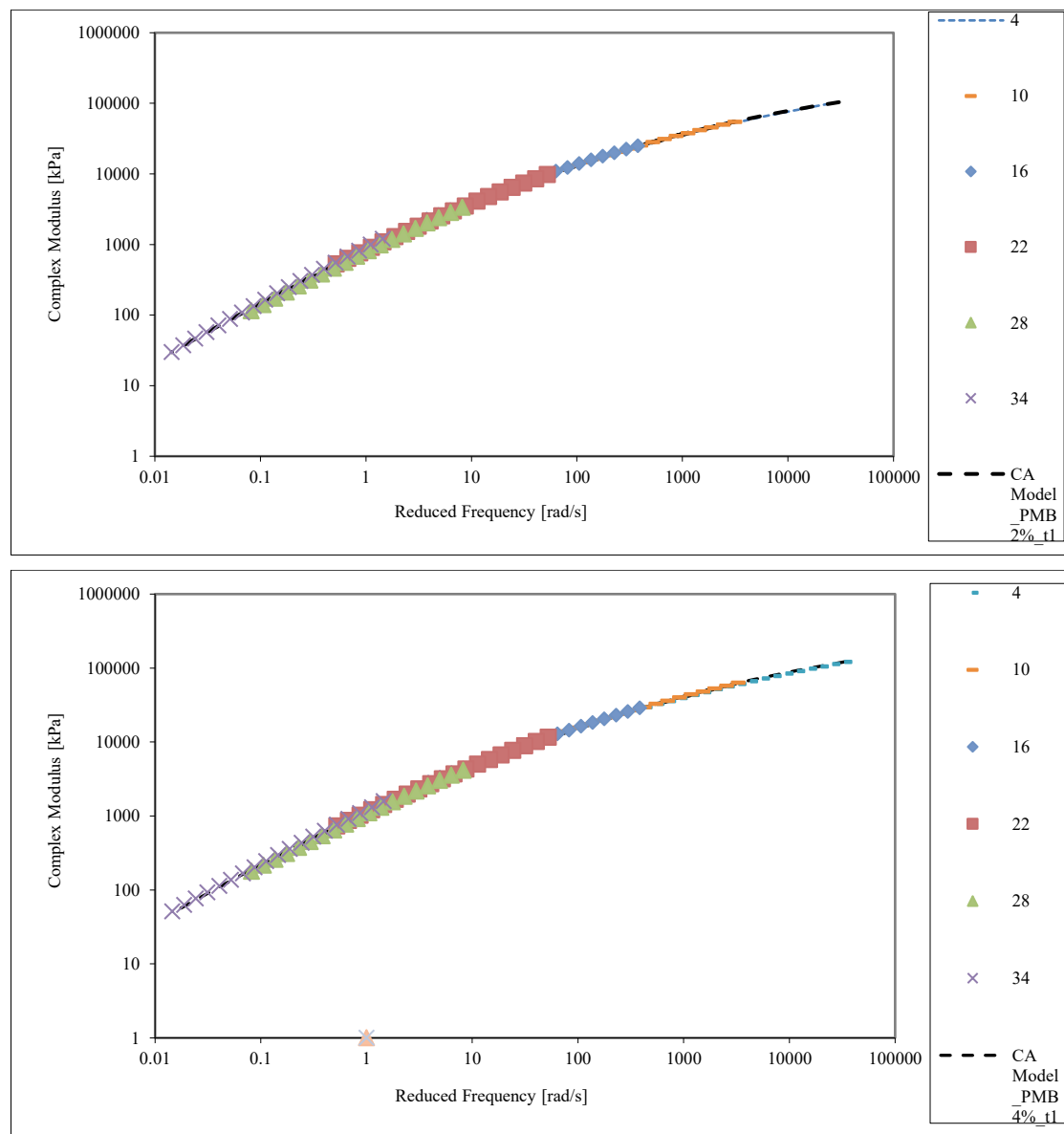
The linear viscoelastic (LVE) characterization of the bituminous binders was carried out through the Frequency Sweep (FS) test to evaluate the fundamental rheological response of the materials. The aim was to assess the influence of Recycled Low-Density Plastic (RLDP) modification on stiffness, viscoelastic balance, and thermal susceptibility, as well as to compare the new binders produced in this work with those obtained from previous studies.

The FS tests were performed using a Dynamic Shear Rheometer (DSR) in 8 mm plate configuration with a 2 mm gap, under controlled strain conditions within the LVE range. The temperature varied from 4 °C to 34 °C, while the loading frequency spanned from 1 rad/s and 100 rad/s. The experimental results were shifted to a reference temperature of 20 °C using the time–temperature superposition principle (TTSP), allowing the construction of continuous master curves that describe binder stiffness over a broad range of reduced frequencies. Due to the convergence of the trials, trial 1 from each binder was chosen to compare them.

CA model	PMB with 2% of RLDP - trial 1	PMB with 2% of RLDP - trial 1	PMB with 4% of RLDP - trial 1	PMB with 4% of RLDP - trial 1
T(0)	20 °C	15 °C	20 °C	15 °C
C1	25.85	26.62	23.22	23.99
C2	182.60	177.92	163.07	158.31
log(Gg)	5.59	5.60	5.79	5.79
log(w0)	1.93	1.20	1.73	0.99
R	1.50	1.50	1.73	1.73

Table 3.1.1 - Master curve parameters at different reference temperatures of PMB with 2% and 4% RLDP.

The superimposed data were fitted with the Christensen–Anderson (CA) model to define the viscoelastic transition. The model parameters showed consistent behaviour across all RLDP-modified binders, with $\log(Gg)$ ranging between 5.59 and 5.79 and R values between 1.50 and 1.73, indicating stable thermorheological characteristics.



Figures 3.1.1 and 3.1.2 – Comparison of CA model fitting curves for PMB with 2% and 4% RLDP.

The resulting master curves of the complex modulus $(|G|)^*$ (Figure 3.1.3) clearly demonstrate the effect of plastic modification. The neat 50/70 binder shows the lowest stiffness across the frequency domain, confirming its predominantly viscous nature.

The addition of 2 % RLDP significantly increases $|G^*|$ values throughout the entire frequency range, indicating a stronger elastic contribution. The 4 % RLDP binder exhibits an even steeper slope and higher modulus, particularly at high frequencies, reflecting improved rigidity and load-bearing capacity. The difference between 2 % and 4 % RLDP becomes more pronounced in the medium-frequency region (10–100 rad/s).

Similarly, the master curve of the phase angle (δ) (Figure 3.1.4) provides a complementary perspective on the viscoelastic balance. The neat binder exhibits the highest δ values, indicating a strong viscous dominance and limited elastic recovery. The 2 % RLDP binder maintains lower δ values across most of the frequency spectrum, revealing an improved elasticity compared to the neat binder. The 4 % RLDP binder shows an even lower phase angle, particularly in the mid-to-high frequency domain, confirming its enhanced elastic nature. At very low frequencies, the 4 % binder demonstrates slower phase reduction, suggesting restricted molecular mobility due to the higher concentration of polymeric components.

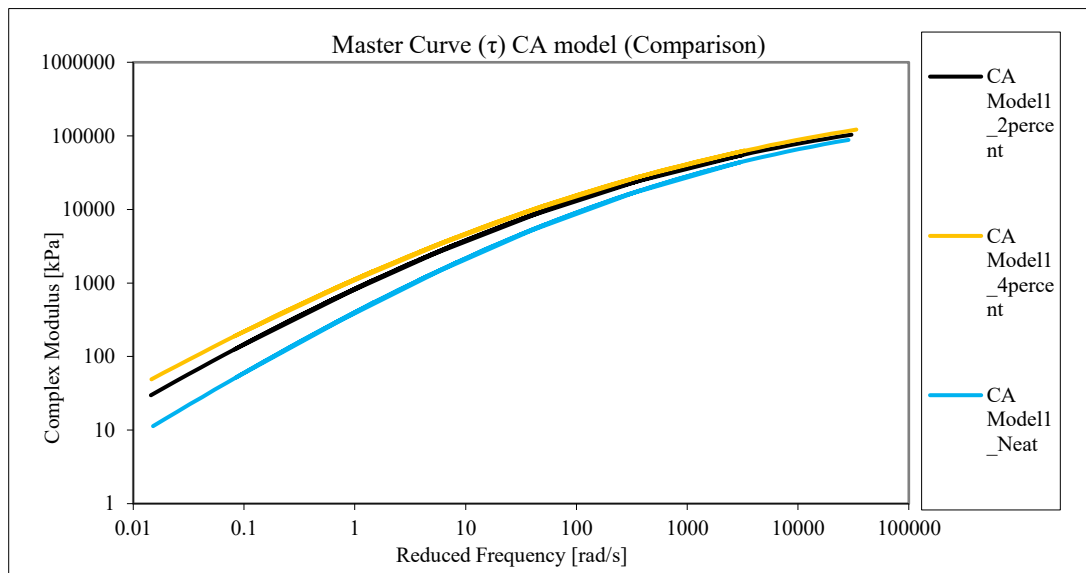


Figure 3.1.3 – Master curves of complex modulus ($|G|$) vs. reduced frequency for Neat50/70, PMB with 2% and 4% RLDP, $T_0 = 20\text{ }^{\circ}\text{C}$.

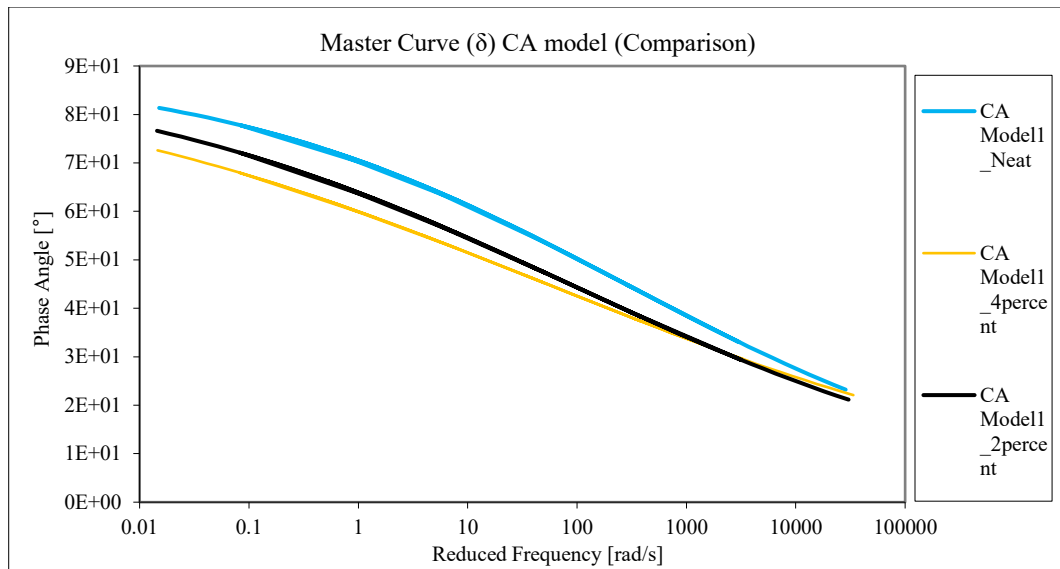


Figure 3.1.4 – Phase angle (δ) vs. reduced frequency comparison between Neat50/70, PMB with 2% and 4% RLDP.

The comparison between the two RLDP formulations reveals a clear reinforcing effect of increased plastic dosage. While both binders exhibit thermorheological consistency, the 4 % system demonstrates a stiffer and more elastic response, whereas the 2 % binder maintains slightly greater viscous adaptability, favouring flexibility and stress relaxation.

To visualize the combined stiffness–elasticity relationship, the Black diagram (Figure 3.1.5) was constructed by plotting $|G^*|$ versus δ for the three binders—neat 50/70, 2 % RLDP, and 4 % RLDP. All three curves follow a smooth monotonic trend, confirming thermorheological simplicity and the validity of the CA model within the LVE region. The neat binder is positioned toward the right-hand side, reflecting high δ and low stiffness values, typical of unmodified bitumen. The 2 % RLDP binder curve shifts leftwards and upward, indicating higher modulus and moderate phase reduction. The 4 % RLDP binder, located furthest to the upper left, shows the greatest stiffness and lowest phase angle, reflecting the most elastic response among the tested materials. The alignment of all curves demonstrates that the RLDP-modified binders maintain structural homogeneity and stability, with no abnormal relaxation behaviour or phase irregularities.

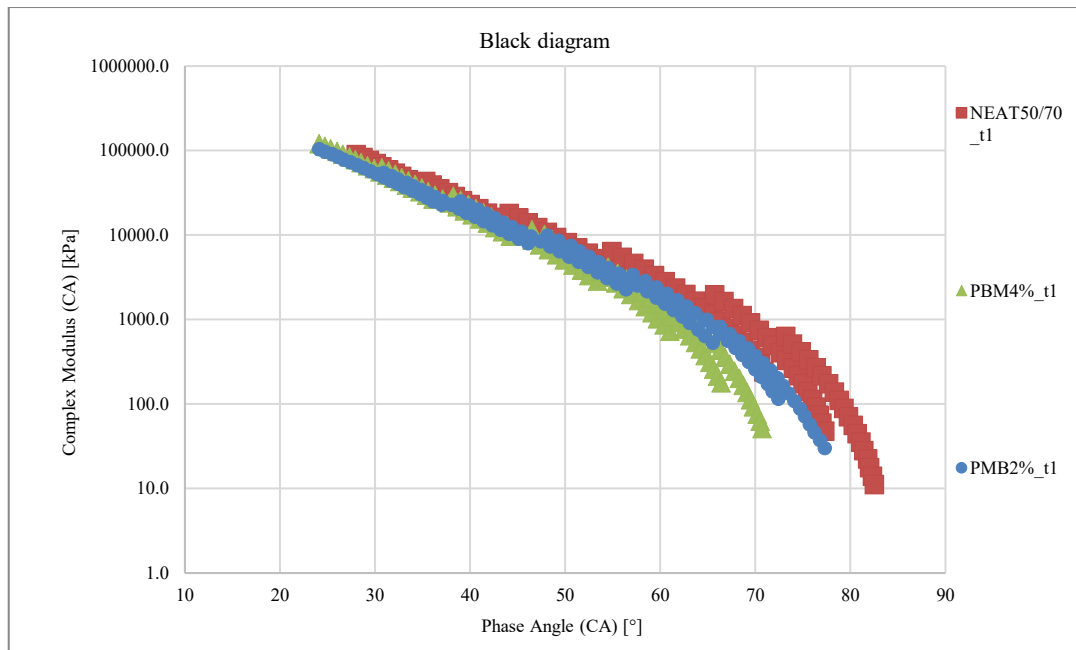


Figure 3.1.5 – Black diagram ($|G|$ vs δ) for Neat 50/70, PMB with 2% and 4% RLDP.

To further quantify thermal sensitivity, equirigidity temperatures were determined by interpolating the CA model at a reference frequency of 10 Hz. The 2 % RLDP binder reached 5 MPa stiffness at 12.1 °C and 35 MPa at 24.2 °C, while the 4 % RLDP binder achieved the same stiffness levels at 13.3 °C and 25.5 °C, respectively. Both binders presented similar viscoelastic transition intervals of approximately 12 °C, typical of polymer-modified systems. The slight upward shift observed in the 4 % RLDP formulation confirms its superior resistance to permanent deformation under elevated temperatures, while the 2 % binder remains more flexible and thus more effective under intermediate climate conditions.

In summary, the linear viscoelastic characterization confirmed that the incorporation of RLDP enhances binder stiffness, elasticity, and thermal stability. The 2 % binder offers a balanced response between flexibility and strength, while the 4 % binder demonstrates higher stiffness and improved resistance to deformation, suitable for warmer service environments. Compared to the neat 50/70 binder, both RLDP-modified systems show a clear improvement in mechanical behaviour without compromising thermorheological consistency. The master curves, Black diagram, and equirigidity analysis together validate the effectiveness of the CA model in describing the viscoelastic response of RLDP-modified binders and provide the rheological

foundation for the fatigue and healing investigations discussed in the following sections.

3.2 Fatigue resistance (LAS test)

The fatigue resistance of the binders was evaluated through the Linear Amplitude Sweep (LAS) test, which provides insight into the material's ability to resist damage under progressively increasing strain amplitudes. The test was carried out following AASHTO TP101-14 and the procedure adapted from De Leonardis (2022). All measurements were performed using an Anton Paar Dynamic Shear Rheometer (DSR) equipped with 8 mm parallel plates and a 2 mm gap. The tests were conducted at two reference temperatures, 15 °C and 20 °C, to represent intermediate pavement service conditions where fatigue failure is most critical.

Before the fatigue analysis, multiple trials were performed for each binder to verify the repeatability and stability of the measurements. For the 2 % RLDP-modified binder at 15 °C, nine independent trials were carried out, of which trials 6, 8, and 9 exhibited convergent behavior and were thus selected for further analysis. For the same binder at 20 °C, six trials were executed, and the last three showed consistent stress–strain envelopes. Similarly, for the 4 % RLDP-modified binder, four trials were completed at both temperatures; at 15 °C, trials 1 and 7 were in good agreement, while at 20 °C the first two were considered representative.

The convergence verification was performed through a statistical comparison of the shear stress–strain curves, ensuring that deviations among selected trials did not exceed 5 %. This filtering process helped eliminate artefacts caused by minor variations in sample thickness or contact conditions between the plates.

Some tests are considered “failed” due to the immediate drop after the peak of Shear Strain, the reason could be because of some external effects, machine error or there was not enough adhesion of binder to the plate and spatula.

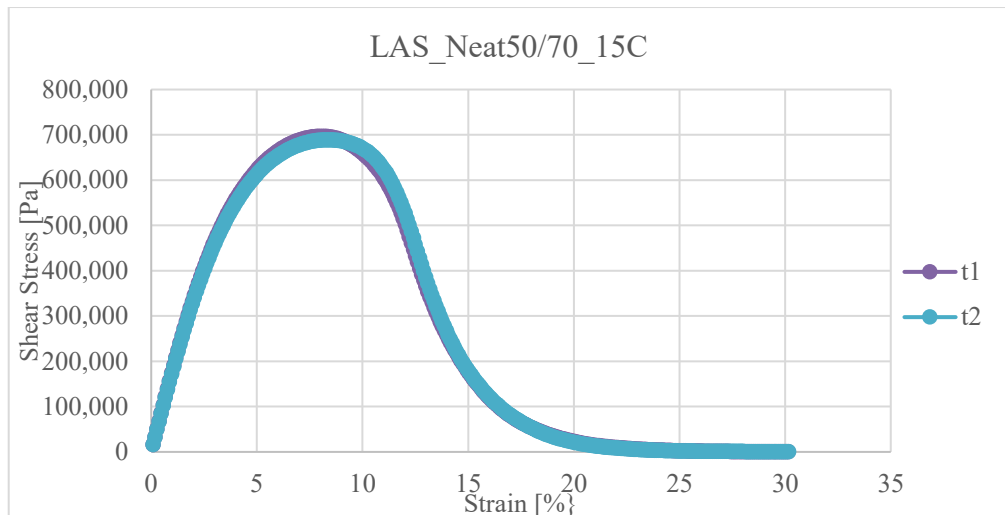


Figure 3.2.1 – LAS 15 ° stress–strain curves for Neat 50/70.

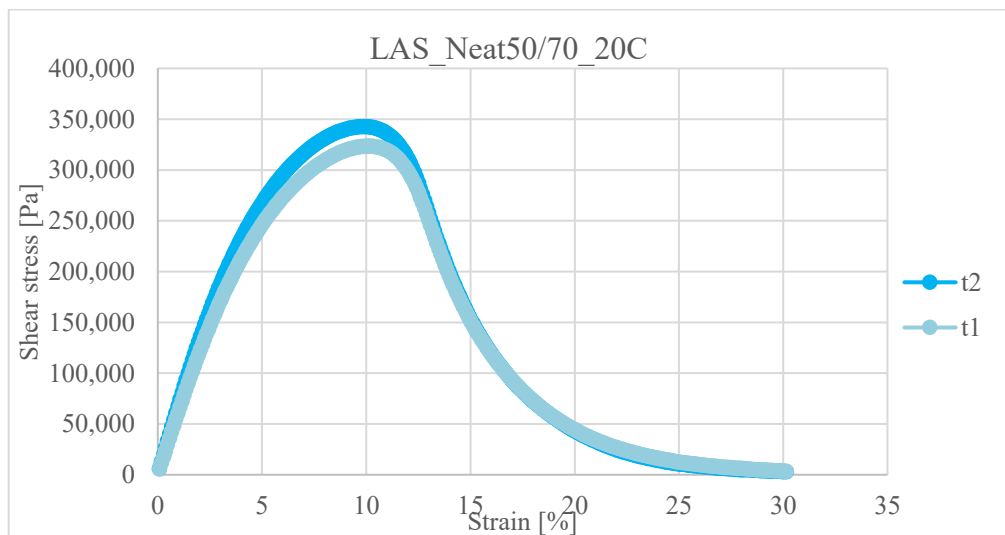


Figure 3.2.2 – LAS 20 °C stress–strain curves for Neat 50/70.

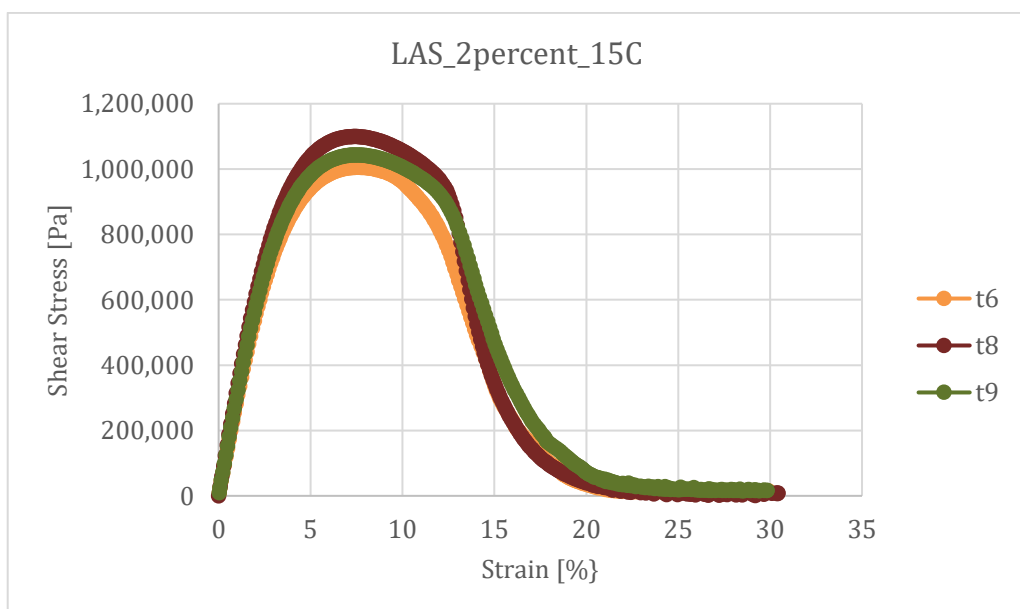


Figure 3.2.3 – LAS 15 °C stress–strain curves for PMB with 2 % of RLDP.

Central limit theorem					
	$\tau(\text{peak})$	$\gamma(\text{at } \tau \text{ peak})$	for $\gamma(\text{at } \tau \text{ peak})$		
Trial	[Pa]	[%]	z-score (Mean Dev)	Outlier? ($ z > 2$)	Status (z thresholds)
1	969955	7.0	-1.2	No	Acceptable ($1 \leq z < 2$)
2	737929	5.7	-5.4	Yes	Outlier ($ z \geq 2$)
3	866750	6.2	-3.8	Yes	Outlier ($ z \geq 2$)
4	891739	5.2	-7.3	Yes	Outlier ($ z \geq 2$)
5	870157	4.2	-10.5	Yes	Outlier ($ z \geq 2$)
6	1005540	7.6	0.8	No	Excellent ($ z < 1$)
7	1090280	6.9	-1.5	No	Acceptable ($1 \leq z < 2$)
8	1099550	7.4	0.3	No	Excellent ($ z < 1$)
9	1043390	7.5	0.4	No	Excellent ($ z < 1$)
			Mean:	7.35	
			SD:	0.30	
Result:					
Trials1-5 are failed and trial 7 is not considered.					

Table 3.2.1 – LAS 15 °C statistical analysis on consistency for PMB with 2 % of RLDP.

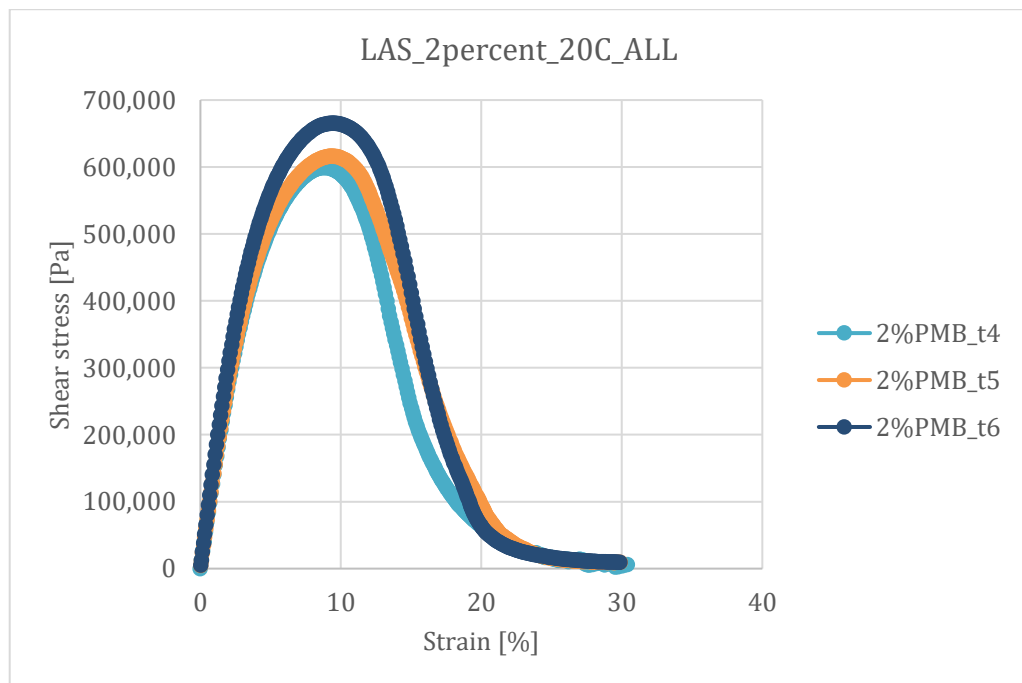
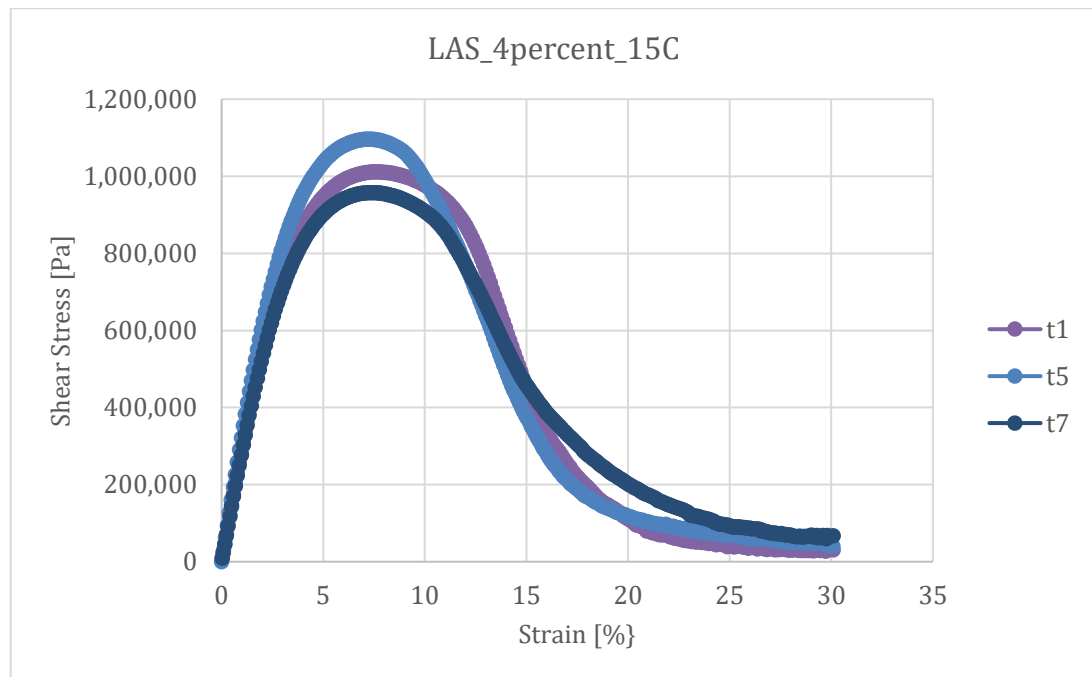


Figure 3.2.4 – LAS 20 °C stress-strain curves for PMB with 2 % of RLDP.

Central limit theorem					
	$\tau(\text{peak})$	$\gamma(\text{at } \tau \text{ peak})$	for $\gamma(\text{at } \tau \text{ peak})$		
Trial	[Pa]	[%]	z-score (Mean Dev)	Outlier? ($ z > 2$)	Status (z thresholds)
Trial 1	461369	8.13	-1.8	No	Acceptable ($1 \leq z < 2$)
Trial 2	484676	7.156	-3.0	Yes	Outlier ($ z \geq 2$)
Trial 3	594776	10.75	1.4	No	Acceptable ($1 \leq z < 2$)
Trial 4	599260	8.797	-1.0	No	Excellent ($ z < 1$)
Trial 5	616272	9.393	-0.3	No	Excellent ($ z < 1$)
Trial 6	665465	9.49	-0.1	No	Excellent ($ z < 1$)
Result:			Mean: 9.6075		
			SD: 0.820981729		
Trials 1 and 2 failed, 3 is not considered					

Table 3.2.2 – LAS 15 °C statistical analysis on consistency for PMB with 4 % of RLDP.



Place Figure 3.2.5 – LAS 15 °C stress–strain curves for PMB with 4 % of RLDP.

Central limit theorem					
	$\tau(\text{peak})$	$\gamma(\text{at } \tau \text{ peak})$	for $\gamma(\text{at } \tau \text{ peak})$		
	[Pa]		z-score (Mean Dev)	Outlier? ($ z > 2$)	Status (z thresholds)
Trial		[%]			
Trial 1	1011490	7.6	0.2	No	Excellent ($ z < 1$)
Trial 2	989623	5.4	-2.1	Yes	Outlier ($ z \geq 2$)
Trial 3	893362	5.4	-2.0	Yes	Outlier ($ z \geq 2$)
Trial 4	980315	7.4	0.0	No	Excellent ($ z < 1$)
Trial 5	1096440	7.2	-0.2	No	Excellent ($ z < 1$)
Trial 6	1062860	7.1	-0.3	No	Excellent ($ z < 1$)
Trial 7	957535	7.4	0.0	No	Excellent ($ z < 1$)
			Mean:	7.40	
			SD:	0.96	
Result:					
Due to the fall after the peak some trials, only the trials 1, 5, and 7 are considered					

Table 3.2.3 – LAS 15 °C statistical analysis on consistency for PMB with 4 % of RLDP.

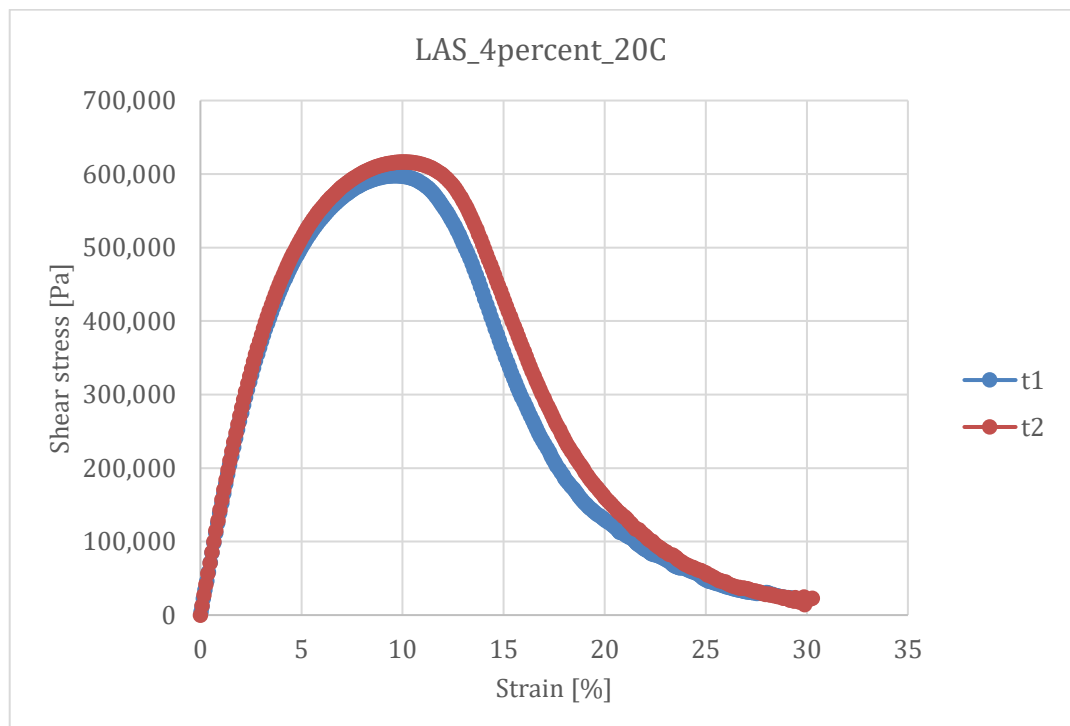


Figure 3.2.6 – LAS 20 °C stress–strain curves for PMB with 4 % of RLDP.

Central limit theorem					
	$\tau(\text{peak})$	$\gamma(\text{at } \tau \text{ peak})$	for $\gamma(\text{at } \tau \text{ peak})$		
Trial	[Pa]	[%]	z-score (Mean Dev)	Outlier? ($ z > 2$)	Status (z thresholds)
1	597802	9.7	-0.71	No	Excellent ($ z < 1$)
2	616525	10.1	0.71	No	Excellent ($ z < 1$)
			Mean:	9.876	
			SD:	0.274357431	
Result:					
All trials are considered					

Table 3.2.4 – LAS 20 °C statistical analysis on consistency for PMB with 4 % of RLDP.

The shear stress–strain response shows a typical shape, characterized by an initial linear region followed by a nonlinear growth up to a distinct peak and then a softening phase as damage accumulates. The peak of the curve corresponds to the strain level at which the material reaches its maximum shear stress (τ_{max}), marking the transition from viscoelastic deformation to fatigue cracking initiation. Comparing the behaviour of the three binders—neat 50/70, 2 % RLDP, and 4 % RLDP—reveals that polymer modification significantly influences both the magnitude of the stress peak and the strain at which it occurs.

At 15 °C, the neat 50/70 binder displayed a τ_{max} at approximately 8 % strain, while both RLDP-modified binders reached their stress peaks earlier, at around 7.5 % strain. This behaviour reflects the higher stiffness induced by the addition of recycled plastic, which limits deformation before the onset of damage. The slightly reduced strain tolerance at peak load indicates that RLDP modification enhances resistance to deformation but reduces ductility at low temperatures—a trend typical for stiffer polymer-modified systems.

At 20 °C, the curves shift toward higher strain values due to increased molecular mobility and reduced viscosity. The neat 50/70 binder reached its τ_{max} at 10 % strain, while the 2 % RLDP binder peaked at 9-10 %, and the 4 % RLDP binder again

approached 10 %. These results suggest that at moderate temperatures, the addition of 4 % RLDP restores the binder's capacity to deform before failure, striking a balance between elasticity and ductility. The 2 % binder, on the other hand, remains slightly more brittle, which may be attributed to a lower concentration of plastic network within the bitumen matrix.

for 15C:		for 20C:	
Specimen type	γ (at τ peak)	Specimen type	γ (at τ peak)
	[%]		[%]
NEAT50/70	8.00	NEAT50/70	10.00
PMB2%	7.00	PMB2%	10.00
PMB4%	7.00	PMB4%	10.00

Table 3.2.5 – Strain at maximum shear stress (γ at τ peak)

The comparison of LAS envelopes among all binders highlights a consistent pattern: at 15 °C, the RLDP-modified binders exhibit a stiffer and more pronounced peak, while at 20 °C the curves flatten slightly, reflecting the softening effect of temperature. The results confirm that temperature plays a dominant role in determining fatigue resistance, but the modification level defines the balance between stiffness and deformability. The 4 % RLDP formulation provides the most stable performance, maintaining higher stress capacity while preserving deformability similar to that of the neat binder.

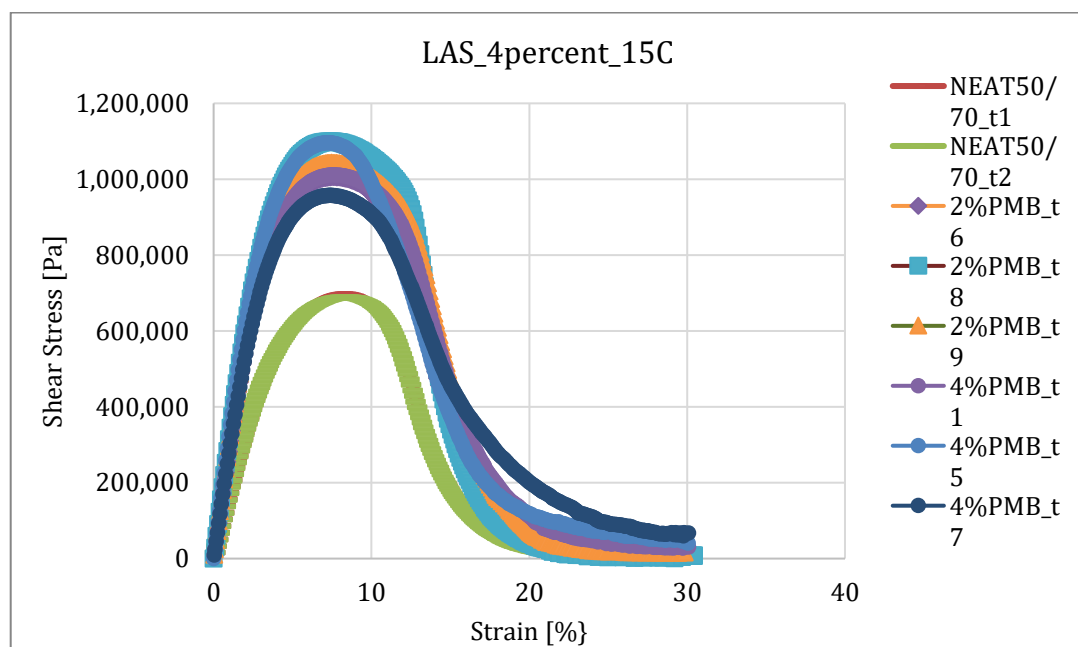


Figure 3.2.7 – Comparison of LAS curves for Neat50/70, 2 %, and 4 % RLDP binders at 15 °C.

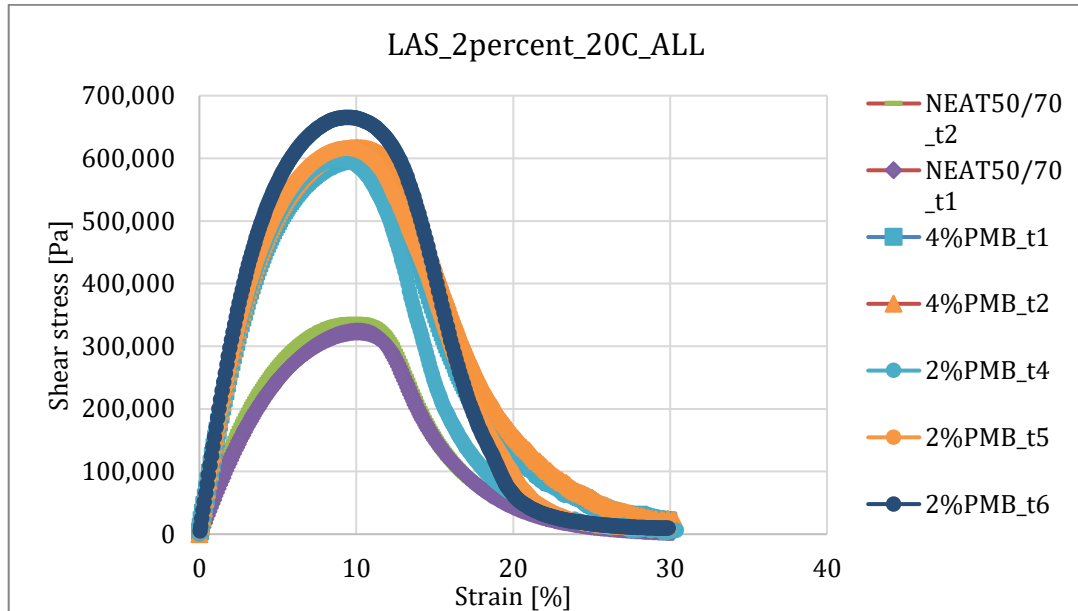


Figure 3.2.8 – Comparison of LAS curves for Neat50/70, 2 %, and 4 % RLDP binders at 20 °C.

Statistical comparison among convergent trials further confirmed the reproducibility of these observations. The mean stress at τ_{\max} and its associated strain exhibited a standard deviation below 4 % for each set of consistent trials, indicating good experimental repeatability. Outlier runs, particularly those showing premature stress drops or irregular curve shapes, were discarded from the analysis.

The evaluation of the strain corresponding to the maximum shear stress is of particular significance because this parameter serves as a reference for subsequent healing tests (LAS-H). In those tests, at temperature 20°C the same strain levels are used as the upper limit for cyclic loading in order to reproduce comparable damage states prior to rest periods. But, for 15°C strain level 7.00% considered as a reference strain, due to the comparison reason with previous tests, in next activities. Thus, the fatigue characterization presented here not only describes the mechanical degradation of the binders under continuous loading but also provides the necessary input for the quantitative assessment of self-healing capacity.

In summary, the LAS analysis demonstrated that the addition of RLDP generally increases binder stiffness and enhances fatigue strength at low temperatures, while at higher temperatures it helps maintain ductility comparable to conventional bitumen. The reproducibility across trials and the consistent shift of the stress–strain envelopes

with temperature confirm the reliability of the adopted testing and data-filtering methodology. These findings lay the experimental foundation for the healing investigation that follows, in which the same binders are evaluated for their ability to recover stiffness and integrity after rest periods using the LAS-Healing (LAS-H) and LAS-Steric Hardening (LAS-SH) protocols.

3.3 Self-healing (LAS-H test)

The LAS-Healing (LASH) tests were conducted to quantify the intrinsic healing potential of the binders following fatigue loading. The experimental procedure followed the same loading protocol as the standard LAS test, with the addition of a rest period between the two loading phases. This methodology allowed the evaluation of the material's ability to recover stiffness and structural integrity after partial damage. Tests were performed on the 2 % and 4 % RLDP-modified binders at 15 °C and 20 °C, under two different conditions: without resting time (0 min) and with a controlled resting period of 30 minutes.

Each LASH test consisted of two consecutive amplitude-sweep loading stages (Phase 1 and Phase 2), separated by the rest interval. The first phase introduced controlled fatigue damage until a predefined strain level—corresponding to the strain at maximum shear stress obtained from the LAS results—was reached.

During the rest period, the sample remained in the DSR testing chamber under constant temperature and no loading, allowing molecular diffusion and re-adhesion to occur within the binder matrix. The second phase then re-loaded the same specimen under identical conditions, and the stress–strain response was compared to that of the first phase.

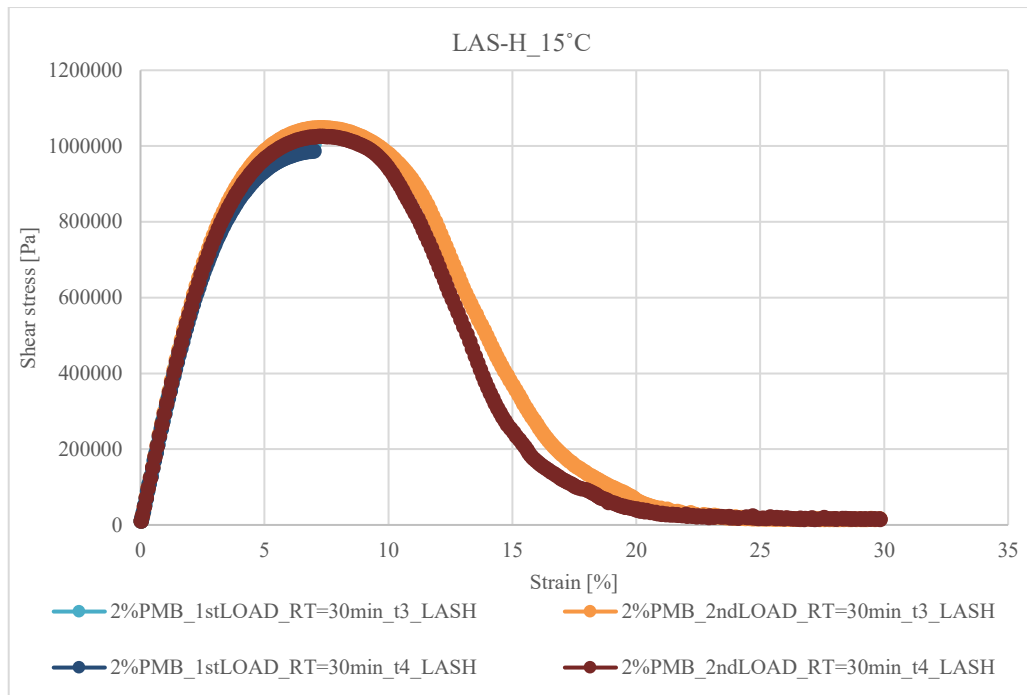


Figure 3.3.1 – LAS-H_15 °C (2 %PMB), where Resting Time = 30min.

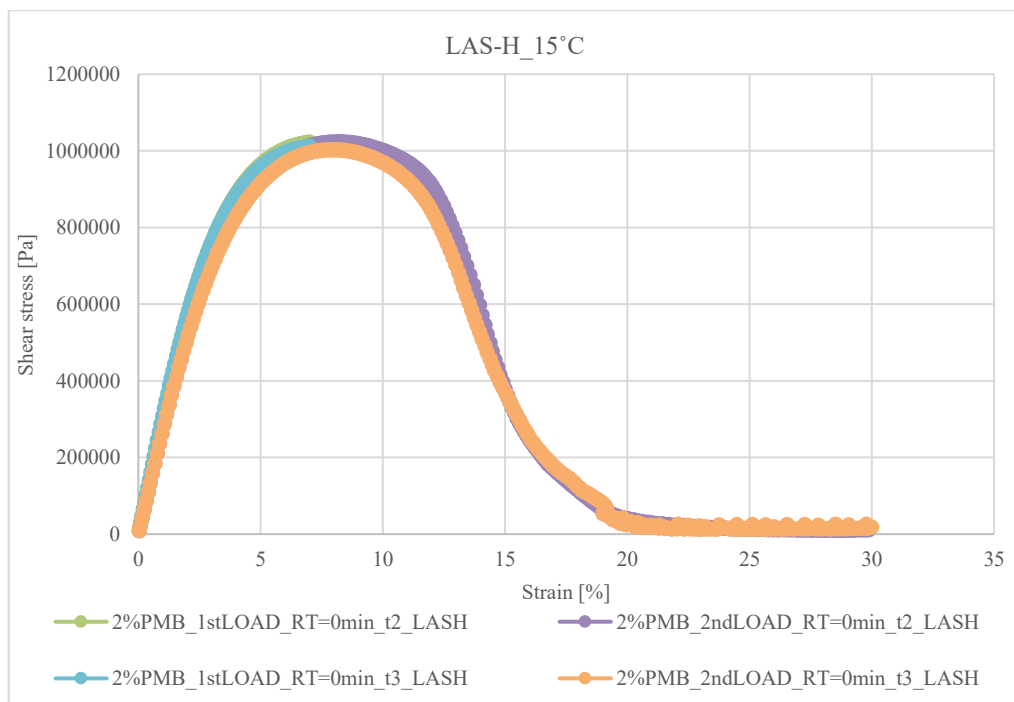


Figure 3.3.2 – LAS-H_15 °C (2 %PMB), where Resting Time = 0min.

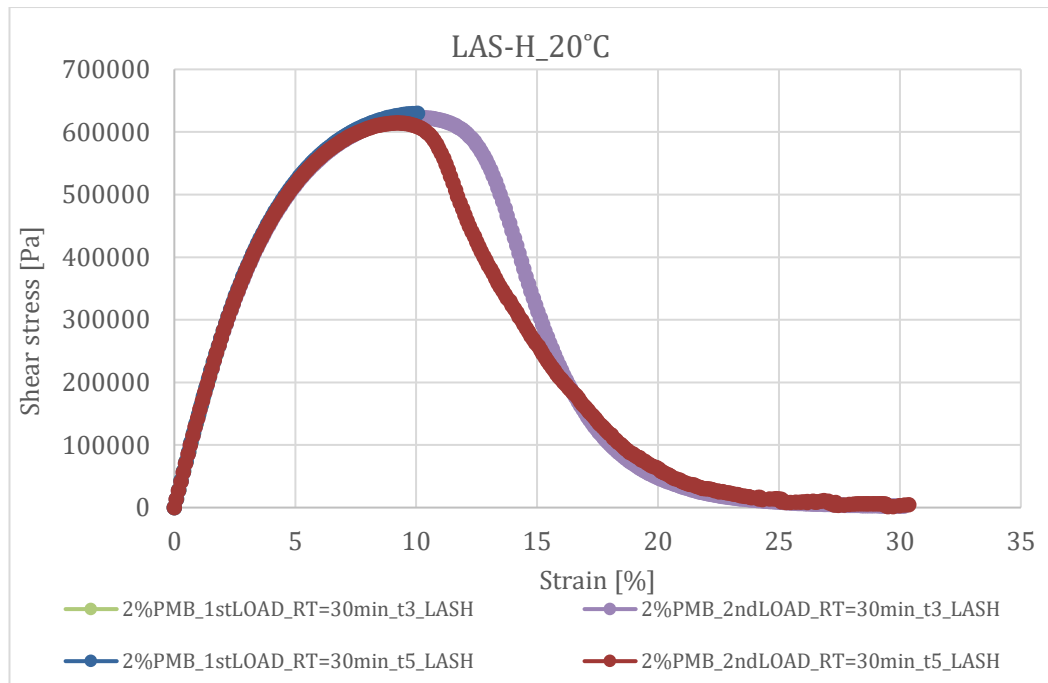


Figure 3.3.3 – LAS-H₂₀ °C (2 %PMB), where Resting Time = 30min.

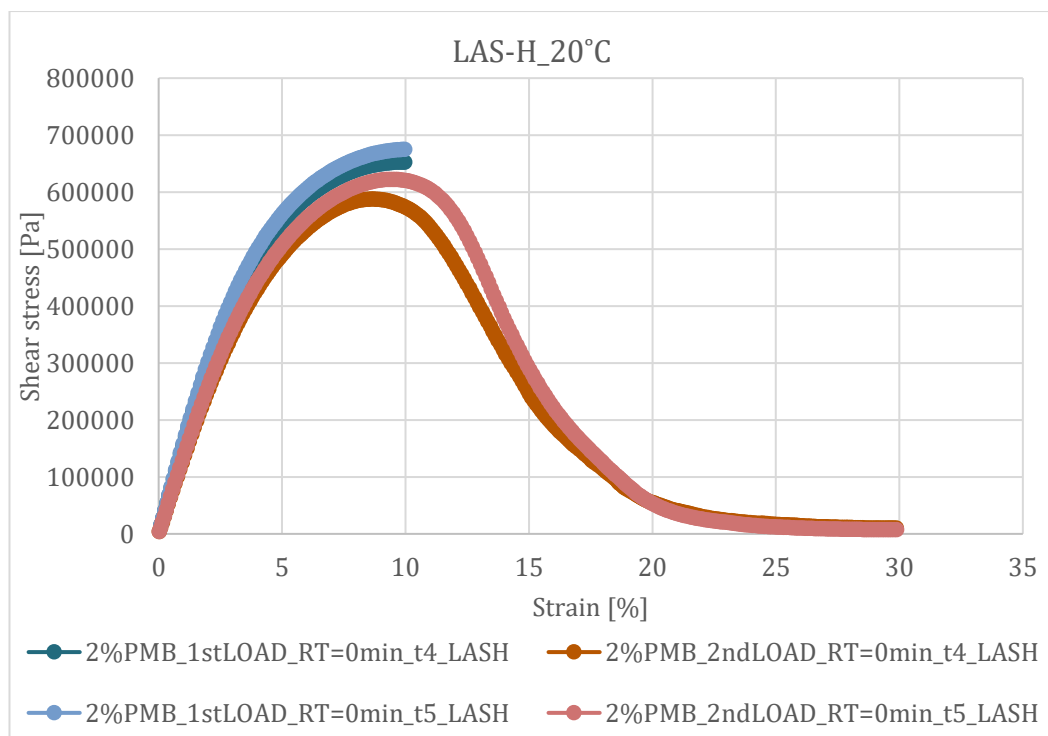


Figure 3.3.4 – LAS-H₂₀ °C (2 %PMB), where Resting Time = 0min.

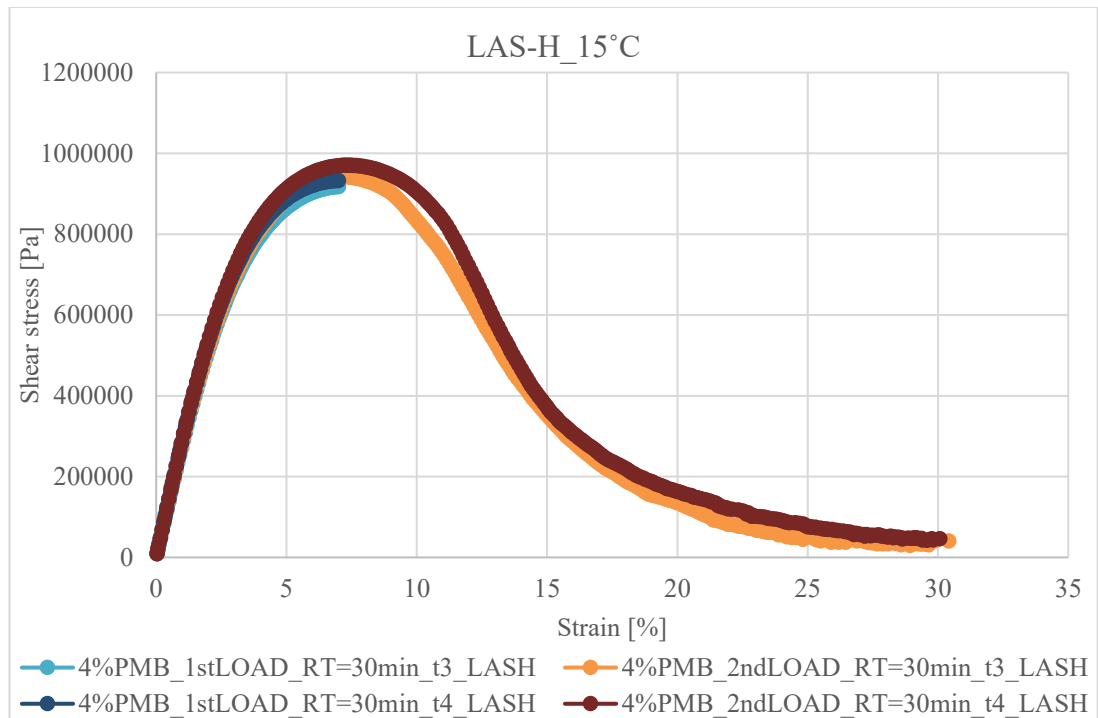


Figure 3.3.5 – LAS-H_15 °C (4 %PMB), where Resting Time = 30min.

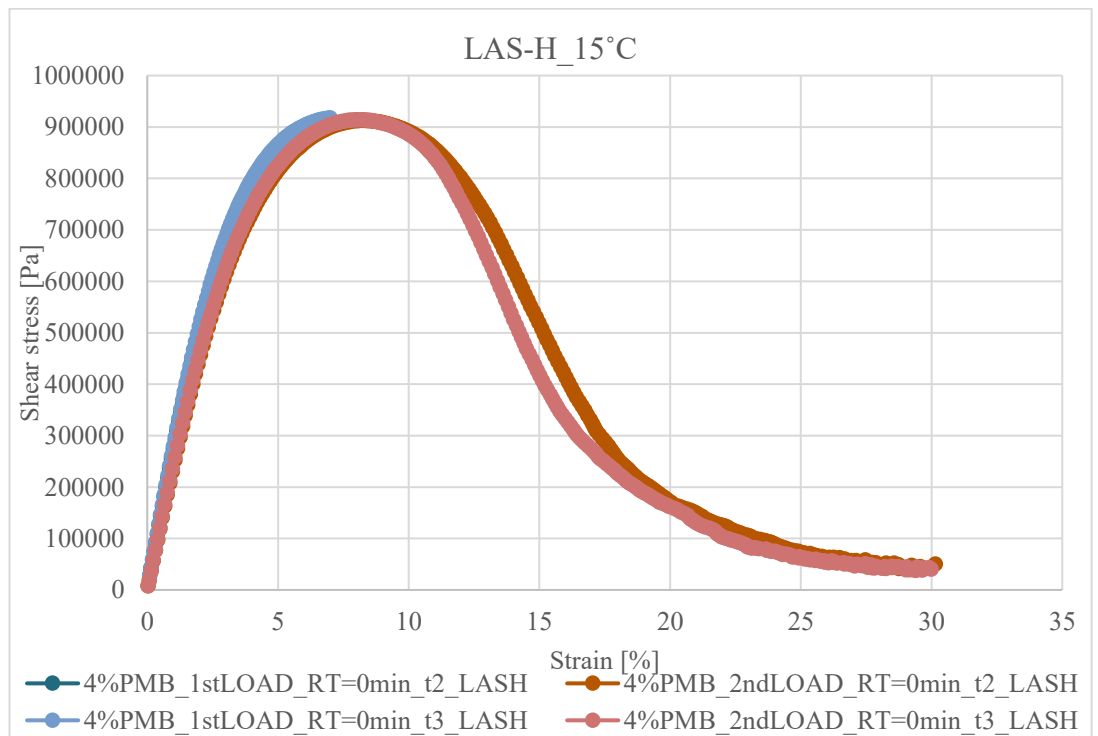


Figure 3.3.6 – LAS-H_15 °C (4 %PMB), where Resting Time = 0min.

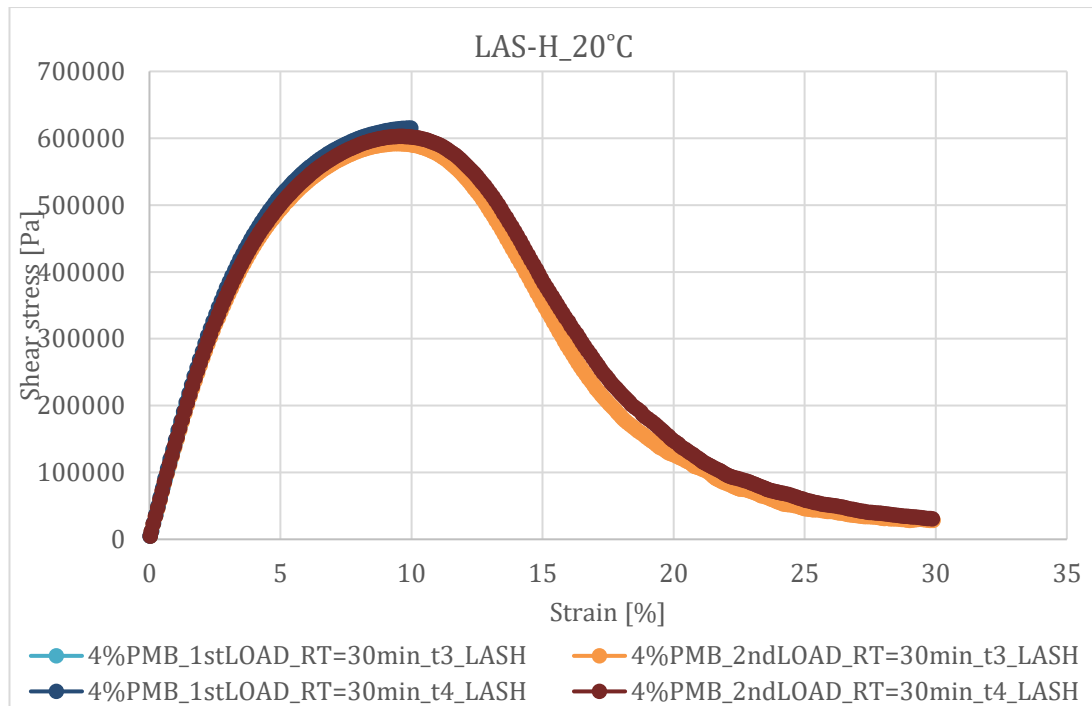


Figure 3.3.7 – LAS-H_20 °C (4 %PMB), where Resting Time = 30min.

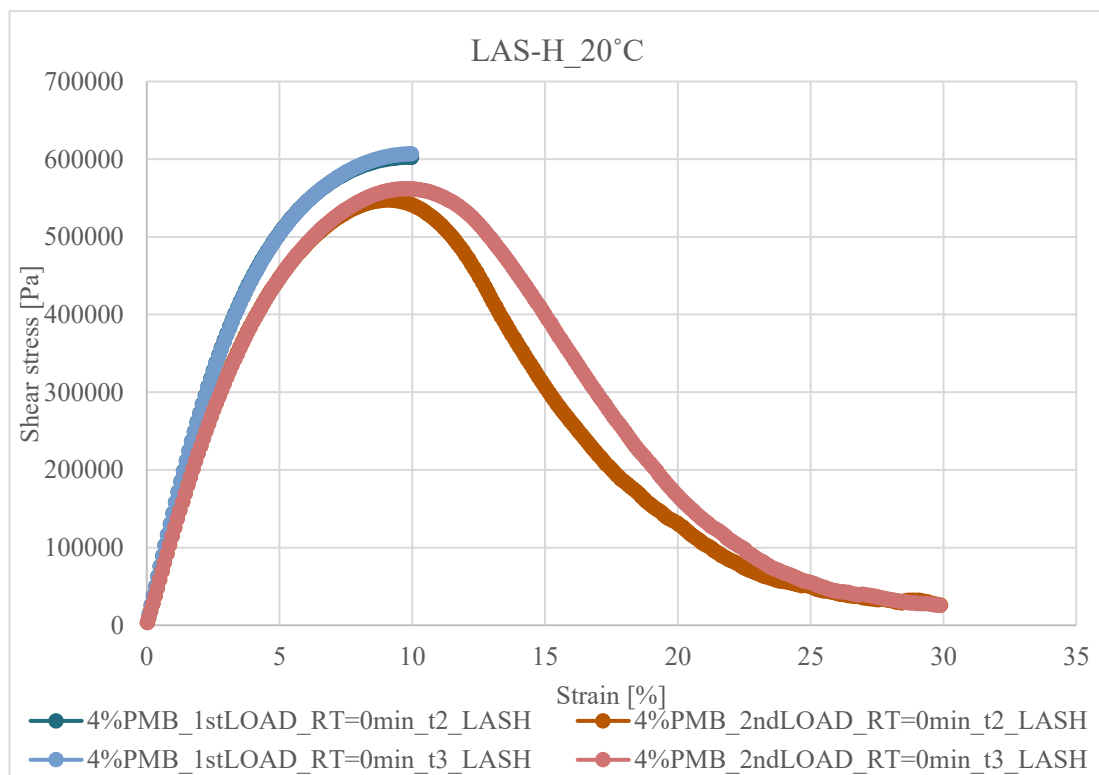


Figure 3.3.8 – LAS-H_20 °C (4 %PMB), where Resting Time = 0min.

The results clearly highlight the beneficial effect of rest time on the recovery of mechanical properties. At 15 °C, both 2 % and 4 % RLDP-modified binders exhibited a distinct increase in shear stress during the second loading cycle following the 30-

minute rest period, compared to the response with no rest time. This behaviour confirms the occurrence of self-healing phenomena and the steric-hardening effect within the binder. The improvement was more pronounced for the 2 % RLDP system, where the stress peak after resting nearly overlapped with that of the initial loading, indicating efficient molecular mobility and re-bonding.

At 20 °C, a similar trend was observed, though the relative recovery was slightly lower. This can be attributed to the higher viscous contribution of the binder at elevated temperatures, which reduces the elastic potential required for full stiffness recovery. The 4 % RLDP binder maintained a high level of stress stability between the first and second loading phases, suggesting that the higher plastic content limited excessive molecular flow and helped preserve the internal structure during damage and recovery.

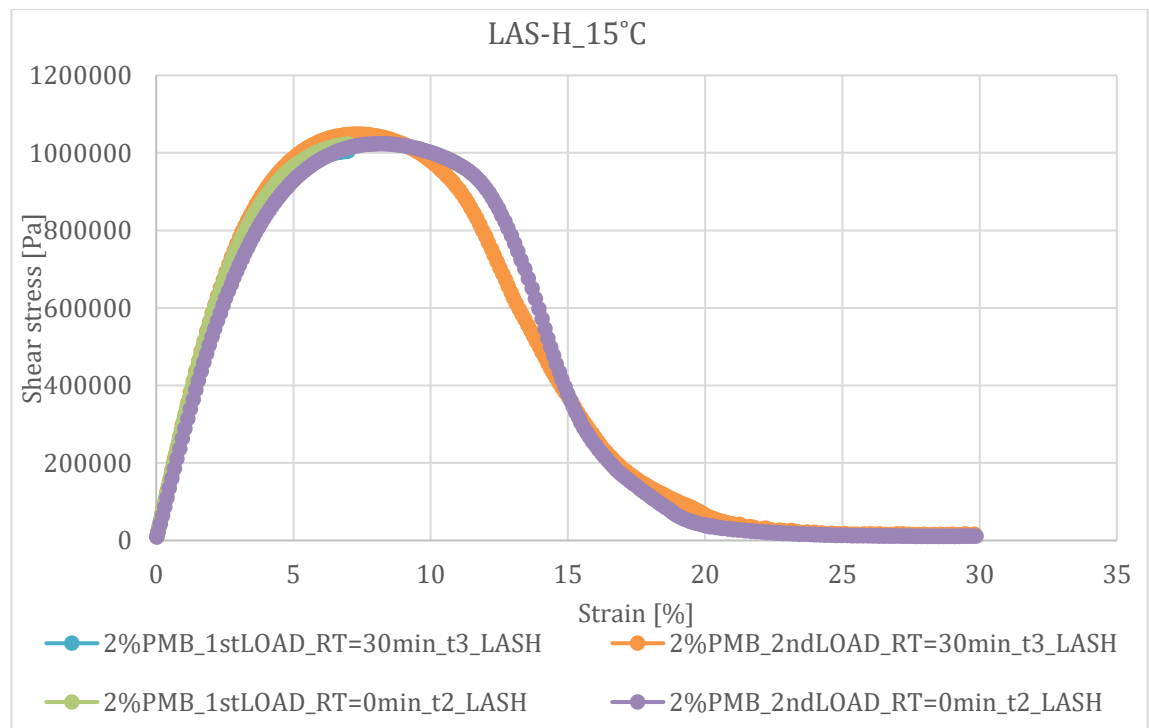


Figure 3.3.9 – LAS-H_15 °C (2 %PMB), where Resting Time = 0min vs Resting Time = 30min.

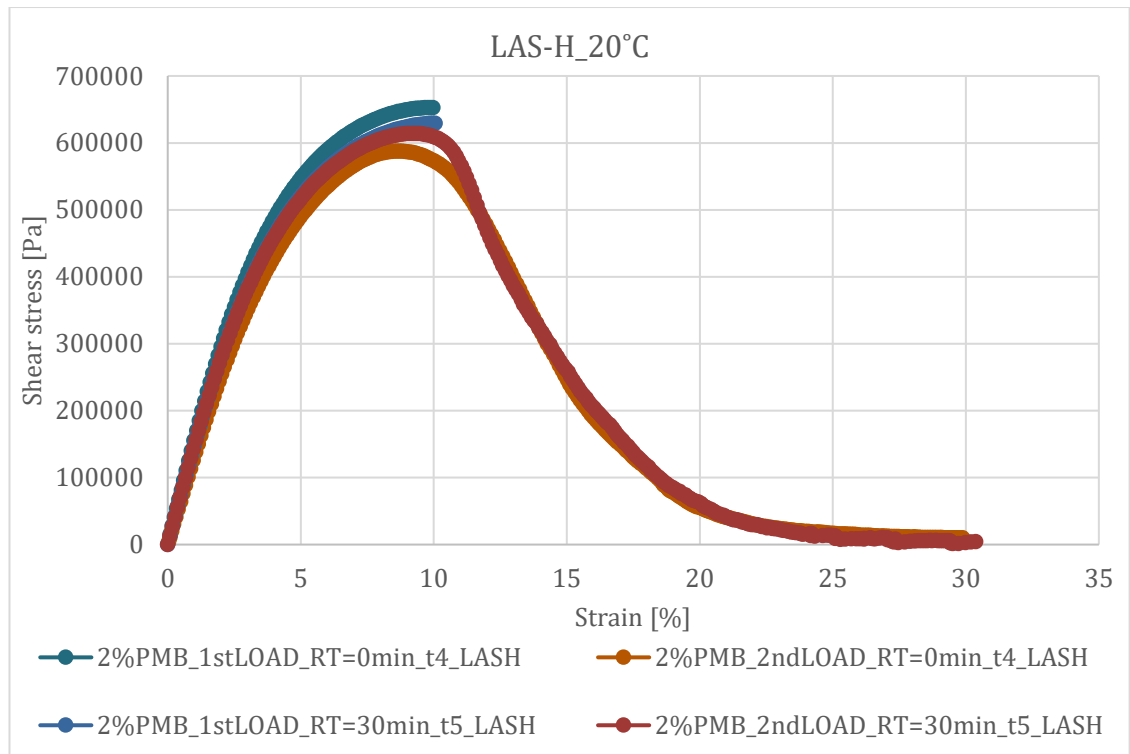


Figure 3.3.10 – LAS-H_20 °C (2 %PMB), where Resting Time = 0min vs Resting Time = 30min.

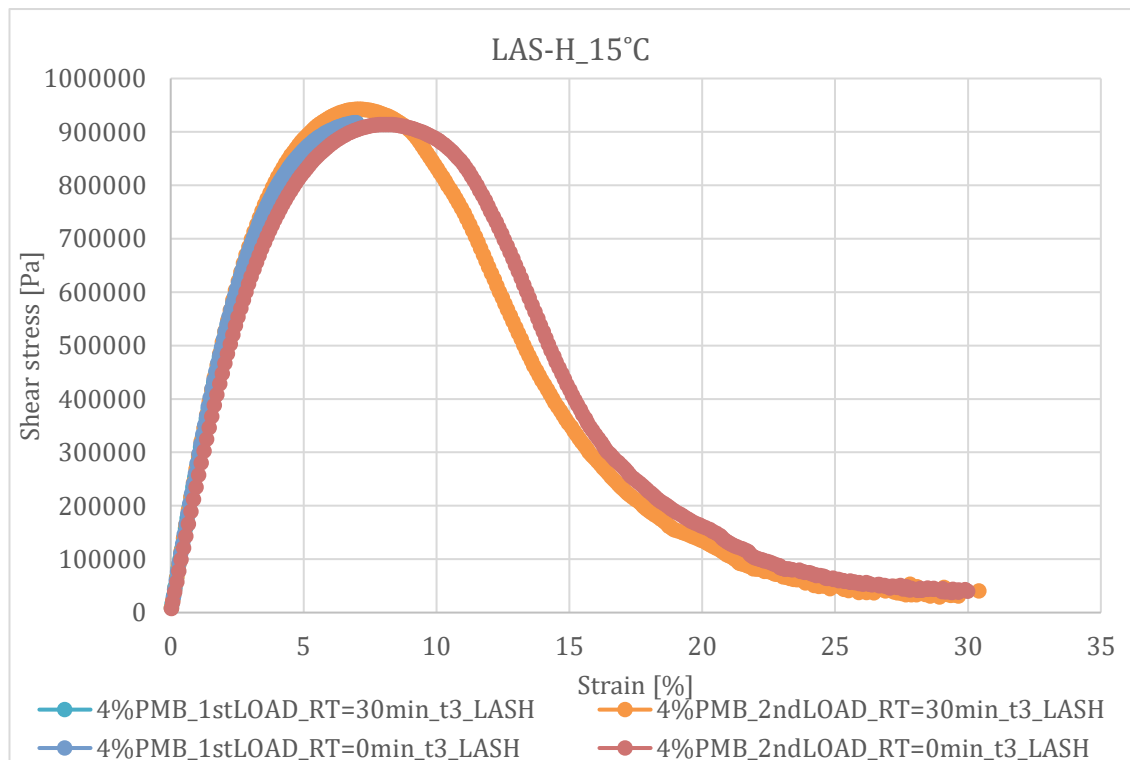


Figure 3.3.11 – LAS-H_15 °C (4 %PMB), where Resting Time = 0min vs Resting Time = 30min.

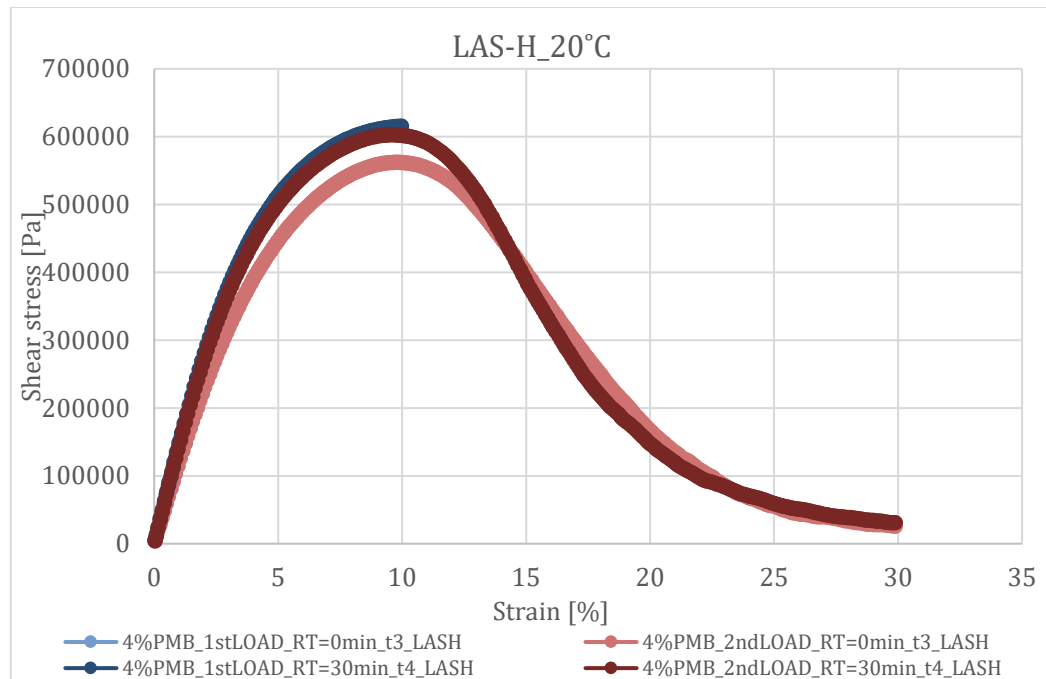


Figure 3.3.12 – LAS-H_20 °C (4 %PMB), where Resting Time = 0min vs Resting Time = 30min.

The LAS-H data were processed in conjunction with LAS-SH (Steric Hardening) reference tests to isolate the true healing contribution from physical stiffening effects. By comparing the second loading curves of LAS-H and LAS-SH tests, it was confirmed that the observed stiffness recovery predominantly originated from self-healing rather than time-dependent hardening, specially at 20 °C .

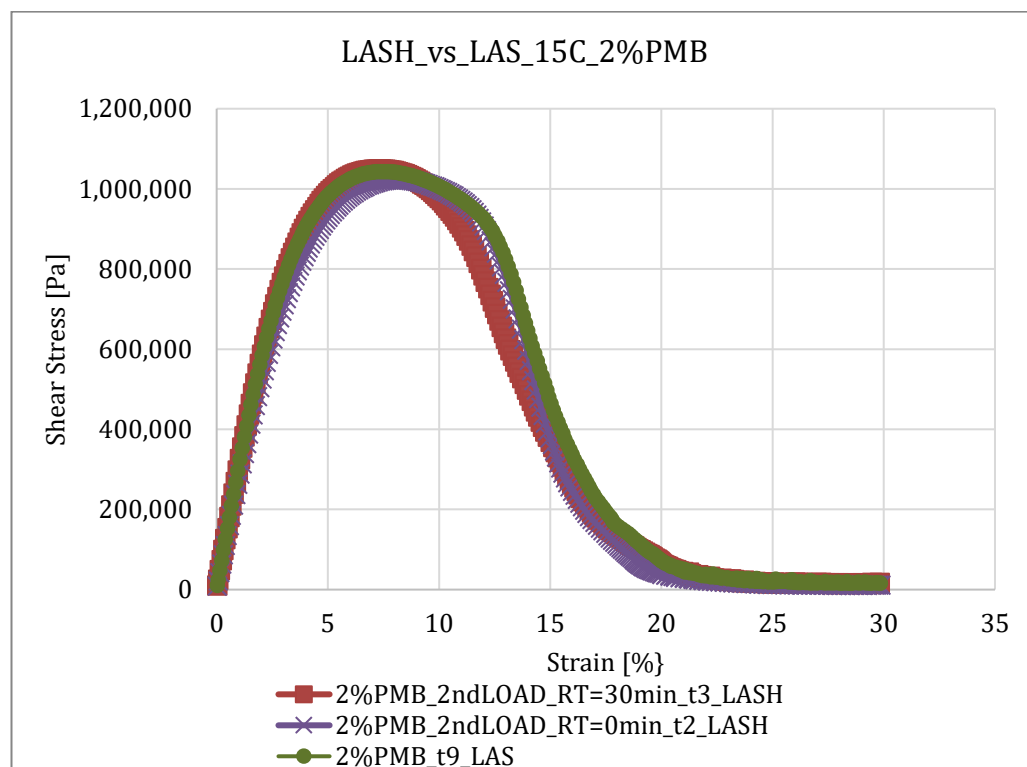


Figure 3.3.13 – At 15 °C (2 %PMB), LASH vs LAS test results.

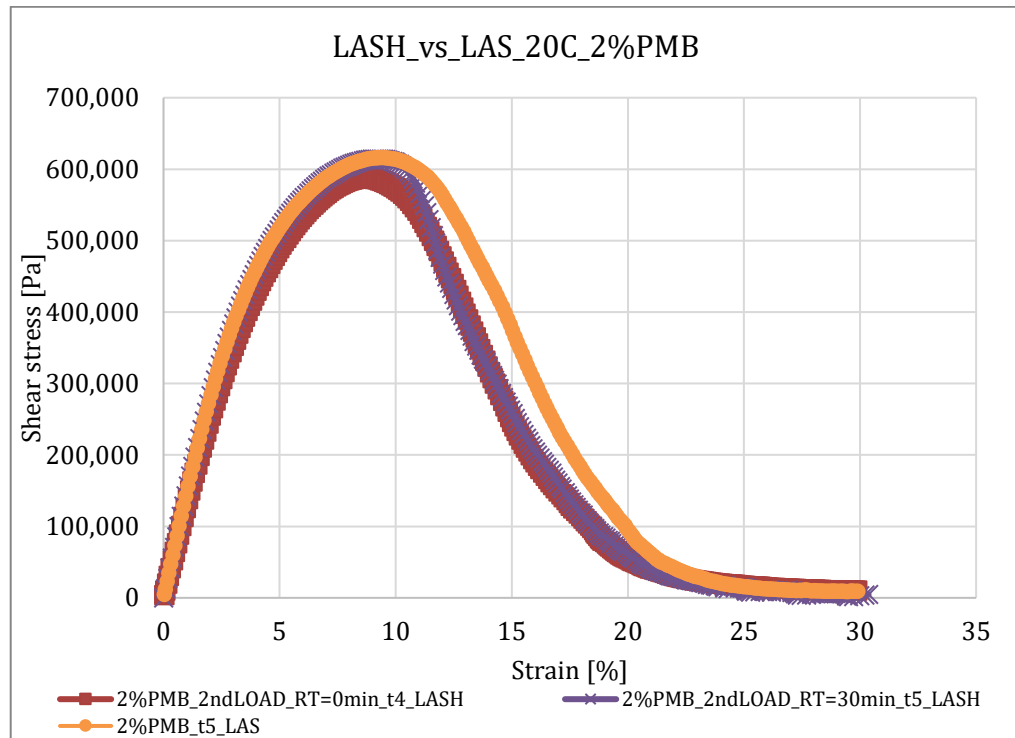


Figure 3.3.14 – At 20 °C (2 %PMB), LASH vs LAS test results.

From the comparative analysis, the following conclusions were drawn:

- At 20 °C, the RLDP-modified binders demonstrated stronger healing potential than at 15 °C, confirming that moderate temperatures promote bitumen self-diffusion without excessive viscous flow.
- The 2 % RLDP binder consistently achieved the highest healing index, indicating that lower additive concentration favours a more flexible polymer-bitumen network, enhancing molecular rearrangement during rest.
- The 4 % RLDP system, while showing slightly lower healing indices, provided greater fatigue durability and structural consistency across tests, suggesting a stiffer network with slower but more stable recovery dynamics.
- Comparisons with neat 50/70 binder data revealed that RLDP modification not only enhances fatigue resistance but also improves the capacity for mechanical recovery after damage, particularly when optimized at 2 %.

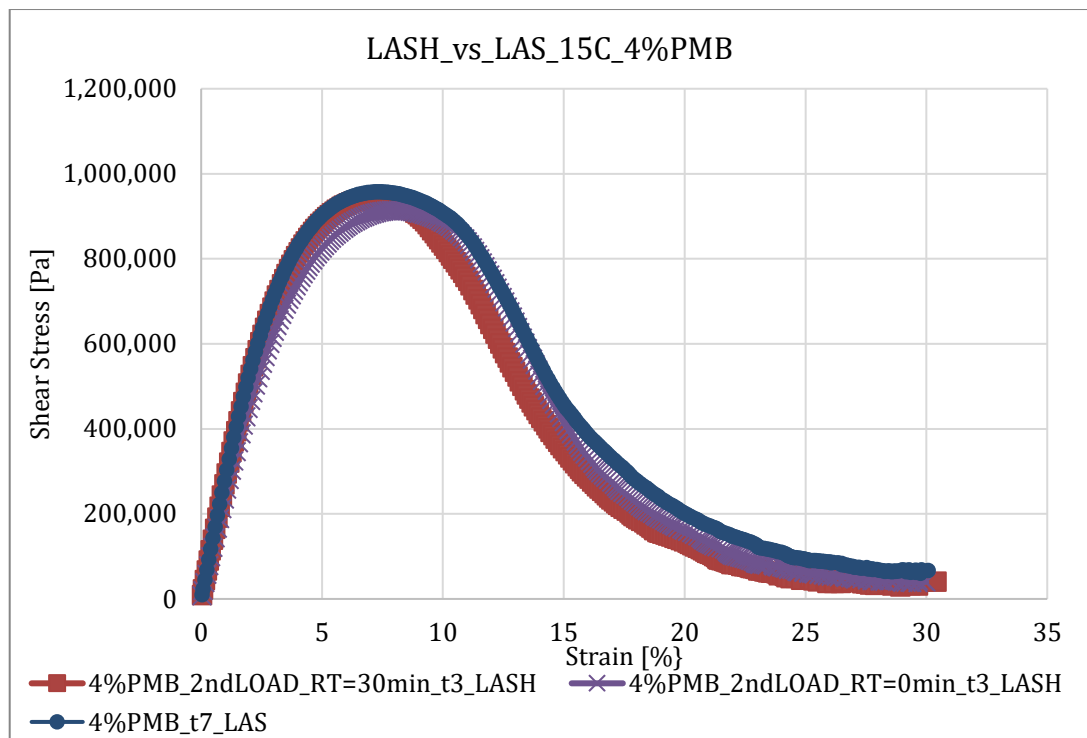


Figure 3.3.15 – At 15 °C (4 %PMB), LASH vs LAS test results.

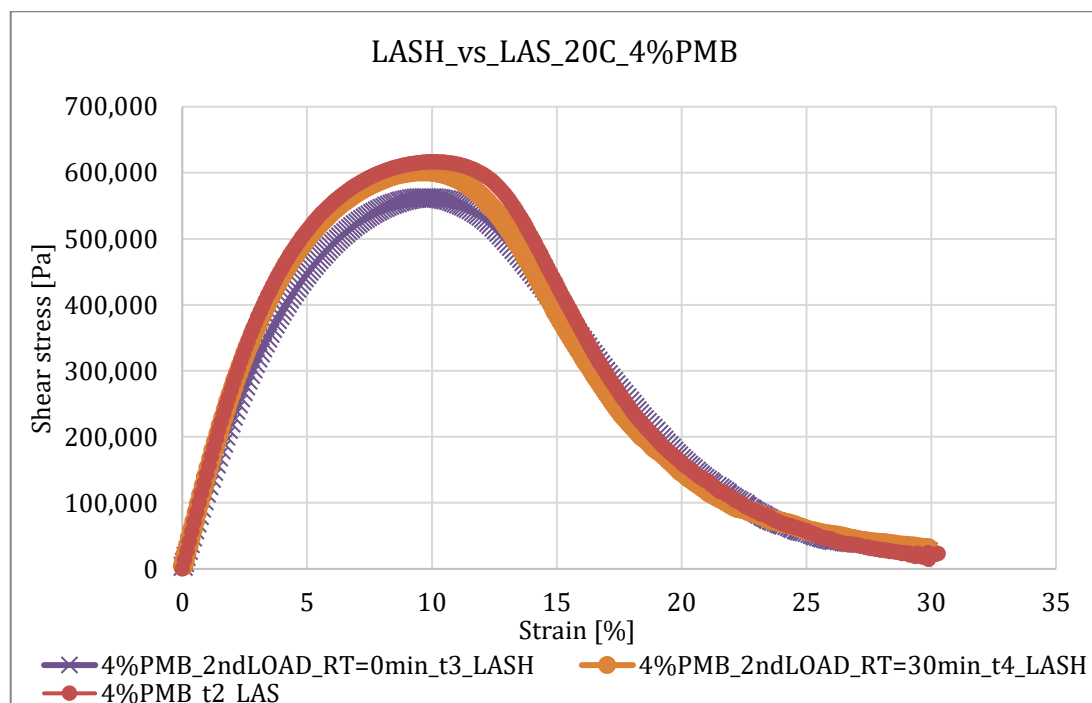


Figure 3.3.16 – At 20 °C (4 %PMB), LASH vs LAS test results.

Overall, the LAS-Healing tests confirmed the intrinsic self-healing capability of recycled-plastic-modified binders. The integration of RLDP contributes to a balance between stiffness and flexibility, enabling the binder to dissipate stress effectively and restore internal cohesion after micro-damage. This behaviour represents a crucial

advantage for sustainable pavement design, as it extends service life and reduces maintenance needs through autonomous recovery mechanisms.

3.4 LAS with Steric Hardening

The LAS-Steric Hardening (LAS-SH) test was carried out to investigate whether the mechanical response observed during LAS-Healing tests was influenced by time-dependent stiffening phenomena rather than by a genuine recovery of viscoelastic properties. This distinction is crucial because asphalt binders may exhibit an apparent strength increase during rest periods that originates from steric or structural rearrangements rather than from true molecular diffusion and self-healing.

In this context, the LAS-SH test was performed on the same RLDP-modified binders (2 % and 4 %) at 15 °C and 20 °C, following the same loading sequence as the LAS-Healing protocol but omitting the rest period between the two loading phases. This approach allows isolating the contribution of physical hardening from that of intrinsic healing.

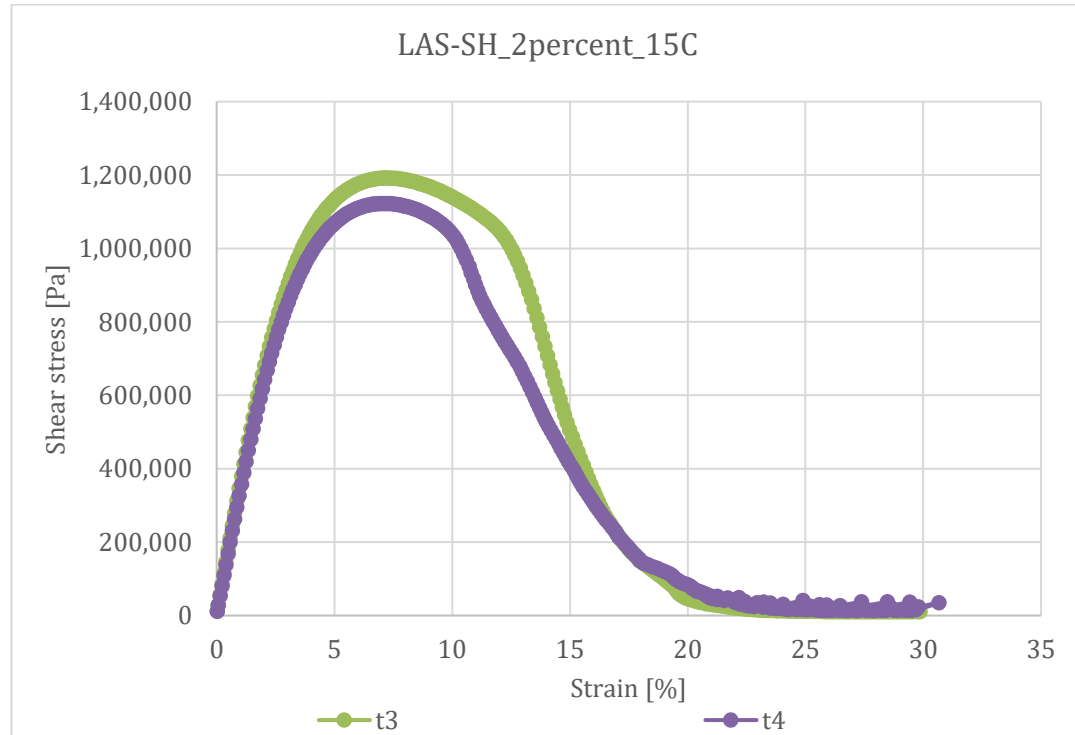


Figure 3.4.1 – LAS-SH 2 % PMB at 15 °C

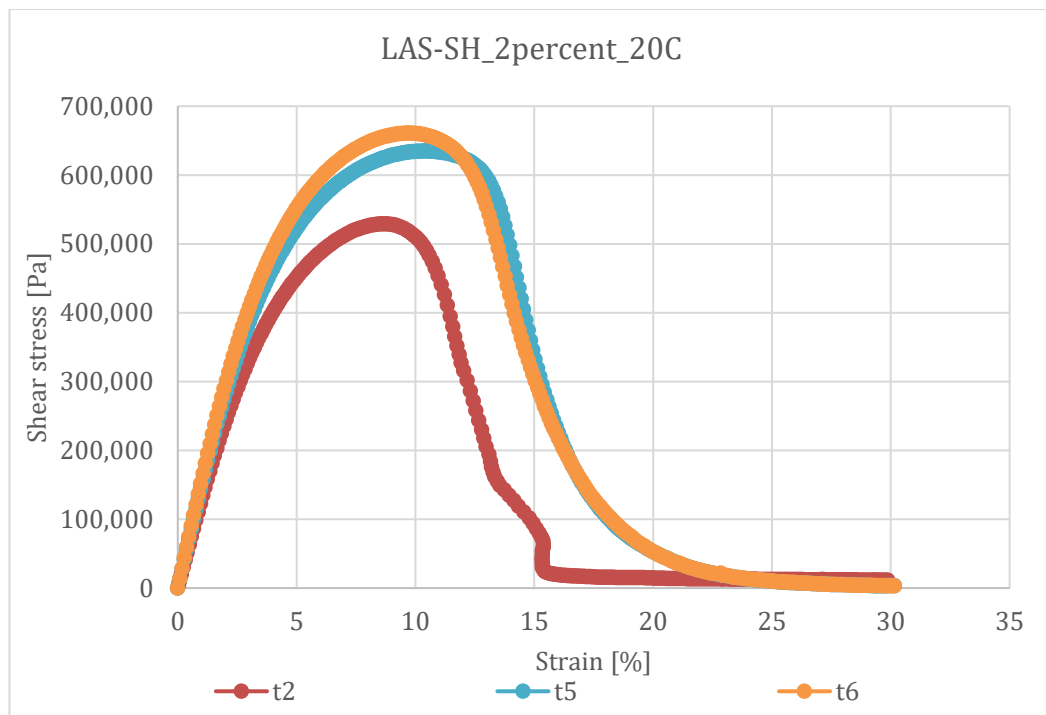


Figure 3.4.2 – LAS-SH 2 % PMB at 20 °C

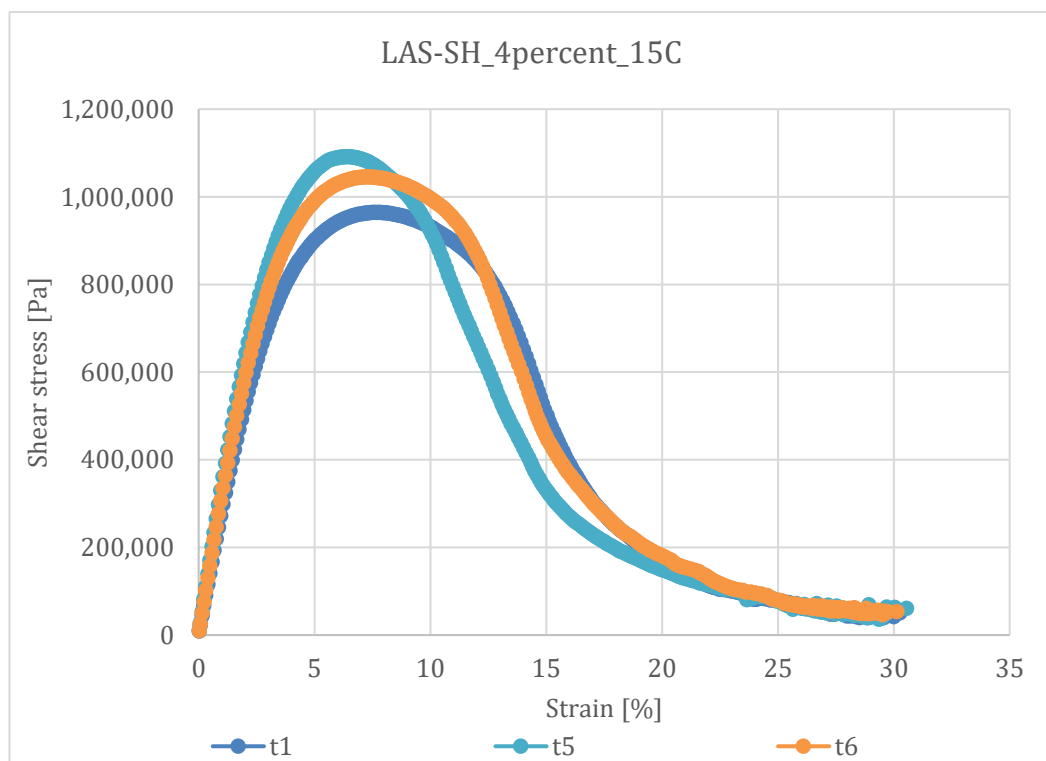


Figure 3.4.3 – LAS-SH 4 % PMB at 15 °C

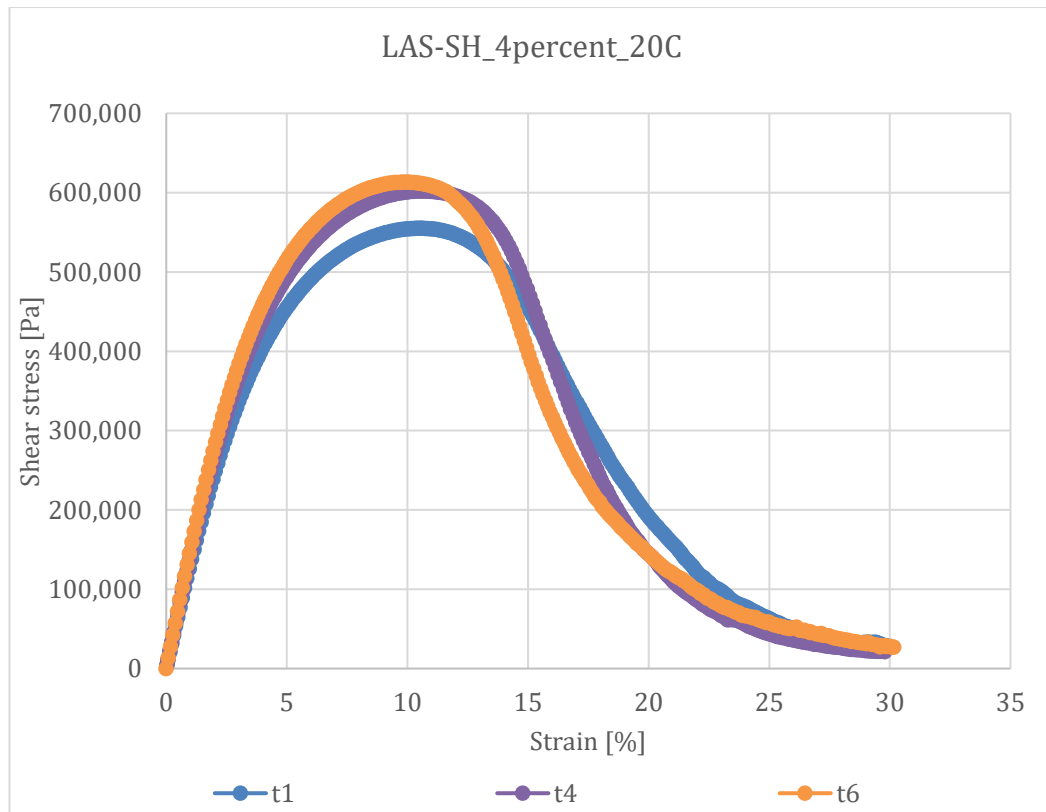


Figure 3.4.4 – LAS-SH 4 % PMB at 20 °C

The shear-stress versus strain curves in Figures 3.4.1 to 3.4.4 reveal consistent patterns across the different binders and temperatures. In all cases, the first loading phase produces a typical bell-shaped response, characterized by an initial linear viscoelastic region followed by a rapid increase in stress until reaching the maximum shear stress (τ_{peak}) and a subsequent sharp drop associated with fatigue damage accumulation.

During the second loading phase, performed immediately after the first without rest, the stress–strain curve almost perfectly overlaps with the first one, confirming the absence of recovery phenomena. This indicates that any variation in mechanical response observed in the LAS-Healing tests can be attributed to the rest period rather than to steric hardening effects.

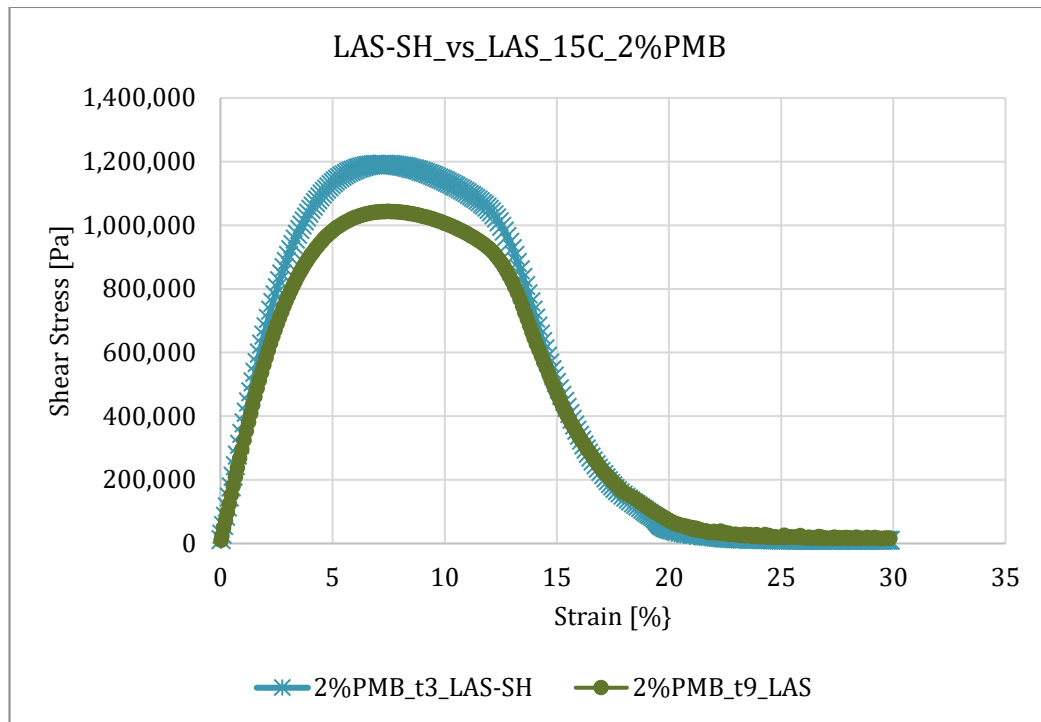


Figure 3.4.5 – At 15 °C (2 %PMB), LAS-SH vs LAS test results.

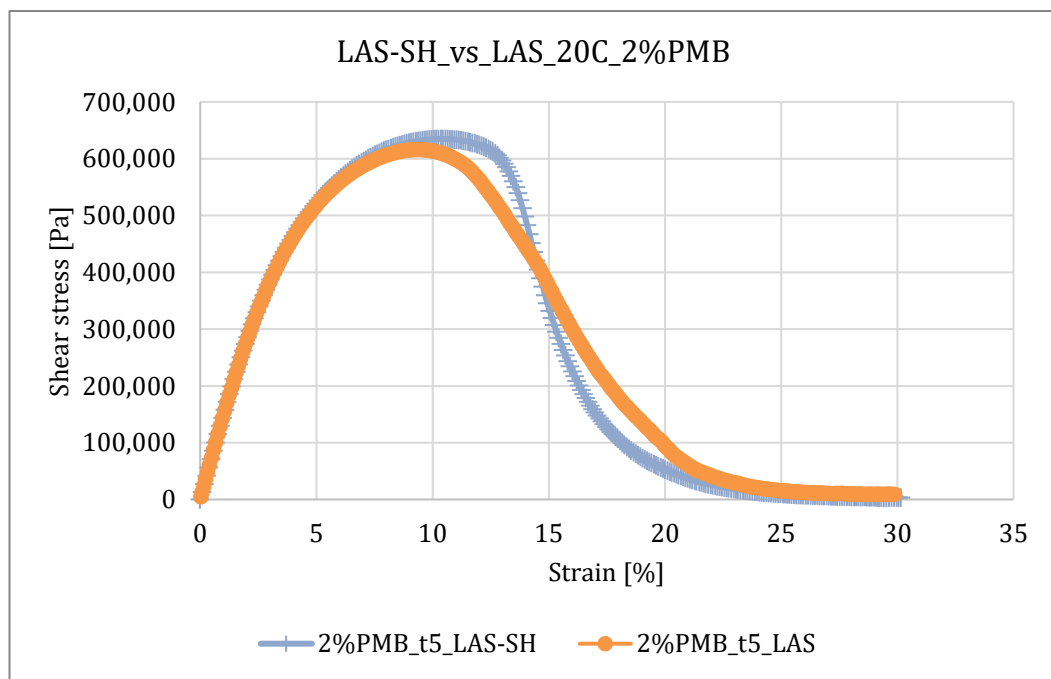


Figure 3.4.6 – At 20 °C (2 %PMB), LAS-SH vs LAS test results.

For the 2 % RLDP binder, both at 15 °C and 20 °C, the first and second loadings exhibit nearly identical τ_{peak} values and strain levels at failure. This suggests that at lower polymer content the molecular structure remains relatively mobile, preventing notable structural stiffening within the short timescale of the test.

Conversely, the 4 % RLDP binder shows a slightly higher stress response at the beginning of the second loading, particularly at 20 °C. This minor increase could be attributed to densification or rearrangement of the polymeric network caused by the first loading, although the overall difference remains small. Therefore, even for the highest plastic content, the steric hardening contribution is considered negligible compared to the effects of true healing observed in the LAS-H tests.

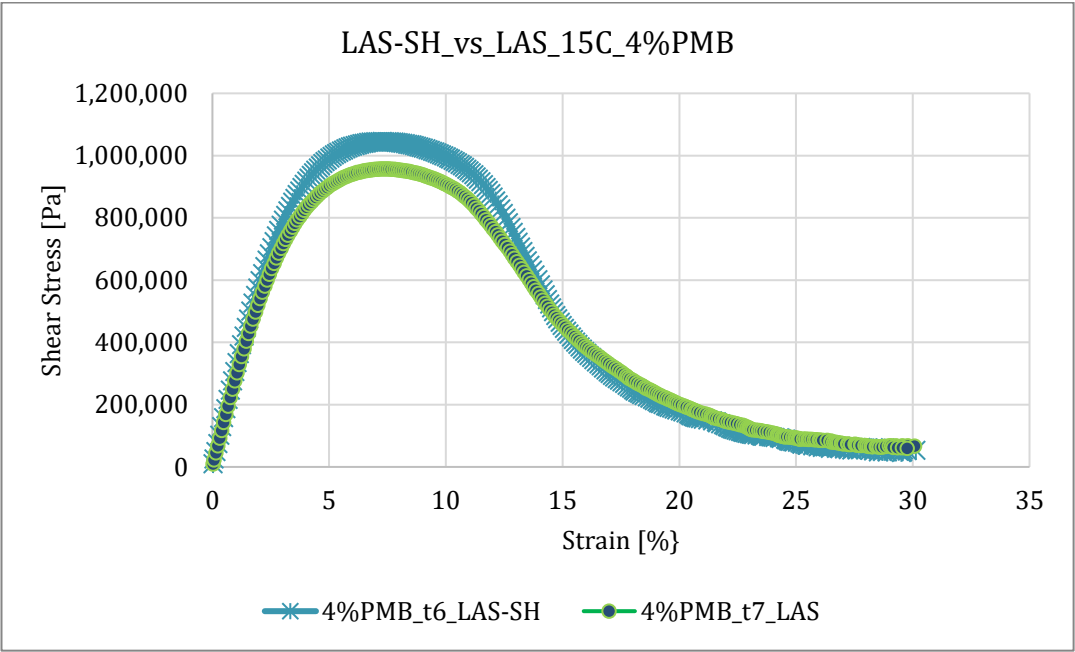


Figure 3.4.7 – At 15 °C (4 %PMB), LAS-SH vs LAS test results.

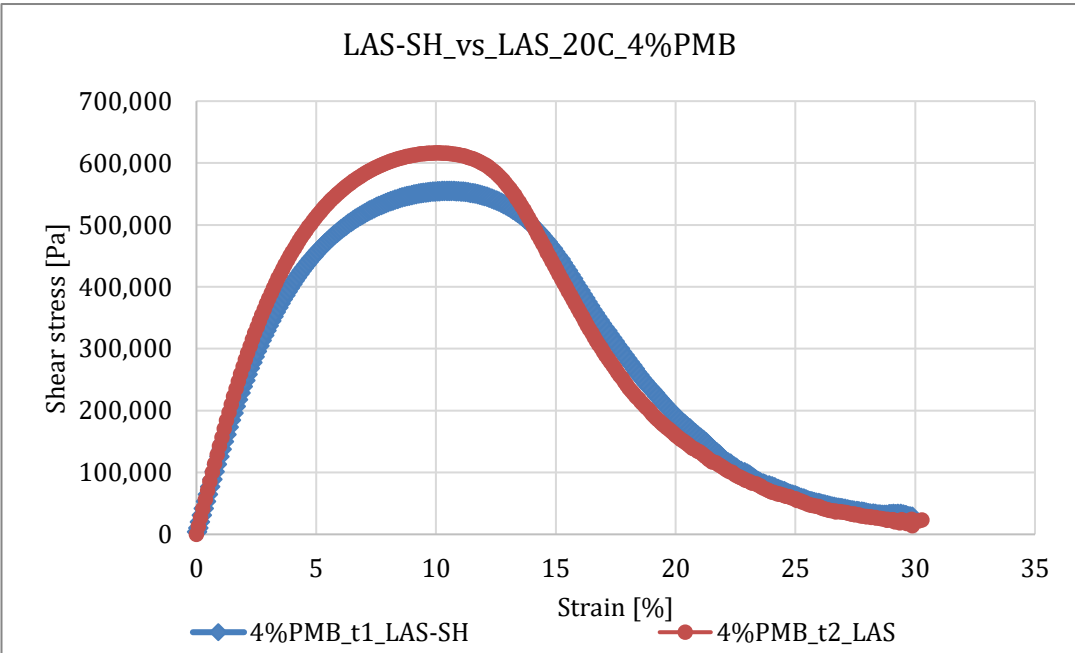


Figure 3.4.8 – At 20 °C (4 %PMB), LAS-SH vs LAS test results.

To quantitatively assess this behaviour, the peak shear stress (τ_{peak}) and corresponding strain (γ_{peak}) were extracted for each trial.

for 15C:		for 20C:	
Specimen type	$\gamma(\text{at } \tau \text{ peak})$	Specimen type	$\gamma(\text{at } \tau \text{ peak})$
	[%]		[%]
PMB2%	7.00	PMB2%	10.00
PMB4%	7.00	PMB4%	10.00

Table 3.4.1 – Strain Values at Peak shear stress for LAS-SH Tests

Overall, the LAS-Steric Hardening analysis confirms that the increase in stiffness and fatigue resistance observed after rest periods in LAS-Healing tests originates primarily from the intrinsic healing capacity of the material rather than from structural hardening. The minimal difference between the two consecutive loadings validates the experimental setup and supports the reliability of the healing quantification procedure applied in this study.

3.5 Quantitative Evaluation of Self-Healing Behavior

Because the S-VECD damage model was not adopted in this research, the quantification of self-healing was carried out using two complementary analytical approaches based solely on the experimental LAS, LAS-H, and LAS-SH results. These approaches were developed to distinguish the portion of stiffness recovery attributable to healing from that caused by steric hardening, and to evaluate how the two RLDP-modified binders respond to damage and rest periods at different temperatures. The two methods differ in structure and purpose: the first focuses on shear stress recovery at a fixed deformation level, while the second evaluates healing through improvements in fatigue life using the AASHTO TP-101 formulation. Taken together, these methods provide a comprehensive picture of the healing behaviour of the modified binders. To organise the subsequent calculations, a consolidated set of averaged results was first prepared (Table 3.5.1 and Table 3.5.2). This table summarises the values that were ultimately selected for analysis, representing only those trials deemed reliable and consistent based on their convergence and experimental stability.

2%PMB_LAS_15C, $\gamma = 7.0\%$ or γ at peak			2%PMB_LAS_20C, $\gamma = 9\%$ or γ at peak		
trial #	τ	γ	trial #	τ	γ
	[Pa]	[%]		[Pa]	[%]
6	1002870	7.0	4	599260	8.8
8	1098530	7.0	5	615472	9.0
9	1041570	7.0	6	664516	9.0
Average	1047657	7.0	Average	626416	8.9
2%PMB_LASH_15C_RT=30min_1st LOAD, $\gamma = 7.0\%$ or γ at peak			2%PMB_LASH_20C_RT=30min_1st LOAD, $\gamma = 9\%$ or γ at peak		
trial #	τ	γ	trial #	τ	γ
	[Pa]	[%]		[Pa]	[%]
3	1004250	7.0	3	620062	9.0
4	986968	7.0			
5	950214	7.0	5	624780	10.0
6	961401	7.0	Average	622421	9.5
Average	975708	7.0			
2%PMB_LASH_15C_RT=30min_2nd LOAD, $\gamma = 7.0\%$ or γ at peak			2%PMB_LASH_20C_RT=30min_2nd LOAD, $\gamma = 9\%$ or γ at peak		
trial #	τ	γ	trial #	τ	γ
	[Pa]	[%]		[Pa]	[%]
3	1047250	7.0	3	618176	9.0
4	1024370	7.0			
5	999627	7.0	5	614000	9.0
6	988999	7.0	Average	616088	9.0
Average	1015062	7.0			
2%PMB_LASH_15C_RT=0min_2nd LOAD, $\gamma = 7.0\%$ or γ at peak			2%PMB_LASH_20C_RT=0min_2nd LOAD, $\gamma = 9\%$ or γ at peak		
trial #	τ	γ	trial #	τ	γ
	[Pa]	[%]		[Pa]	[%]
1	852047	6.7	4	587864	8.7
2	1012570	7.0	5	621190	9.0
3	995301	7.0			
Average	953306	7.0	Average	604527	9
2%PMB_LAS-SH_15C, $\gamma = 7.0\%$ or γ at peak			2%PMB_LAS-SH_20C, $\gamma = 9\%$ or γ at peak		
trial #	τ	γ	trial #	τ	γ
	[Pa]	[%]		[Pa]	[%]
3	1190820	7.0	2	529261	8.7
4	1122100	7.0	5	628464	9.0
			6	658385	9.0
Average	1156460	7.0	Average	605370	8.9

Table 3.5.1 – Results of 2%PMB at reference γ and at peak γ

4%PMB_LAS_15C, $\gamma = 7.0\%$ or γ at peak			4%PMB_LAS_20C, $\gamma = 9\%$ or γ at peak		
trial #	τ	γ	trial #	τ	γ
	[Pa]	[%]		[Pa]	[%]
1	1008520	7.0	1	595915	9.0
			2	612472	9.0
7	956407	7.0			
Average	982464	7.0	Average	604194	9.0
4%PMB_LASH_15C_RT=30min_1st LOAD, $\gamma = 7.0\%$ or γ at peak			4%PMB_LASH_20C_RT=30min_1st LOAD, $\gamma = 9\%$ or γ at peak		
trial #	τ	γ	trial #	τ	γ
	[Pa]	[%]		[Pa]	[%]
1	955828	7.0			
2	940474	7.0	3	599801	9.0
3	918001	7.0	4	610489	9.0
4	933044	7.0	Average	605145	9.0
Average	936837	7.0			
4%PMB_LASH_15C_RT=30min_2nd LOAD, $\gamma = 7.0\%$ or γ at peak			4%PMB_LASH_20C_RT=30min_2nd LOAD, $\gamma = 9\%$ or γ at peak		
trial #	τ	γ	trial #	τ	γ
	[Pa]	[%]		[Pa]	[%]
1	1002890	7.0			
2	961651	7.0	3	590541	9.0
3	942623	7.0	4	600778	9.0
4	969479	7.0	Average	595660	9.0
Average	969161	7.0			
4%PMB_LASH_15C_RT=0min_2nd LOAD, $\gamma = 7.0\%$ or γ at peak			4%PMB_LASH_20C_RT=0min_2nd LOAD, $\gamma = 9\%$ or γ at peak		
trial #	τ	γ	trial #	τ	γ
	[Pa]	[%]		[Pa]	[%]
1	934891	7.0	1	581197	9.0
2	898977	7.0	2	547558	9.0
3	903908	7.0	3	558739	9.0
Average	912592	7.0	Average	562498	9
4%PMB_LAS-SH_15C, $\gamma = 7.0\%$ or γ at peak			4%PMB_LAS-SH_20C, $\gamma = 9\%$ or γ at peak		
trial #	τ	γ	trial #	τ	γ
	[Pa]	[%]		[Pa]	[%]
1	961173	7.0	1	548522	9.0
5	1091910	6.4	4	594516	9.0
6	1044810	7.0	6	610376	9.0
Average	1032631	6.8	Average	584471	9.0

Table 3.5.2 – Results of 4%PMB at reference γ and at peak γ

3.5.1 Method 1 — Healing Assessment at a Fixed Reference Strain

The first method is based on the comparison of shear stress values at a fixed strain level. This approach was chosen because the strain corresponding to peak shear stress differed noticeably from trial to trial, especially in the modified binders. In several repetitions, the peak occurred at strains higher than the expected value, ranging between 7% and 10%. This variability makes direct peak-to-peak comparison unreliable and can lead to misleading conclusions about healing capacity. To ensure consistent evaluation, a reference strain was defined for each temperature, corresponding to the typical strain range where the peak shear stress occurred during the LAS tests: 7% for 15°C and 9% for 20°C.

At these reference strain levels, shear stress values were taken from the LAS curve (representing the undamaged material), the first load of LAS-H (the damaged state), the second load of LAS-H after a 30-minute rest period (potentially healed state), and the second load of LAS-SH (steric hardening baseline). When these values are placed side-by-side, they allow a direct comparison between the recovered stress and the portion of stiffness increase caused only by steric re-arrangement. The steric component was removed using the LAS-SH curve so that only true healing remained.

The behaviour at 15°C was consistent across all binders. After subtracting the steric hardening effect, the net recovery was extremely small, confirming that the increase in shear stress during the reloading of LAS-H was almost entirely due to steric hardening rather than molecular healing. At this temperature, both the 2% and 4% RLDP binders behave as relatively stiff materials, with limited molecular mobility. As a result, internal microcracks do not close effectively and the material does not regain measurable stiffness, even after a resting period.

At 20°C, the behaviour was fundamentally different. When the same reference-strain comparison was made, both RLDP-modified binders showed measurable recovery after rest. The 2% RLDP binder displayed the highest degree of recovery, achieving a healing index of roughly 60%, indicating that a significant portion of the damage induced during the first load was reversed during the rest period. The 4% RLDP binder exhibited a lower healing index, approximately 26%, which suggests that the

increased stiffness from higher plastic dosage reduces the ability of the material to realign and re-bond its molecular structure. Method 1 therefore confirms that healing is strongly temperature-dependent and that lower polymer dosage favours a more flexible configuration conducive to healing.

Next formulations were assumed for calculation of “Healing Index”:

$$\Delta Damage = \tau_{peak}(LAS-H_{(1stload)}) - \tau_{peak}(LAS-H_{(2ndLoad)_{RT=0min}})$$

$$\Delta SH = \tau_{peak}(LAS-SH) - \tau_{peak}(LAS-H_{(2ndLoad)_{RT=0min}})$$

$$\Delta (H + SH) = \tau_{peak}(LAS-H_{(2ndLoad)_{RT=30min}}) - \tau_{peak}(LAS-H_{(2ndLoad)_{RT=0min}})$$

$$\Delta H = \frac{\Delta(H+SH) - \Delta SH}{\Delta Damage}$$

1) Calculation of “Healing Index” of 2%PMB with RLDP at 15°C:

trial #	15C_PMB2%	τ (ref) [Pa]	τ (ref) [MPa]	γ [%]	G*
AVG	LAS	1047657	1.048	7.0	0.15
AVG	LAS-H 1st Load (RT=30min)*	975708	0.976	7.0	0.14
AVG	LAS-H 2nd Load (RT=0min)	953306	0.953	7.0	0.14
AVG	LAS-H 2nd Load (RT=30min)	1015062	1.015	7.0	0.15
AVG	LAS-SH	1156460	1.156	7.0	0.17

Table 3.5.1.1 – Results of average values at 15°C of 2%PMB at reference γ and at peak γ

$$\Delta Damage = 0.976 - 0.953 = 0.022 [MPa]$$

$$\Delta SH = 1.156 - 0.953 = 0.203 [MPa]$$

$$\Delta (H + SH) = 1.015 - 0.953 = 0.062 [MPa]$$

$$\Delta H = \frac{0.062 - 0.203}{0.022} = -6.31, \text{ which means, no “healing”, due to the negative value}$$

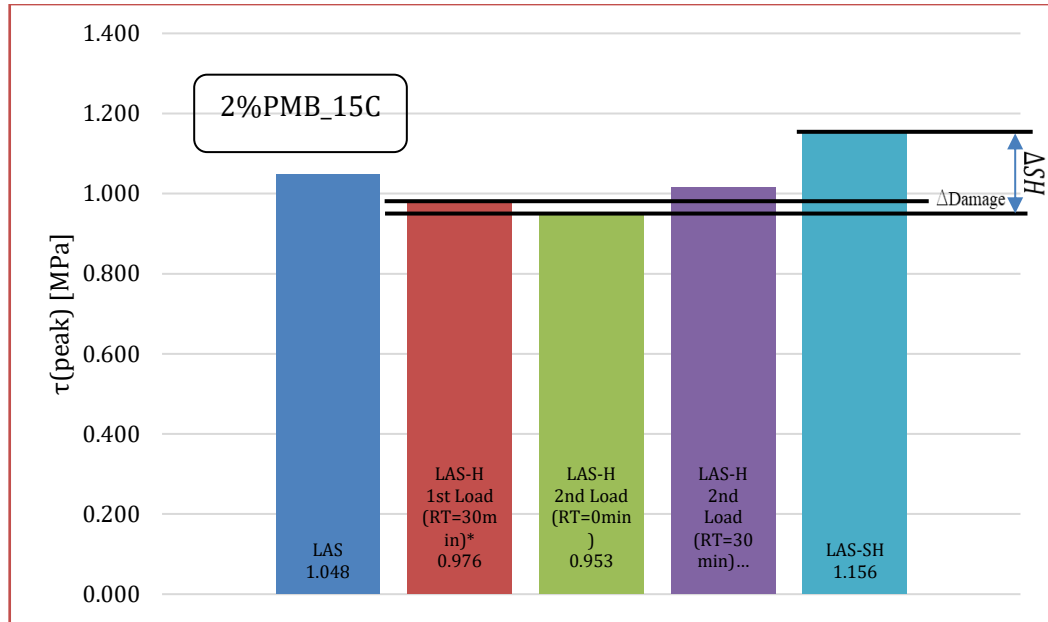


Figure 3.5.1.1 – At 15 °C (2 %PMB), comparison of results of all protocols used.

2) Calculation of “Healing Index” of 2%PMB with RLDP at 20°C:

trial #	20C_PMB2%	τ(ref) [Pa]	τ(ref) [MPa]	γ [%]	G*
AVG	LAS	626416	0.626	9.0	0.070
AVG	LAS-H 1st Load (RT=30min)*	622421	0.623	9.0	0.069
AVG	LAS-H 2nd Load (RT=0min)	604527	0.605	9.0	0.067
AVG	LAS-H 2nd Load (RT=30min)	616088	0.616	9.0	0.068
AVG	LAS-SH	605370	0.606	9.0	0.067

Table 3.5.1.2 – Results of average values at 15°C of 2%PMB at reference γ and at peak γ

$$\Delta Damage = 0.623 - 0.605 = 0.018 \text{ [MPa]}$$

$$\Delta SH = 0.606 - 0.605 = 0.001 \text{ [MPa]}$$

$$\Delta (H + SH) = 0.616 - 0.605 = 0.011 \text{ [MPa]}$$

$$\Delta H = \frac{0.011 - 0.001}{0.018} = 0.60, \text{ which means HI=60\%}.$$

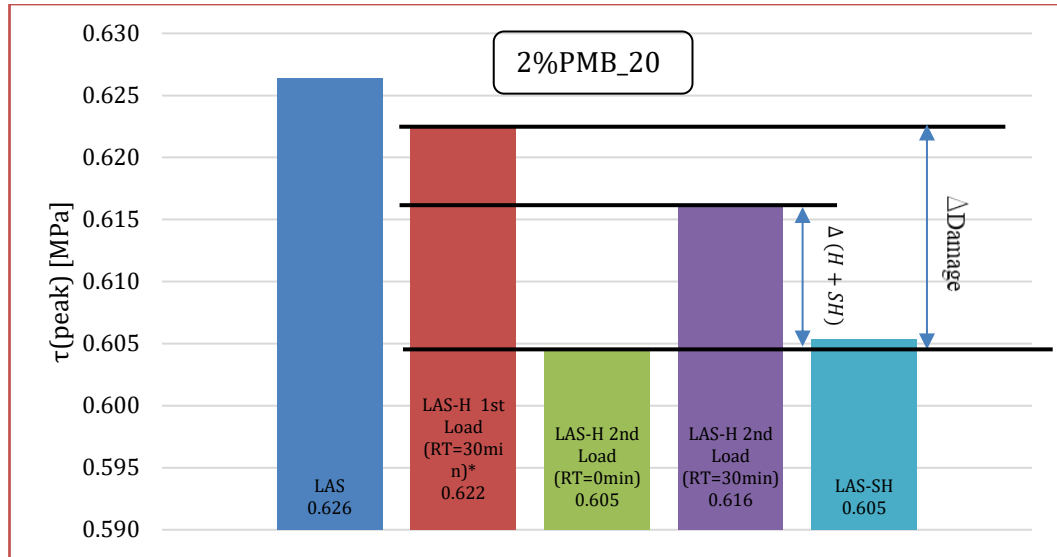


Figure 3.5.1.2 – At 20°C (2 %PMB), comparison of results of all protocols used.

3) Calculation of “Healing Index” of 4%PMB with RLDP at 15°C:

trial #	15C_PMB4%	τ(ref) [Pa]	τ(ref) [MPa]	γ [%]	G*
AVG	LAS	982463.500	0.982	7.00	0.140352
AVG	LAS-H 1st Load (RT=30min)*	936836.750	0.937	7.00	0.133834
AVG	LAS-H 2nd Load (RT=0min)	912592.000	0.913	7.00	0.13037
AVG	LAS-H 2nd Load (RT=30min)	969160.750	0.969	7.00	0.138452
AVG	LAS-SH	1032631.000	1.033	7.00	0.147519

Table 3.5.1.3 – Results of average values at 15°C of 4%PMB at reference γ and at peak γ

$$\Delta Damage = 0.937 - 0.913 = 0.024 [MPa]$$

$$\Delta SH = 1.033 - 0.913 = 0.120 [MPa]$$

$$\Delta (H + SH) = 0.969 - 0.913 = 0.057 [MPa]$$

$$\Delta H = \frac{0.057 - 0.120}{0.024} = -2.62, \text{ which means no “healing”, due to the negative value.}$$

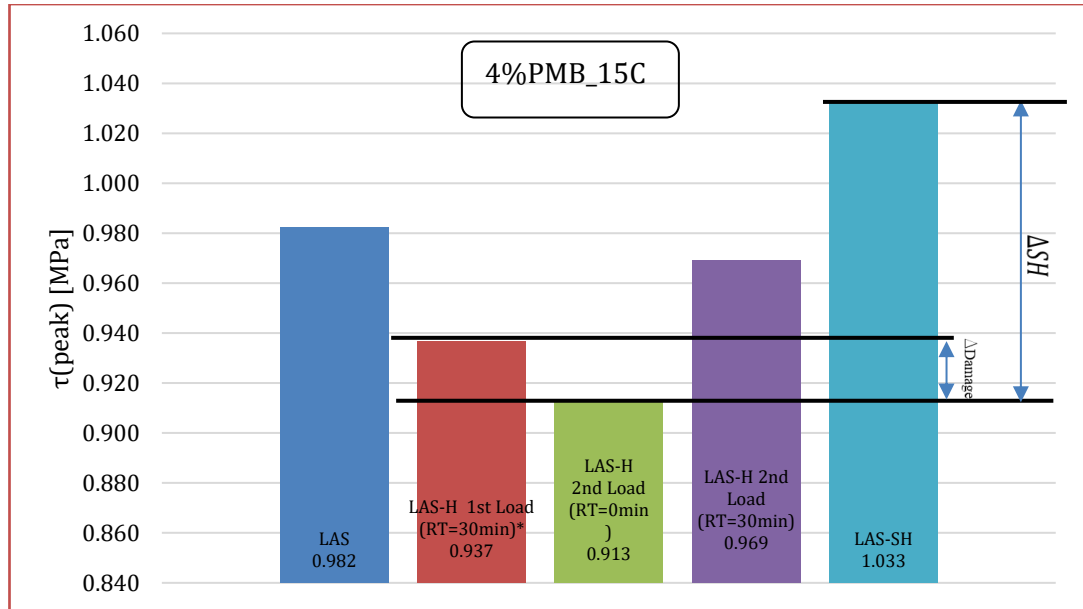


Figure 3.5.1.3 – At 15°C (4%PMB), comparison of results of all protocols used.

4) Calculation of “Healing Index” of 4%PMB with RLDP at 20°C:

trial #	20C_PMB4%	τ(ref) [Pa]	τ(ref) [MPa]	γ [%]	G*
AVG	LAS	604194	0.604	9.0	0.067
AVG	LAS-H 1st Load (RT=30min)*	605145	0.605	9.0	0.067
AVG	LAS-H 2nd Load (RT=0min)	562498	0.562	9.0	0.062
AVG	LAS-H 2nd Load (RT=30min)	595660	0.596	9.0	0.066
AVG	LAS-SH	584471	0.584	9.0	0.065

Table 3.5.1.4– Results of average values at 20°C of 4%PMB at reference γ and at peak γ

$$\Delta Damage = 0.605 - 0.562 = 0.043 [MPa]$$

$$\Delta SH = 0.584 - 0.562 = 0.022 [MPa]$$

$$\Delta (H + SH) = 0.596 - 0.562 = 0.033 [MPa]$$

$$\Delta H = \frac{0.033 - 0.022}{0.043} = 0.26, \text{ which means HI}=26\%.$$

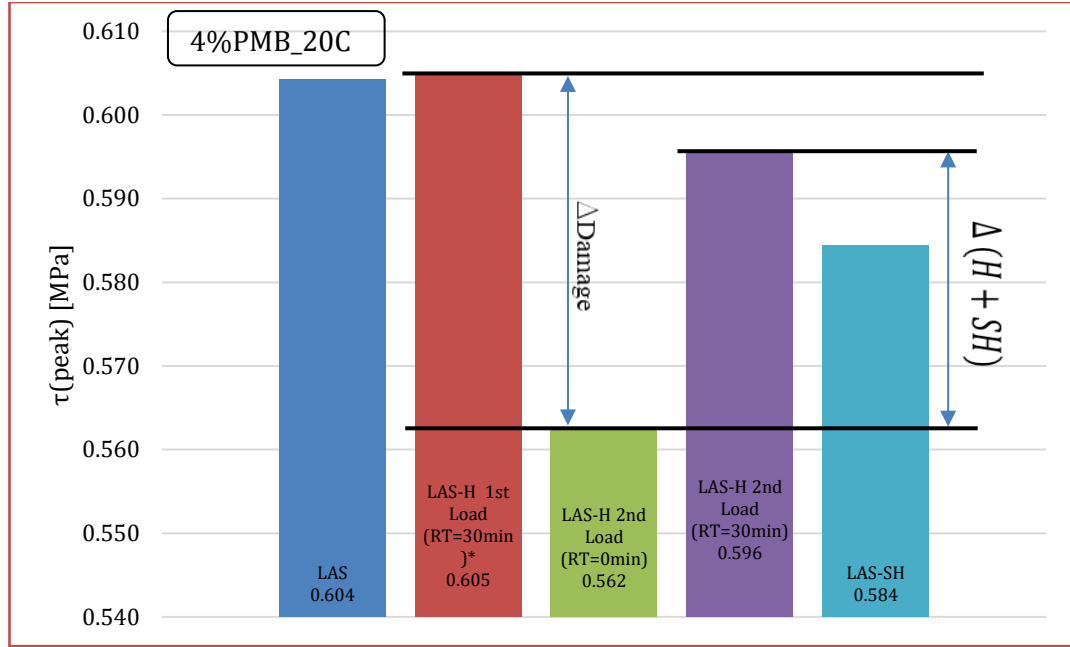


Figure 3.5.1.4 – At 20°C (4%PMB), comparison of results of all protocols used.

3.5.2 Method 2 — Self-Healing Analysis Based on the AASHTO TP-101

framework defined in AASHTO TP-101, which forms the basis of the Linear Amplitude Sweep (LAS) procedure. Although the standard was originally developed for estimating binder fatigue life under continuous strain-controlled loading, its damage-based formulation can also be applied to interrupted tests such as LAS-Healing (LAS-H). For this reason, the LAS-H results obtained in this thesis were processed using the TP-101 analytical procedure, allowing fatigue lives from the first and second loading phases to be compared in order to identify the presence of healing. According to AASHTO TP-101, fatigue behaviour in LAS is described through Continuum Damage Mechanics (CDM), where the deterioration of the binder is represented by an internal damage variable D . During the amplitude sweep, the strain increases linearly from 0 to 30 % over approximately 3,100 cycles at 10 Hz. For each measured point, damage accumulation is computed incrementally as:

$$D(t) \cong \sum_{i=1}^N [\pi \gamma_0^2 (C_{i-1} - C_i)]^{\frac{\alpha}{1+\alpha}} (t_i - t_{i-1})^{\frac{1}{1+\alpha}}$$

where

- $|G_0^*|$ is the undamaged modulus (second data point of LAS),
- $\gamma(t)$ is the applied shear strain at that measurement,
- $\alpha = 1/m$ is derived from the frequency sweep master curve, and
- Δt is the time increment between measurement points.

As the test progresses, the material integrity is expressed through:

$$C(t) = \frac{|G^*(t)|}{|G_0^*|}$$

and the relationship between integrity and damage is fitted using the TP-101 regression form:

$$\log(C_0 - C(t)) = \log(C_1) + C_2 * \log(D(t))$$

yielding the LAS fatigue model constants C_1 and C_2 . These values are then used to compute the fatigue law parameters:

$$A = \frac{(f(D_f))^k}{k(\pi * C_1 * C_2)^\alpha}$$

$$B = 2 * \alpha$$

and the predicted fatigue life is finally obtained from:

$$N_f = A * \gamma_{max}^{-B}$$

where γ_{max} is the maximum strain reached before complete material softening.

2%PMB_15C_LAS_AVERAGE

A	B	Applied Strain [%]	Nf
5.427E+05	3.738	1	542,733
		5.0	1,324
	γ (at τ peak)=	7.50	291

2%PMB_20C_LAS_AVERAGE

A	B	Applied Strain [%]	Nf
3.027E+05	3.074	1	302,661
		5.0	2,149
	γ (at τ peak)=	9.98	257

2%PMB_15C_RT=30min_LASH_AVG

A	B	Applied Strain [%]	Nf
3.986E+05	3.643	1	398,565
		5.0	1,133
		7.3	280

2%PMB_20C_RT=30min_LASH_AVG

A	B	Applied Strain [%]	Nf
3.560E+05	3.107	1	355,991
		5.0	2,399
		9.7	309

2%PMB_15C_RT=0min_LASH_AVG

A	B	Applied Strain [%]	Nf
5.837E+05	3.651	1	583,722
		5.0	1,638
		8.01	293

2%PMB_20C_RT=0min_LASH_AVG

A	B	Applied Strain [%]	Nf
2.659E+05	3.073	1	265,895
		5.0	1,890
		9.3	276

2%PMB_15C_LAS-SH_AVERAGE

A	B	Applied Strain [%]	Nf
4.682E+05	3.747	1	468,179
		5.0	1,126
	γ (at τ peak)=	7.15	295

2%PMB_20C_LAS-SH_AVERAGE

A	B	Applied Strain [%]	Nf
2.894E+05	3.036	1	289,356
		5.0	2,184
	γ (at τ peak)=	9.25	337

Table 3.5.2.1– Results analysis of average values of 2%PMB, with respect to AASHTO TP 101.

4%PMB_15C_LAS_AVERAGE

A	B	Applied Strain [%]	Nf
9.450E+05	3.986	1	944,987
		5.0	1,545
	γ (at τ peak)=	7.48	311

4%PMB_20C_LAS_AVERAGE

A	B	Applied Strain [%]	Nf
7.229E+05	3.349	1	722,852
		5.0	3,297
	γ (at τ peak)=	9.88	337

4%PMB_15C_RT=30min_LASH_AVG

A	B	Applied Strain [%]	Nf
5.586E+05	3.923	1	558,608
		5.0	1,012
	γ (at τ peak)=	7.04	264

4%PMB_20C_RT=30min_LASH_AVG

A	B	Applied Strain [%]	Nf
5.172E+05	3.354	1	517,230
		5.0	2,339
	γ (at τ peak)=	9.14	309

4%PMB_15C_RT=0min_LASH_AVG				4%PMB_20C_RT=0min_LASH_AVG				
A	B	Applied Strain [%]	Nf		A	B	Applied Strain [%]	Nf
1.220E+06	3.952	1	1,219,870		5.612E+05	3.330	1	561,188
		5.0	2,108				5.0	2,640
	γ (at τ peak)=	8.15	306			γ (at τ peak)=	9.44	318

4%PMB_15C_LAS-SH_AVERAGE			
A	B	Applied Strain [%]	Nf
8.599E+05	4.008	1	859,890
		5.0	1,358
	γ (at τ peak)=	7.13	328

4%PMB_20C_LAS-SH_AVERAGE			
A	B	Applied Strain [%]	Nf
8.657E+05	3.347	1	865,694
		5.0	3,963
	γ (at τ peak)=	10.33	349

Table 3.5.2.2– Results analysis of average values of 4%PMB, with respect to AASHTO TP 101.

At 15°C, the fatigue-life curves showed considerable overlap and scatter, consistent with a material that behaves predominantly in a stiff and brittle manner. The LAS-H tests with and without rest produced fatigue-life curves similar in shape, and no significant shift was observed in the LAS-H (30-minute) curve. Likewise, the LAS-SH curves were almost indistinguishable from the rest and provided no evidence of healing. These similarities once again indicate that, at low temperature, the rest period does not allow the material to recover from damage. The dominance of steric hardening is evident, and the fatigue behaviour is mainly governed by the inherent rheological rigidity of the binder.

At 20°C, however, the fatigue-life curves revealed an entirely different pattern. The LAS-H test with a 30-minute rest consistently showed the highest fatigue life at the beginning of the curve, particularly at low strain amplitudes where the effect of healing is most pronounced. In contrast, the LAS-H test with zero rest time showed a clear reduction in fatigue resistance, consistent with the expected behaviour of a fully damaged material. The LAS-SH curve, representing steric hardening alone, always remained below the LAS-H (30-minute rest) curve, demonstrating that the increase in fatigue life was not caused by steric effects but by actual molecular healing. The larger

upward shift observed for the 2% RLDP binder further confirms that a moderate amount of RLDP allows better healing than the stiffer 4% RLDP binder.

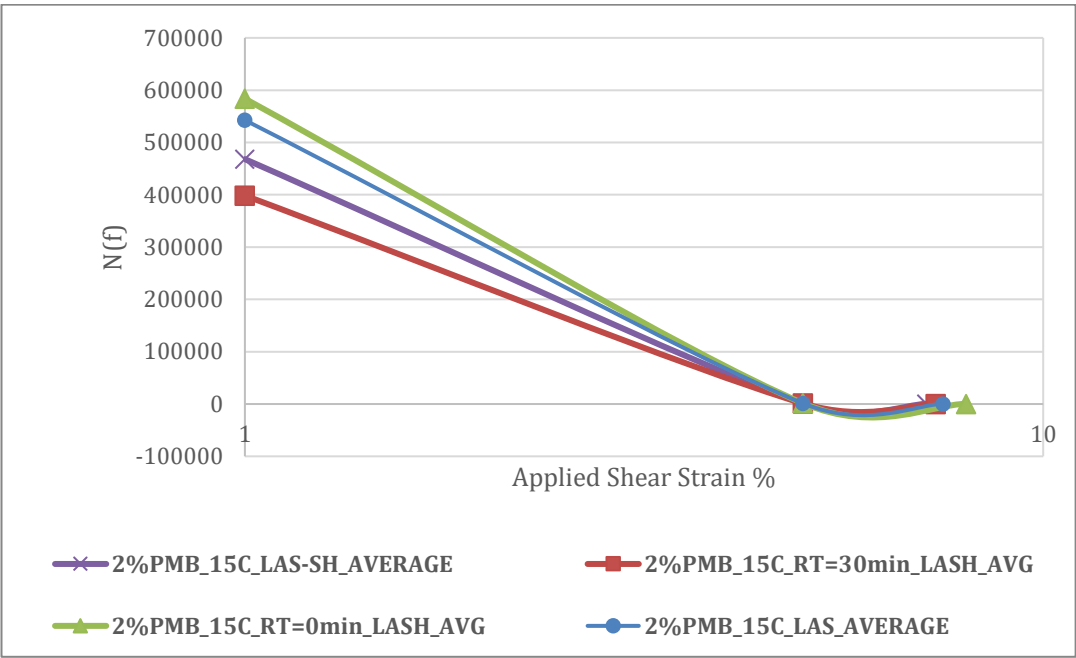


Figure 3.5.2.1 – At 15°C (2%PMB), comparison of results of all protocols used, with respect to AASHTO TP 101.

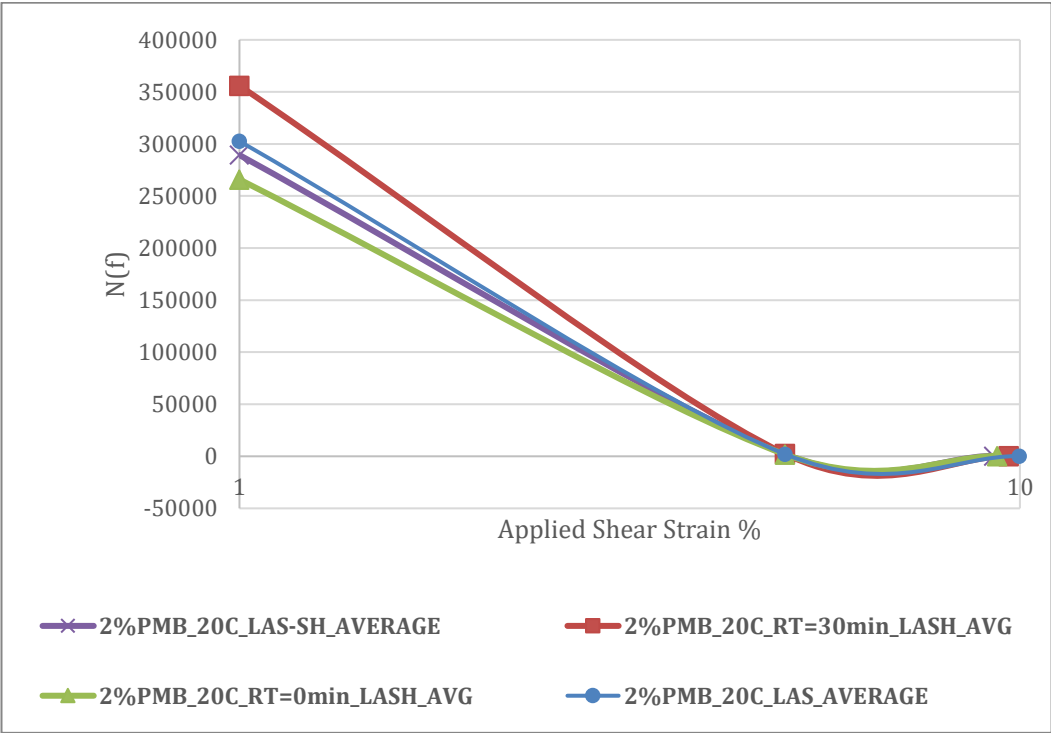


Figure 3.5.2.2 – At 20°C (2%PMB), comparison of results of all protocols used, with respect to AASHTO TP 101.

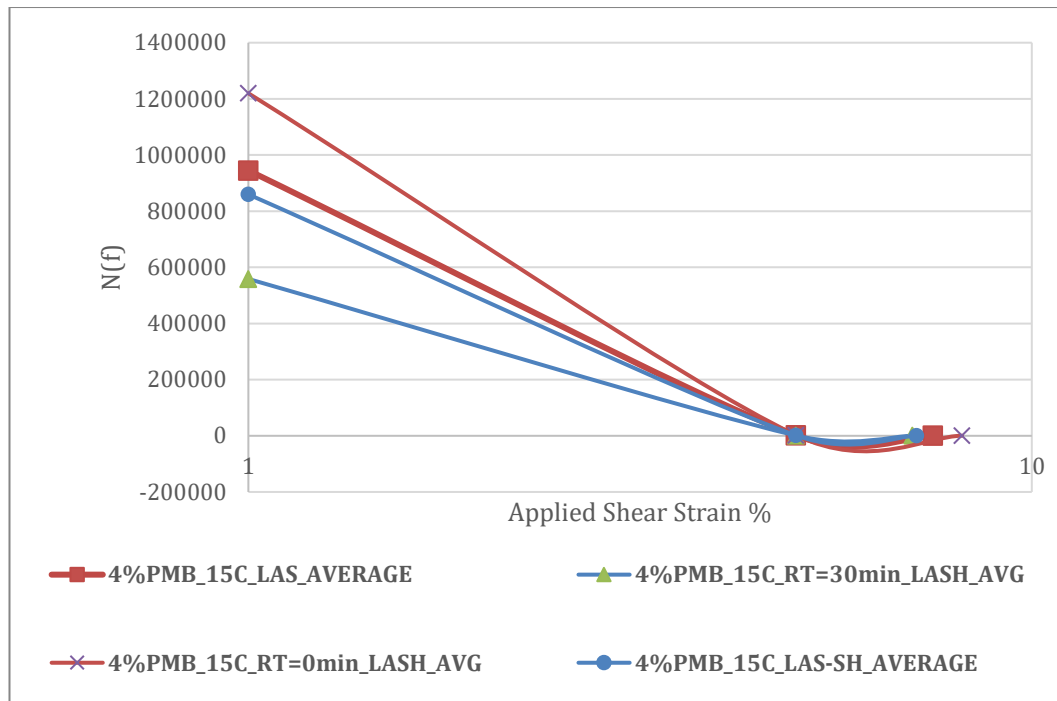


Figure 3.5.2.3 – At 15°C (4%PMB), comparison of results of all protocols used, with respect to AASHTO TP 101.

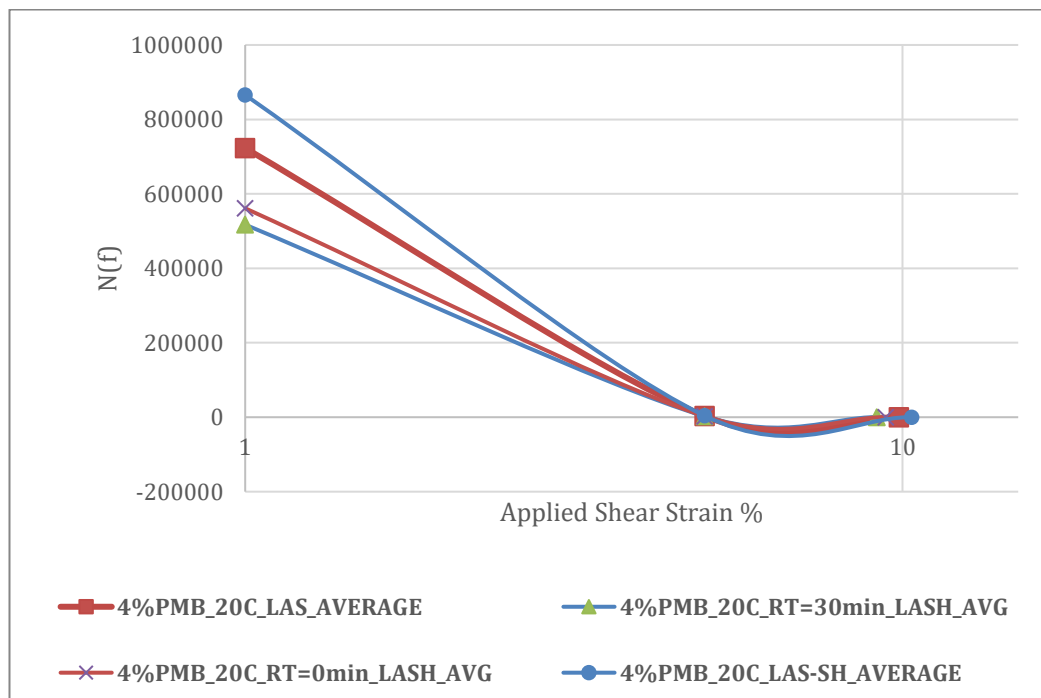


Figure 3.5.2.4 – At 20°C (4%PMB), comparison of results of all protocols used, with respect to AASHTO TP 101.

Both methods—despite their methodological differences—arrive at the same physical conclusions. The binders show no meaningful healing at 15°C, where the increase in stiffness after rest is entirely due to steric hardening and not molecular restoration. At 20°C, healing is consistently observed, with the 2% RLDP binder demonstrating stronger healing capacity than the 4% RLDP binder, both in local stiffness recovery and in fatigue-life enhancement. This combined evaluation confirms that healing in bituminous binders is highly temperature-dependent and strongly influenced by the level of polymer modification. The dual-method analysis adopted here provides a reliable and robust assessment of healing behaviour, offering a clear interpretation even without the use of the S-VECD framework.

CHAPTER 4 – CONCLUSION

The objective of this thesis was to investigate the fatigue resistance and self-healing behaviour of bituminous binders modified with Recycled Low-Density Plastic (RLDP), comparing two newly prepared formulations (2% and 4% RLDP) with a reference neat 50/70 binder. Through an integrated experimental program consisting of Frequency Sweep (FS), Linear Amplitude Sweep (LAS), LAS-Healing (LASH), and Steric Hardening (LAS-SH) tests, combined with two independent quantitative healing assessment methods, the study provided a comprehensive evaluation of the mechanical response and recovery potential of RLDP-modified binders under service-like conditions. The results collectively highlight the dual benefit of RLDP blending: enhanced mechanical performance and improved sustainability, with specific behaviours depending on the dosage level.

The linear viscoelastic characterization showed that both RLDP-modified binders maintained thermorheologically consistent behaviour, confirming that the addition of recycled plastic does not alter the fundamental viscoelastic structure of the binder. The master curves developed through the CA model demonstrated a distinct shift toward higher stiffness with increasing RLDP content. At both low and intermediate frequencies, the 4% RLDP binder exhibited the highest $|G^*|$ values, indicating superior resistance to deformation, whereas the 2% RLDP binder displayed a moderate stiffness increase while preserving a more balanced viscoelastic profile. The equirigidity temperatures interpolated at 5 MPa and 35 MPa reinforced these trends, with RLDP-modified binders showing improved high-temperature stiffness, which is desirable for rutting resistance.

Fatigue analysis through LAS testing highlighted clear distinctions in performance among the three binders. At both 15°C and 20°C, the introduction of RLDP increased the strain level at maximum shear stress, revealing enhanced fatigue endurance compared to the neat binder. The 4% RLDP binder consistently demonstrated the highest fatigue resistance, delaying damage accumulation and enduring greater deformation before reaching the critical stress peak. The 2% RLDP binder also improved fatigue properties relative to the neat binder, though to a lesser degree than

the 4% formulation, suggesting that RLDP dosage plays a decisive role in fatigue performance.

The healing-related protocols provided further insight into the recovery potential of the binders. The LAS-H tests showed that temperature strongly governs healing, with negligible or no healing observed at 15°C for both RLDP binders—where the observed recovery was largely attributable to steric hardening effects confirmed by LAS-SH control tests. At 20°C, however, RLDP-modified binders displayed measurable healing behaviour. The 2% RLDP binder exhibited the highest stiffness recovery after the 30-minute rest period, whereas the 4% RLDP binder showed partial recovery but with significantly lower efficiency. These outcomes suggest that while higher RLDP contents enhance stiffness and fatigue resistance, they may concurrently restrict molecular mobility, reducing the binder's ability to heal micro-damage. This balance between stiffness enhancement and healing ability underscores the importance of selecting an optimal RLDP dosage depending on the intended pavement performance requirements.

The quantitative healing assessments further validated these trends. The first method—based on comparing shear stress values at reference strains—confirmed the absence of healing at 15°C and highlighted healing indices of approximately 60% for the 2% RLDP binder and 26% for the 4% RLDP binder at 20°C. Although this method is simple and provides an immediate indication of recovery, it does not account for the full strain history and is sensitive to variations in peak strain among trials. The second method, based on AASHTO TP-101 fatigue-life evaluation, incorporated the entire stress-strain response. Despite complications arising from curve shapes after the peak stress, especially for the 4% RLDP binder, the method confirmed that at 20°C the binders subjected to a rest period exhibited longer fatigue lives than those without rest—consistent with the presence of healing. Both methods converged on the same conclusion: the 2% RLDP binder possesses superior healing capacity, while the 4% RLDP binder prioritizes fatigue resistance at the expense of healing efficiency.

Overall, the findings of this thesis highlight the valuable contribution of recycled plastics in enhancing binder performance. RLDP increases stiffness, improves fatigue resistance, and—at moderate dosages—preserves or even enhances the self-healing

potential of bituminous binders. The 4% RLDP binder offers the highest mechanical strength but reduced healing capacity, whereas the 2% RLDP binder provides an optimal balance between improved mechanical performance and significant healing capability. These results demonstrate that recycled plastic modification can serve as a viable and sustainable alternative to traditional polymer modification techniques, supporting both performance improvement and circular-economy goals in modern pavement engineering.

Future work may explore the performance of RLDP-modified binders in mixture-scale testing, long-term aging scenarios, and extended healing cycles, as well as the optimization of plastic composition and blending techniques. Nonetheless, the present study establishes a solid scientific basis for the use of RLDP as an effective and environmentally responsible modifier capable of enhancing both the durability and resilience of asphalt pavement materials.

BIBLIOGRAPHY

- [1] Anupam, B. R., Sahoo, U. C., & Chandrappa, A. K. (2022). A methodological review on self-healing asphalt pavements. *Construction and Building Materials*, 321, 126395.
- [2] Little, D. N., Bhasin, A., & Darabi, M. K. (2015). Damage healing in asphalt pavements: Theory, mechanisms, measurement, and modeling. In *Advances in asphalt materials* (pp. 205-242). Woodhead Publishing.
- [3] Qiu, J. (2012). Self healing of asphalt mixtures: towards a better understanding of the mechanism.
- [4] Airey, G. D. (2003). State of the art report on ageing test methods for bituminous pavement materials. *International Journal of Pavement Engineering*, 4(3), 165-176.
- [5] Hofko, B. (2022). M&S highlight: Di Benedetto et al.(2004), Fatigue of bituminous mixtures. *Materials and Structures*, 55(2), 34.
- [6] Carpenter, S. H., Ghuzlan, K. A., & Shen, S. (2003). Fatigue endurance limit for highway and airport pavements. *Transportation research record*, 1832(1), 131-138.
- [7] Kim, Y. R., Little, D. N., & Lytton, R. L. (2003). Fatigue and healing characterization of asphalt mixtures. *Journal of materials in Civil Engineering*, 15(1), 75-83.
- [8] Tang, J., Liu, Q., Wu, S., Ye, Q., Sun, Y., & Schlangen, E. (2016). Investigation of the optimal self-healing temperatures and healing time of asphalt binders. *Construction and Building Materials*, 113, 1029-1033.
- [9] Collop, A. C., & Cebon, D. (1995). A theoretical analysis of fatigue cracking in flexible pavements. *Proceedings of the Institution of Mechanical Engineers, Part C: Journal of Mechanical Engineering Science*, 209(5), 345-361.
- [10] Mazzoni, G., Stimilli, A., Cardone, F., & Canestrari, F. (2017). Fatigue, self-healing and thixotropy of bituminous mastics including aged modified bitumens and different filler contents. *Construction and Building Materials*, 131, 496-502.
- [11] Bhasin, A., Little, D. N., Bommavaram, R., & Vasconcelos, K. (2008). A framework to quantify the effect of healing in bituminous materials using material properties. *Road Materials and Pavement Design*, 9(sup1), 219-242.
- [12] Hunter, R. N., Self, A., Read, J., & Hobson, E. (2015). *The shell bitumen handbook* (Vol. 514). London, UK:: Shell Bitumen.

- [13] Tabaković, A., & Schlangen, E. (2020, June). Self-healing asphalt for road pavements. In *Proceedings of the 9th International Conference on Maintenance and Rehabilitation of Pavements—Mairepav9* (pp. 307-317). Cham: Springer International Publishing.
- [14] Emtiaz, M., Imtiyaz, M. N., Majumder, M., Idris, I. I., Mazumder, R., & Rahaman, M. M. (2023). A comprehensive literature review on polymer-modified asphalt binder. *CivilEng*, 4(3), 901-932.
- [15] Yang, Q., Lin, J., Wang, X., Wang, D., Xie, N., & Shi, X. (2024). A review of polymer-modified asphalt binder: Modification mechanisms and mechanical properties. *Cleaner Materials*, 12, 100255.
- [16] Baglieri, O., Aurilio, R., Miglietta, F., Tsantilis, L., & Baaj, H. (2025). Article of RILEM TC 278-CHA: evaluation of self-healing properties of asphalt binders—outcomes and challenges. *Materials and Structures*, 58(7), 1-16.
- [17] AASHTO Designation: T 315-12. Determining the Rheological Properties of Asphalt Binder Using a Dynamic Shear Rheometer (DSR).
- [18] AASHTO Designation: TP 101-14. (2013). Estimating Damage Tolerance of Asphalt Binders Using the Linear Amplitude Sweep.
- [19] Santagata, E., Baglieri, O., Tsantilis, L., & Dalmazzo, D. (2013). Evaluation of self healing properties of bituminous binders taking into account steric hardening effects. *Construction and Building Materials*, 41, 60-67.
- [20] Bashin, A., Masad, E., Kutay, M. E., Buttlar, W., Kim, Y. R., Marasteanu, M., ... & Carvalho, R. L. (2012). Applications of advanced models to understand behavior and performance of asphalt mixtures. *Transportation Research Circular*, (E-C161).
- [21] Giustozzi, F., & Nizamuddin, S. (Eds.). (2022). *Plastic waste for sustainable asphalt roads*. Woodhead Publishing.
- [22] Giustozzi, F., Enfrin, M., Xuan, D. L., Boom, Y. J., Masood, H., Audy, R., & Swaney, M. (2022). Use of road-grade recycled plastics for sustainable asphalt pavements: final performance and environmental assessment (No. AP-R669-22).
- [23] AASHTO T391-20 (2024). Estimating Fatigue Resistance of Asphalt Binders Using the Linear Amplitude Sweep.
- [24] Baglieri, O., Miglietta, F., Tsantilis, L., & Santagata, E. (2024). Effects of non-linearity and thixotropy in linear amplitude sweep testing for the evaluation of self-healing of bituminous binders. *Materials and Structures*, 57(4), 54.

- [25] Nouali, M., Dony, A., & Carter, A. (2024). Evaluation of fatigue life of asphalt binders using the time sweep and linear amplitude sweep tests: A literature review. *Journal of Traffic and Transportation Engineering (English Edition)*.
- [26] De Leonardis, A. (2022). Effetti di non linearità e sovrapposizione tempo–temperatura nell’autoriparazione dei leganti bituminosi= Effects of non-linearity and time-temperature superposition in the self-healing of bituminous binders (Doctoral dissertation, Politecnico di Torino).